CA1
DTC 847
86
M35
c.2

CANADIAN ASTRONAUTICS LIMITED

TP 7919E

MICROSTRIP MLS ANTENNA DEVELOPMENT

Prepared For: Transportation Development Centre
Montreal, Quebec

August 1986

Prepared By: P.R. Cowles and P.C. Strickland
Canadian Astronautics Limited
1050 Morrison Drive
Ottawa, Ontario

CAL Document #: 344-CAL-FR-10400

NOV 1987

The contents of this report reflect the views of the contractor and not necessarily the official views or policies of the Transportation Development Centre.

Un sommaire en français de ce rapport est inclus avant la table des matières.

PROJECT TEAM

The project team at Canadian Astronautics comprised:

Dr. P.R. Cowles
Mr. P.C. Strickland
Mr. S. Bailey
Mr. R. Woodhall

Transport Canada / Transports Canada
Development / Développement

REPORT DOCUMENTATION FORM

1. Transport Canada Report No.	2. TDC Project No.	3. Recipient's Catalogue No.
TP7919E	6320	

4. Title and Subtitle	5. Report Date
Microstrip MLS Antenna Development	August 1986
	6. Performing Organization Report No.

7. Author(s)	8. Transport Canada File No.
P.R. Cowles, P.C. Strickland	D1455-153-4

9. Performing Organization Name and Address	10. DSS File No.
Canadian Astronautics Limited (CAL) 1050 Morrison Drive Ottawa, Ontario K2H 8K7	11SD.T8200-4-4543
	11. DSS or Transport Canada Contract No.
	OSD84-00266

12. Sponsoring Agency Name and Address	13. Type of Report and Period Covered
Transportation Development Centre (TDC) Complex Guy Favreau 200 Dorchester Blvd. West, Suite 601, West Tower Montreal, Quebec H2Z 1X4	Final, Feb. 85-Aug. 86
	14. Sponsoring Agency Code

15. Supplementary Notes	16. TDC Project Officer
	Micha Avni

17. Abstract

This report describes the work performed and results obtained during the development of a microstrip azimuth antenna for a microwave landing system (MLS). The objective was to determine whether the antenna would meet current MLS antenna performance requirements.

A series of design, breadboard and test activities was undertaken, leading to the fabrication of a complete antenna. Final tests on the antenna were successful and it was shown to conform to requirements.

18. Key Words	19. Distribution Statement
Microwave Landing System, Microstrip Antenna, Phased Array, Navigational Aids.	Limited number of copies available from the Transportation Development Centre on request.

20. Security Classification (of this report)	21. Security Classification (of this page)	22. No. of Pages	23. Price
Unclassified	Unclassified	112	

TDC CDT 79 005
Rev 86

Canada

Transports Canada / Transport Canada
Développement / Development

FORMULE DOCUMENTAIRE DU RAPPORT

1. Nº du rapport Transports Canada	2. Nº de l'étude — CDT	3. Nº de catalogue du destinataire
TP7919E	6320	

4. Titre et sous-titre	5. Date du rapport
MICROSTRIP MLS ANTENNA DEVELOPMENT	August 1986
	6. Nº du rapport de l'organisme executant

7. Auteur(s)	8. Nº de dossier Transports Canada
P.R. Cowles, P.C. Strickland	D1455-153-4

9. Nom et adresse de l'organisme executant	10. Nº de dossier — ASC
Canadian Astronautics Limited (CAL) 1050 Morrison Drive Ottawa, Ontario K2H 8K7	11SD.T8200-4-4543
	11. Nº de contrat — ASC ou Transports Canada
	OSD84-00266

12. Nom et adresse de l'organisme parrain	13. Genre de rapport et période visée
Centre de développement des transports (CDT) Complexe Guy-Favreau 200 ouest, boul. Dorchester, Suite 601, tour ouest Montréal, Québec H2Z 1X4	Final, fév. 85-août 86
	14. Code de l'organisme parrain

15. Remarques additionnelles	16. Agent de projet — CDT
	Micha Avni

17. Resume

Ce rapport fait état des travaux accomplis et des résultats obtenus lors de l'étude et de la mise au point d'une antenne azimutale à microrubans destinée à un système d'atterrissage hyperfréquence (MLS). Il s'agissait de déterminer si l'antenne répondrait aux critères de performance actuels des systèmes MLS.

À cet fin, les chercheurs ont procédé à une série d'études, de montages expérimentaux et d'essais qui ont abouti à la fabrication d'une antenne fonctionnelle. Les essais finaux effectués sur l'antenne ont été concluants, le dispositif ayant satisfait aux critères de performance établis.

18. Mots-clés	19. Diffusion
Système d'atterrissage hyperfréquence, antenne à microrubans, réseau en phase, aides à la navigation.	Le Centre de développement des transports dispose d'un nombre limité d'examplaires.

20. Classification de sécurité (de ce rapport)	21. Classification de sécurité (de cette page)	22. Nombre de pages	23. Prix
non classifié	non classifiée	112	

CDT TDC 9005 Rev 86

Canada

ACKNOWLDGEMENTS

The authors particularly wish to thank Dr. R. Mishra and Mr. J. Hazel of the National Research Centre Antenna Group for measurements made at short notice on antenna 002. This group has subsequently had notice of closure.

SUMMARY

This report describes the work performed and the results obtained during the study and development of a microstrip MLS azimuth antenna. The objective was to demonstrate that a microstrip antenna would meet current Microwave Landing System (MLS) performance requirements.

To achieve this, a series of design and piece-part breadboard and test activities were undertaken, leading to the fabrication of a full sized antenna. Final tests on the complete breadboard antenna were successful, and the antenna was shown to conform to the requirements.

Early work defined that the general form of the antenna was to be a set of 54 series rectangular microstrip patch arrays. The number 54 was chosen to conform with existing systems, while the series array configuration offers a particularly simple form of antenna which can be "printed" onto one side of a conventional double-sided copper-clad laminate.

The series array, however, is sensitive to any errors in the assumed properties of the individual elements, these properties being the effective electrical length of the patch and its radiation conductance. Mutual coupling between patches in the direction of the series array creates the largest uncertainty; if it were not for this, patch properties could be accurately calculated. Hence, a detailed programme of patch characterization was undertaken for patches with a wide range of physical parameters - dimension and spacing.

This characterization was followed by the building and testing of increasingly complex array configurations. Firstly, a synthesis technique was used to devise a series array configuration which fulfilled the elevation pattern requirements. A single array was then made, comprising some 29 patches of various widths disposed along a 50 ohm transmission line. This configuration was to be (perhaps with minor modifications) repeated 54 times to form the complete azimuth antenna. Tests on the single array were successful, indicating that the patch characterization was accurate. A quadruple array was equally successful, allowing a full sized antenna to be built with confidence. Tests on this array showed that there was some inconsistency within the PTFE dielectric. Although some minor "trimming" gave results which were within specifications, a new batch of material was procured with closer dielectric tolerances. This second antenna performed excellently in all respects.

A study of mechanical, thermal and structural aspects of the MLS antenna was conducted in parallel with the electrical breadboarding. A critical look was taken at environmental and reliability requirements and the properties of available materials were evaluated with particular regard to their thermal sensitivity. A construction method using graphite fibre composites is proposed which, along with careful choice of printed laminate, results in a thermally insensitive lightweight antenna.

While this study was directed at the azimuth function, much of the development work is equally applicable to the remaining MLS antenna types - elevation, data and out of coverage.

SOMMAIRE

Ce rapport fait état des travaux accomplis et des résultats obtenus lors de l'étude et de la mise au point d'une antenne azimutale à microrubans destinée à un système d'atterrissage hyperfréquence (MLS). Il s'agissait de déterminer si l'antenne répondrait aux critères de performance actuels des systèmes MLS.

À cet fin, les chercheurs ont procédé à une série d'études, de montages expérimentaux et d'essais qui ont abouti à la fabrication d'une antenne fonctionnelle. Les essais finaux effectués sur l'antenne ont été concluants, le dispositif ayant satisfait aux critères de performance établis.

Les travaux préliminaires avaient permis d'établir que l'antenne devrait se composer d'un ensemble de 54 réseaux série de microrubans en forme de plaquettes rectangulaires. Ce nombre a été retenu pour assurer la conformité avec les systèmes existants, tandis que la configuration en réseau série permet de réaliser une forme d'antenne relativement simple pouvant être "imprimée" sur une des faces d'une plaque cuivrée classique.

Toutefois, le réseau série est sensible à tout écart par rapport aux propriétés théoriques de chaque élément, ces propriétés étant la longueur électrique effective de la plaquette et sa conductance de rayonnement. Le couplage mutuel entre les plaquettes, dans le sens du réseau en série, est la principale source d'incertitude; sans cela, les propriétés des plaquettes pourraient être calculées avec précision. Pour lever les doutes, un programme détaillé de caractérisation a été entrepris sur des plaquettes de dimensions et d'espacements très variés.

Cette caractérisation a été suivie par la construction et l'essai de réseaux en configuration de plus en plus complexes. D'abord, une technique de synthèse a été utilisée pour définir une configuration de réseaux série qui répondrait aux exigences concernant le diagramme d'élévation. Puis, on a procédé à la fabrication d'un réseau simple comprenant quelque 29 plaquettes de largeurs diverses disposées sur une ligne de transmission de 50 ohms.

Cette configuration devait être répétée 54 fois (avec peut-être quelques modifications mineures) pour constituer une antenne azimutale complète. Les essais effectués sur le réseau simple ont été concluants, ce qui indiquait que la caractérisation des plaquettes était précise. Après des essais tout aussi concluants sur un réseau quadruple, les experts ont construit en toute confiance une antenne grandeur nature. Les essais effectués sur ce réseau ont permis de déceler certaines inégalités dans la rigidité diélectrique du PTFE. Même si certains "réglages d'appoint" mineurs ont permis d'obtenir des résultats conformes aux spécifications, les chercheurs ont préféré recommencer avec un nouveau lot de matériaux dont les caractéristiques diélectriques étaient plus constantes. La deuxième antenne a donné d'excellents résultats sous tous les aspects.

Une étude des propriétés mécaniques, thermiques et structurales de l'antenne a été effectuée en même temps que l'on procédait aux montages expérimentaux du strict point de vue électrique, en portant une attention spéciale à l'environnement et à la fiabilité. De même, les propriétés des matériaux disponibles ont été évalués, particulièrement en ce qui concerne leur sensibilité aux variations de température. Une méthode de construction à partir d'un matériau composé de fibres de graphite ainsi qu'un choix judicieux de plaques imprimées ont permis de réaliser une antenne légère et thermiquement stable.

Même si cette étude portait sur la fonction azimutale, la plupart des travaux de développement s'appliquent également aux autres fonctions des systèmes d'atterrissage, notamment la fonction de guidage en altitude, la transmission de données sur l'état des pistes et les avertissements de non couverture MLS.

TABLE OF CONTENTS

1.0	**INTRODUCTION**	1
	1.1 Background	2
	1.2 Review of Antenna Technology	4
	1.3 Summary of the Work	7
2.0	**MLS ANTENNA REQUIREMENTS**	9
	2.1 General Requirements	9
3.0	**MICROWAVE DESIGN**	15
	3.1 Series Array Synthesis	16
	3.2 Characteristics of Elements	19
	3.3 Azimuth Design And Corporate Feed	20
	3.4 The Integral Monitor	22
4.0	**MECHANICAL DESIGN**	38
	4.1 Breadboard Antenna	38
	4.2 Study of Mechanical, Thermal and Structural Design	38
5.0	**TEST PLAN**	45
	5.1 Test Articles	46
	5.1.1 Configuration of MLS Antenna	46
	5.1.2 Configuration of Intermediate Test Pieces	46
	5.2 Test Equipment	51
6.0	**TEST RESULTS AND DISCUSSION**	53
	6.1 Characteristics of Single Patches	53
	6.2 Quadruple Array	53
	6.3 The Corporate Feed	56
	6.4 Antenna 001	59
	6.5 Antenna 002	59
7.0	**CONCLUSIONS AND RECOMMENDATIONS**	63
8.0	**REFERENCES**	64
	APPENDIX: Radiation patterns of MLS antennas	65

LIST OF FIGURES

1-1	MLS Antenna	3
1-2	Azimuth MLS and Elevation Beams	5
1-3	MLS Azimuth Subsystem	6
3-1	Microstrip Patch Array Configuration and Definitions	18
3-2	Variation of Bandwidth with Frequency for Different Dielectric Substrate Parameters	23
3-3	Microstrip Junction Patch Model	24
3-4	Ideal Elevation Array Pattern	25
3-5	Elevation Illumination Function Resulting From a Simple Fourier Transformer	26
3-6	Optimized Elevation Illumination Function	27
3-7	Predicted Elevation Array Factor	28
3-8	Taylor Distribution Function	29
3-9	Modified Split-Tee Power Divider	30
3-10	Comporate Feed Layout	31
3-11	Power Divider Layout for K1 to K10 and K24 to K27	32
3-12	Power Divider Layout for K11 to K23	33
3-13	Statistical Sidelobe Distribution Resulting from Array Errors	34
3-14	Proposed Integral Monitor	35
4-1	Two Structural Types	42
4-2	Variation of Laminate Dielectric Constant with Temperature	43
4-3	Proposed Construction of MLS Antenna	44
5-1	Test Sequence	47
5-2	Early Test Pieces	48
5-3	Comporate Feed	49
5-4	Complete MLS Antenna on NRC Test Range	50
5-5	Equipment and Physical Layout of NRC Facility	52
6-1	Transmission Line Extension	54
6-2	Radiation Conductance as a Function of Patch Width and Spacing	55
6-3	Radiation Pattern in Elevation Plane of Quadruple Series Array	57
6-4	Contour Plot Radiation Pattern of Antenna 002, 5.06 GHz with Beam on Boresight	60
A1-1 TO A1-21	RADIATION PATTERNS OF ANTENNA 001	68 to 88
A1-22 TO A1-32	RADIATION PATTERNS OF ANTENNA 002	89 to 100

LIST OF TABLES

1-1	Statement of Work and Activity Breakdown	8
2-1	Performance Requirements	10
2-2	Electrical Interfaces	11
2-3	Mechanical Interfaces	12
2-4	Physical Characteristics	13
2-5	Environmental Conditions	14
3-1	Corporate Feed Distribution	36
3-2	Split-Tee Power Dividers Design Values	37
5-1	Test Articles	46
6-1	Corporate Feed, Phase and Amplitude	58
6-2	Antenna 001 Transmission Phases Before and After Trimming, 5.06 GHz	61
6-3	Antenna 002, Transmission Phases and Amplitudes	62
A1-1	SUMMARY OF RADIATION PATTERNS, ANTENNA 001	66
A1-2	SUMMARY OF RADIATION PATTERNS, ANTENNA 002	67

1.0 INTRODUCTION

The Microwave Landing System (MLS) defined by the International Civil Aviation Organization (ICAO) is to become the standard instrument for guiding aircraft to land in conditions of poor visibility.

Current MLS antennas comprise arrays of waveguide radiators. From the radio frequency (RF) viewpoint, these are reasonably satisfactory but they carry significant mass and cost disadvantages. The antenna mass makes the design of a rugged but frangible antenna particularly difficult, while precision milling or spark erosion is generally regarded as an expensive operation, even with automated machinery. It is recognized that cost and mass savings can be effected by pursuing microstrip technology. This has been demonstrated by the successful deployment of a number of airborne microstrip arrays as well as large number of terrestrial applications [1,2]. A number of problem areas have prevented the widespread adoption of microstrip antennas until recent times. These are:

- energy loss in the dielectric substrate
- unrepeatability of the dielectric substrate
- difficulty in analysis of the array
- difficulties with mechanical and environmental aspects

The first two items are now within the reach of an easy solution since highly accurate, stable and low loss dielectrics are on the market. Two examples are glass-reinforced Teflon as used in this project and polyimide (NOMEX) Honeycomb [3], which has been used in space applications but which is eminently suitable for ground use.

Analysis of the array is complicated by the existence of feed line radiation, the presence of the dielectric substrate, the complex mode structure and by the strong inter-element coupling. A number of formulations have been proposed for dealing with individual elements [4,5] but no one general solution yet exists for a whole array. In this project this was circumvented by establishing a progressive breadboarding programme starting with single elements and leading in steps to the whole array.

This report present the results of work performed by Canadian Astronautics Limited (CAL) for the Transportation Development Centre (TDC) on the design, construction and testing of a prototype MLS microstrip antenna. The work reported here forms the second part of a two part programme. The first part [6], undertaken during the period April until October 1983 was a general study of microstrip antenna techniques; the second part deals with the implementation of microstrip technology.

Earlier work [6] identified the series fed rectangular microstrip patch as being an antenna configuration worthy of further study and breadboarding. The resulting antenna is shown in figure 1-1. It comprises 54 linear arrays, each of which is identical, fed at the top and terminated at the bottom. The linear arrays produce the elevation radiation pattern, while the widthwise arrangement generates the azimuth beam. This separability of elevation and azimuth functions is used to advantage during the antenna design process and thus leads to the method adopted here, which comprised initial identification of microstrip patch parameters, leading to

elevation and then azimuth array design. Given that the individual elevation arrays perform well, then the azimuth power distribution can be devised. In a working MLS antenna, the azimuth beam is swept rapidly through an angle of ±40°. The breadboard was designed to work at two fixed beam positions; at 0° and 40°. This was achieved by means of a fixed power divider, the "corporate feed" and two sets of interconnecting cables. In Figure 1-1 a cable set can be seen at the top of the array leading to the corporate feed which resides behind the array.

This development is seen as particularly important in Canadian National terms. Recent developments in antenna technology have shown a considerable shift towards microstrip style antennas in a number of aerospace, terrestrial, military and civilian areas. Much development work on the theory and practice of these antennas is underway in the USA (Ball Brothers), in Japan (MELCO), in Europe at the Ecole Polytechnique Federale, Lausanne and in the UK (GEC-Marconi). It is often the case that equipment sales and marketing efforts are fuelled by a sound antenna design since the antenna is frequently a critical system component.

1.1 Background

Angular positional information is provided to an aircraft via the MLS elevation and azimuth swept beams by the technique known as Time Reference Scanning Beam (TRSB). The two beams sweep a volume from 0° to 20° in elevation and ±40° in azimuth to a range of 20 nautical miles (31 km) and to a height of 20,000 ft. (6,100 m). Such an operational volume is far superior to the current Instrument Landing System (ILS) in terms of allowable aircraft approach manoeuvers and glide slope angles. Further advantages of MLS over ILS are:

- cost, particularly of installation and maintenance
- high accuracy
- possible common location of azimuth and elevation antennas
- high reliability due to all-digital circuitry
- 200 channels compared with 40 for ILS
- less sensitivity to site conditions and layout

It is the intention of ICAO to replace all ILS systems by MLS by the year 2000, Additional MLS will be required worldwide because the system is eminently suitable for smaller airports and airports in difficult terrain.

The operational volume is scanned by both azimuth and elevation beams at accurately controlled sweep rates. By measuring time differences between reception of "up", "down", "to" and "fro" beams the aircraft can locate its direction relative to the MLS. With the addition of Distance Measuring Equipment (DME) a complete knowledge of position is obtained. The scan arrangement of the azimuth and elevation MLS beams is shown in Figure 1-2, scan frequencies are 13 and 39 per second for Azimuth and Elevation respectively. Differentiation of the received signals is achieved by time multiplexing the various ground station transmissions.

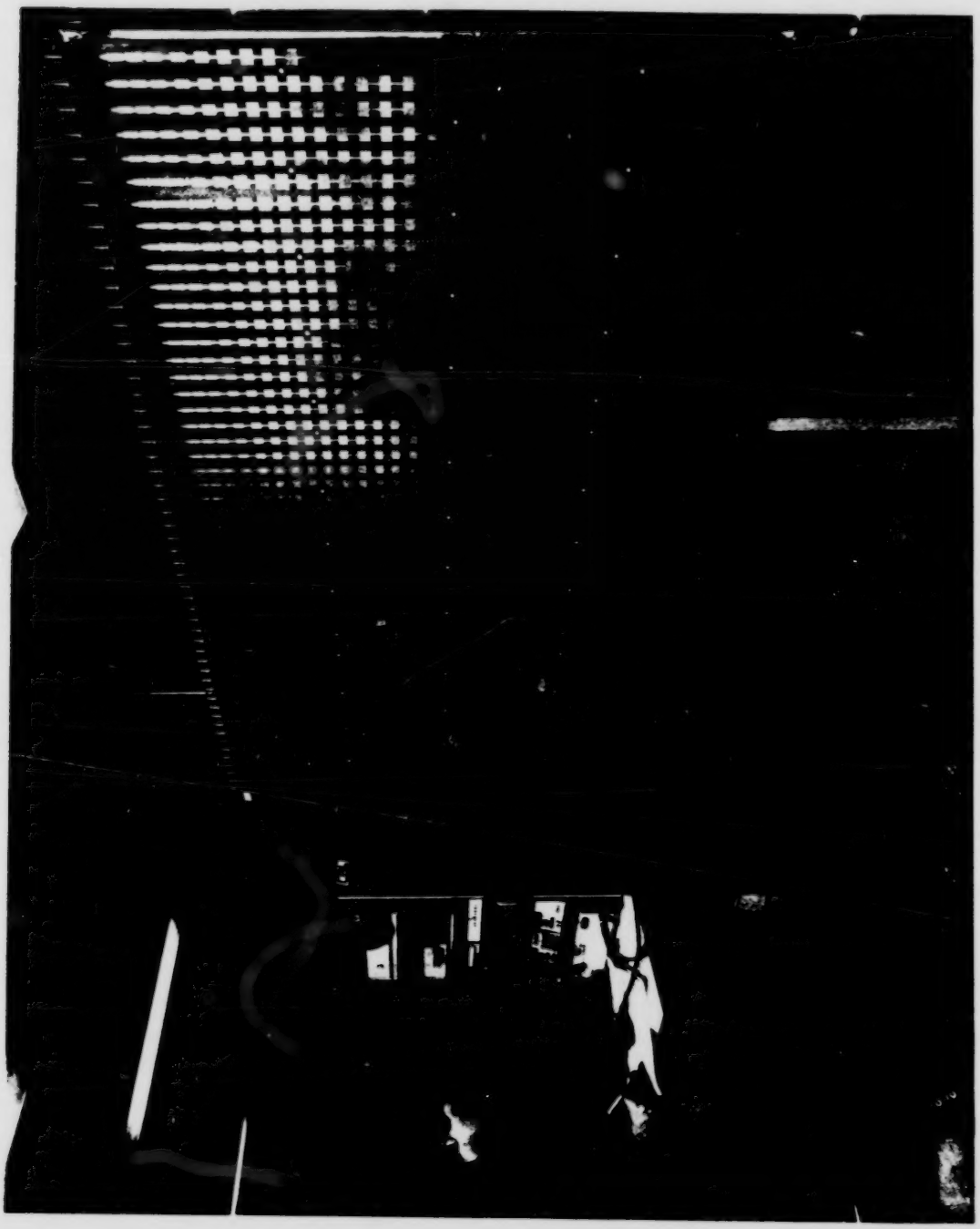

Figure 1-1 MLS Antenna

To illustrate the relationship of the MLS Azimuth antenna to the whole system, the Azimuth subsystem is shown in block diagram form in Figure 1-3.

1.2 Review of Antenna Technology

A fan shaped beam, scanning through a wide angle can in principle be generated by a number of antenna types. Mechanical scanning can easily be discounted as other simpler, lighter and more reliable techniques are available. Of the general types - reflector antennas and phased arrays- probably only the TORUS reflector can comfortably achieve such scan angles. However, this would necessitate an aperture much larger than a scanning phased array and would in any case require a significantly large feed structure which may well have the complexity of a stand alone array. We are therefore reduced to the scanning phased array as the obvious choice for MLS azimuth (or elevation) antennas. Given this choice, the array design is complicated by the existence of "mutual coupling" between array elements. This exists both in the series distribution networks feeding the elements and in radiative coupling via free-space or surface coupled modes. Its principal effect is to modify the impedance and radiation characteristics of a single solitary element when taken to an array environment. These parameter changes can be severe, even catastrophic, if they are not fully accounted in the design stage. Some simple array elements and array configurations can be dealt with entirely theoretically, which leads to an antenna that works first time around. Most arrangements, however, cannot be so analysed even when the most recent advances in antenna theory are summoned. In these cases, a series of practical tests on elements and groups of elements must be made to arrive at a good knowledge of the immersed element characteristics. Such tests were performed on the microstrip elements in this study.

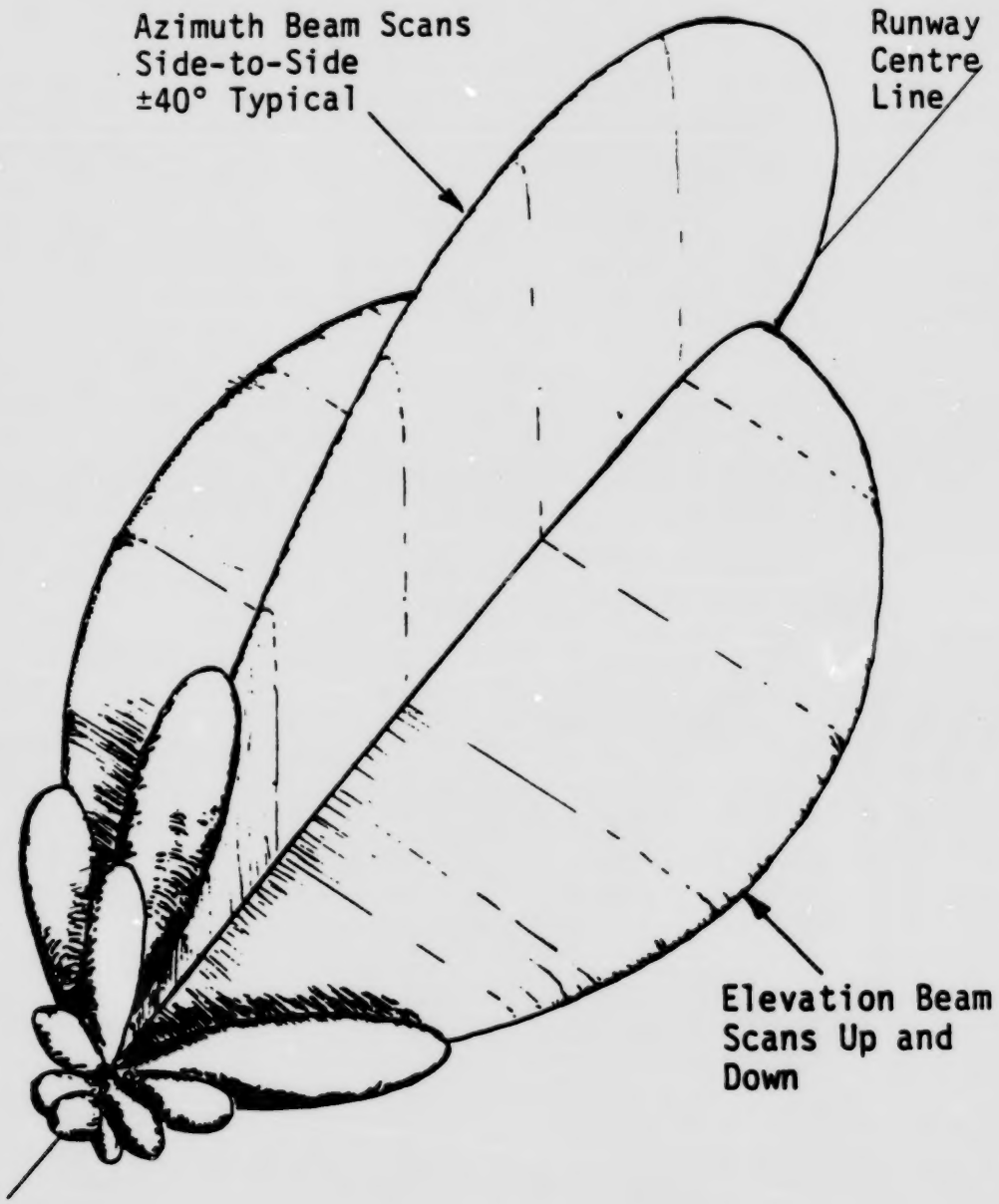

Figure 1-2 Azimuth MLS and Elevation Beams

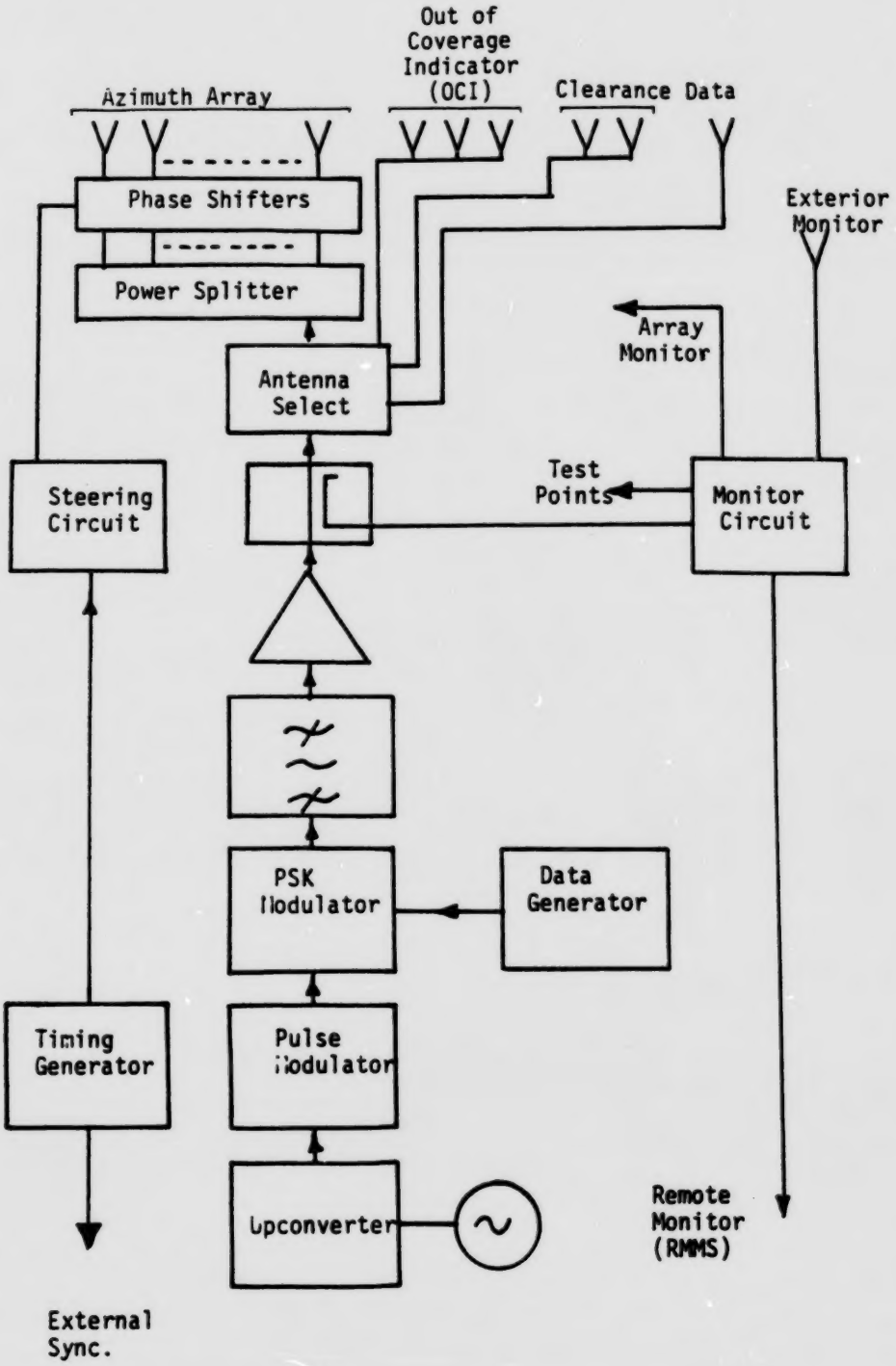

Figure 1-3 MLS Azimuth Subsystem

1.3 Summary of the Work

Starting with the concept of using an array of series-fed rectangular patches which were to be made by conventional printed circuit techniques, the program of work followed a step-by-step development process.

Certain features of the antenna were fixed from the start. For example, the choice of 54 series arrays across the antennas width is dictated by the desire for compatibility with existing MLS systems. Element spacing in the azimuth direction is limited because of the scan requirements and the need to avoid grating lobes at maximum scan angle.

Early work comprised the characterisation of individual elements. This was followed by short arrays and a full length array to gain confidence. Elevation radiation patterns of the full length array and of a subsequent quadruple array were totally satisfactory, having remarkable similarity to the predicted array patterns. These tests then allowed the full scale antenna to be manufactured.

In support of the final tests, a 54 way power divider was made, tested and integrated with the array elements. This used similar microstrip technology and identical substrate material to the arrays. Measurements on the first antenna, 001, were disappointing. Bench tests of the phase and amplitude of signals passing from beginning to end of the series array elements showed a substantial variation in phase. Investigation showed that the batch of laminate used for this antenna exhibited significant variations in dielectric constant. These variations correlated with the striated appearance of the dielectric surface which can be observed in Figure 1-1. At the very best, the laminate was at the extreme edge of its dielectric constant tolerance band. The antenna was "patched" to obtain a more uniform terminal phase and tested for radiation pattern performance, which complied with the RF requirements.

Discussions with TDC resulted in a second attempt to produce an antenna which would receive no "patching". Laminate was procured from the same source with a tighter control and tolerance on dielectric constant. Bench tests on the printed arrays showed an excellent uniformity of transmission phase and the radiation performance measurements on the antenna, 002, were very satisfactory.

A breakdown of the activities defined in the Statement of Work and the status of these activities is shown in table 1-1.

SOW REFERENCE	SOW ACTIVITY	NOTES
4.1	Develop detailed work plan, activity schedule, project management control and documentation procedures.	Work performed within established CAL procedures
4.2	Design, manufacture and test a prototype vertical linear array for a microstrip MLS azimuth antenna according to the specification in Appendix 1. Include integral monitor which can be used to simulate "far field" signal.	Results presented in Section 6.2 (quadruple array) Baseline design presented in Section 3.4
4.3	Engineer the mechanical packaging of the microstrip azimuth antenna. Give consideration to environmental and frangibility aspects.	Study reported in Section 4.2. Section 4.2
4.4	Demonstrate design feasibility using five strip vertical linear array	Design progressed from 1-4-54, section 6. No design iteration was required.
4.5	Design, manufacture and test a full MLS azimuth antenna. All test equipment including corporate feed and static phase adjustment hardware shall be provided.	Results for full sized antennas 001 and 002 in Section 6. Completed; hardware for 0° and 40° beam squints was made.
4.6	Prepare and submit to TDC a technical report Deliver hardware	 Delivery to be agreed

Table 1-1 Statement of Work and Activity Breakdown

2.0 MLS ANTENNA REQUIREMENTS

The MLS antenna must produce its scanning shaped beam when installed in any one of a number of possible operating environments. Maintenance should be zero or simple and infrequent over the design life. The following section is an attempt to produce a resumé specification for a complete commercial MLS antenna. The values presented are a result of the use of a number of sources; manufacturers specifications and literature from both the US and Canada, ICAO documents and discussions with MLS system suppliers and with officials of Transport Canada.

For the breadboard developed during this project, the RF performance requirements of Table 2-1 are appropriate.

2.1 General Requirements

These are subdivided into the following areas:

- performance requirements
- physical properties
- interface
- environment

Where values have proved difficult to obtain, suggested or tentative figures are given in parentheses.

PARAMETER	VALUE
Frequency Range	5030 MHz to 5090 MHz
Polarisation	Vertical
Gain	[25 dBi]
Elevation Patterns	-13 dB below horizon 8 dB deg^{-1} at horizon uniform from 0.8° to 9.0° cosecant from 9.0° to 15.0°
Azimuth Pattern	Azimuth half power beamwidth 2.0 ± TBD. Defined at boresight at 5060 MHz. Azimuth sidelobe level -20 dB max
Radiation Pattern, crosspolar	not specified [0 dBi max]
Scan Angle	± 40° in azimuth
Scan Rate	20,000 deg. sec^{-1}
Reliability	[200,000 hours MTBF, 5000 FIT]

Table 2-1 Performance Requirements

PARAMETER	VALUE
RF Interfaces	
Number of input ports	54
Impedance, into antenna	50 ± [2] ohms
Impedance, out of antenna	50 ± [2] ohms
Transmission Line	Coaxial
Input Power	10 W
Connector Type	SMA Female
Test Port	
Purpose	to sample all 54 input lines
Type	[type N female]
Impedance, into antenna	50 ± TBD ohms
Impedance, out of antenna	50 ± TBD ohms
Power Interface	
Purpose	radome heating
Type	single phase, 2 wire and earth
Connector	TBD
Voltage	115 ± TBD
Current	[20 A max]

Table 2-2 Electrical Interfaces

PARAMETER	VALUE
Fixing to base	
Characteristics	TBD
Weight	[30 kg] maximum
Shear force	[9300 N] maximum
Overturning Moment	[14000 NM] maximum
Interface with Phase Shifters	
Characteristics	TBD

Table 2-3 Mechanical Interfaces

PARAMETER	VALUE
Envelope, height width depth	[2.2 m] [2.0 m] [0.6 m]
Mass	[25 kg]
Frangibility	TBD, to comply with FAA ICAO and TDC requirements
Design lifetime	[20 years]
Colour	TBD

Table 2-4 Physical Characteristics

Parameter	Operating or Non-Operating	Value
Temperature	OP	-50°C to 55°C
Humidity	OP	0% to 100%
Wind	OP NOP	[100 Kmh^{-1}, 44 ms^{-1}] [240 Kmh^{-1}, 67 ms^{-1}]
Solar flux	OP	1135 WM^{-2}
Altitude	OP NOP	0 to 4000 m 0 to 15000 m
Shock	OP NOP	Seismic zone III of Uniform Builders Code Transportation shocks TBD
Snow load	NOP	1.7 Kgm^{-2}
Ground snow	OP	1 m
Ice load	NOP	50 mm radial ice
Salt and fog	OP	MIL-STD 810 Method 509.1
Rain	OP	51 mmh^{-1}
Hail	OP	13 mm dia.
Sand and dust	OP	Size up to 150 microns

Table 2-5 Environmental Conditions

3.0 MICROWAVE DESIGN

The electrical specifications for the microstrip MLS antenna have been presented in Table 2-1. As far as microwave design is concerned, the key parameters are the frequency band, scan angle, azimuth beamwidth, sidelobe levels and elevation pattern shape. Other RF specifications are important in the phase shifter design but have little impact on the of the microstrip radiating elements. The azimuth beamwidth and sidelobe level dictate the azimuth aperture dimension. The antenna azimuth design and corporate feed are considered in Section 3.3 of this report. Section 3.2 deals with the elevation array design. The principal characteristics of the elevation pattern are the rate of roll-off at the horizon, the flat beamwidth, cosecant squared illumination to 15 degrees above the horizon and the sidelobe level below the horizon. It is rapid roll-off of the pattern at the horizon which dictates the elevation aperture. Section 3.1 deals with the design and characterisation of the microstrip radiating elements. Series fed arrays are very sensitive to errors in the estimated radiation impedances, losses and propagation velocity of the non-uniformly loaded transmission line. Complicating this is the fact that the patches are strongly coupled in the E plane due to their close proximity. Consequently accurate charactisation of the microstrip patch elements was necessary under various conditions of patch width and mutual coupling.

Three principals were essential to the radio frequency microwave design of the MLS antenna.

a) It was assumed that the elevation and azimuth functions are separable. That is that the performance of one is not dependent on the configuration of the other. This implies that the mutual coupling between series arrays in the azimuth direction was negligibly small which was indeed the case.

b) Mutual coupling in the series array or elevation direction is strong and that measurements are required to determine the element parameters in the array environment. This coupling was found to be very strong and highly influential on element parameters. These were successfully characterized by measurement.

c) The complex elevation radiation pattern may be synthesized directly without the need for physical iterations. In practice, because principals a and b were valid, the synthesis procedure described below series arrays which performed to requirements without recourse to iteration or tuning.

3.1 Series Array Synthesis Procedure-

In describing the antenna and the design methods, reference is made to figure 3-1 which defines the configuration and terms used. The 54 identical series arrays each generate the requisite elevation radiation pattern. Azimuth beam shape and beam scan is achieved by arranging these series arrays side by side and feeding them with 54 appropriate phase and voltage drives. It is the separability of the antenna performance in the two orthogonal (azimuth and elevation) planes that allows the synthesis of the elevation series arrays to proceed in isolation from the azimuth design.

Series array synthesis is based on four software procedures: FOUR PATCH AN2 and AN1 which are operated consecutively to arrive at a dimensional description of the patches and a performance prediction. Synopsis of the program functions are given below.

FOUR

This routine takes the elevation pattern requirements as its input, this is prepared in the "ideal" form shown in Figure 3-4. The operator is required to define the series array length and an initial patch spacing. The program performs a Fourier Transform on the "ideal" patterns and produces as output the excitations of the patches at the positions specified. The output of this program forms an approximate starting point for further optimization and is not in itself definitive.

PATCH

This program takes the output of the previous routine FOUR and generates a list of patch positions, widths, resonant lengths and connecting line lengths. It uses measured data on patch conductances and extensions (described in section 3.2) expressed as best fit functions. The program has as its basis an iterative loop which successively refines the crude starting assumptions of patch geometry.

AN1

This programs takes the patch geometry from PATCH and performs a chain matrix transmission line analysis of forward and reflected waves along the length of the array.

The series array radiation pattern is determined and compared to the original requirement template. An error function is generated which is used to modify the array geometry and the calculation proceeds iteratively until a close match is obtained.

The output from this program is used to manufacture the mask to etch the array.

AN2

This program takes the data file from AN1 and calculates and displays the array radiation pattern in hard copy form.

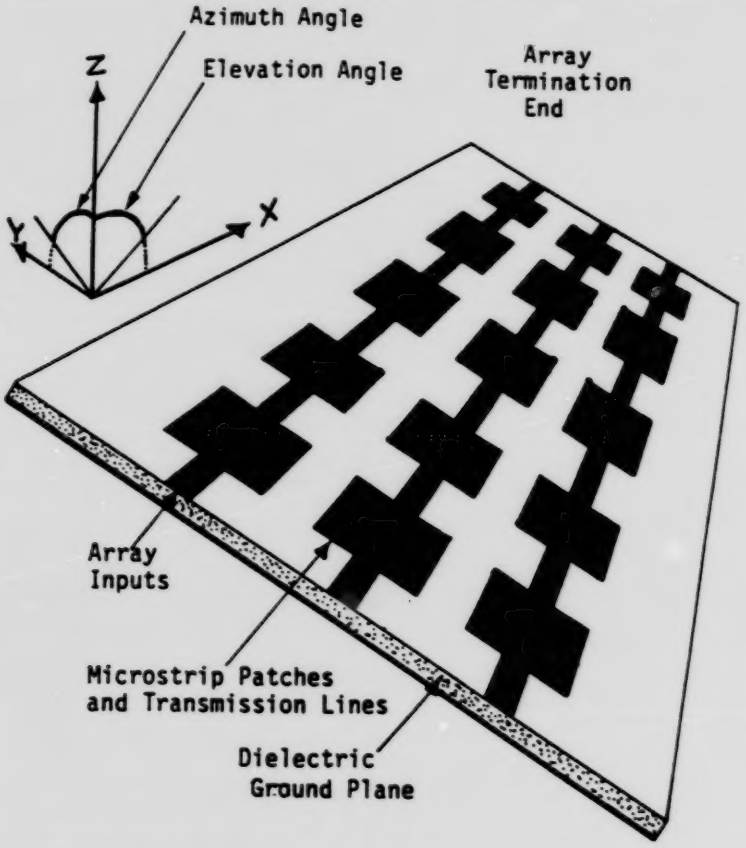

List of Symbols

C	velocity of light
f	operating frequency
f_t	maximum operating frequency
g_o	radiation conductance of a patch
h	thickness of dielectric substrate
s	patch spacing, along the array
w	patch width
w_{max}	maximum permissible patch width
Z_o	characteristic transmission line impedance
ϵ_r	dielectric constant of substrate
S_1, S_2	measured maximum and minimum reflection coefficients
Δ_1, Δ_2	near and far connecting line extensions

Figure 3-1 Microstrip Patch Array Configuration and Definitions

3.2 Characteristics of Elements

Element design comprises selection of dielectric substrate material and thickness, a check that this choice does not infringe criteria for avoiding surface mode generation and the selection of patch dimensions for the early measurement program.

With microstrip antennas, it is possible to trade-off dielectric constant, dielectric thickness and bandwidth. In the case of the MLS antenna, the bandwidth requirement is not particularly onerous. Nevertheless there is often a direct link between an antennas bandwidth and its sensitivity to thermal expansion and contraction and to constructional errors. A more than adequate bandwidth is therefore desireable. Referring to Figure 3-2 which relates percentage bandwidth and frequency to dielectric constant and thickness, our chosen parameters are shown. By using a standard, available material (1/16" PTFE-woven glass) a bandwidth of around 2.5% can be obtained which is more than twice that demanded by the RF requirements, 1.2%.

Surface waves can also be enhanced or controlled by choice of dielectric constant and thickness. These waves, which can exist in TE and TM forms are coupled to the dielectric and propagate along the surface. They create an "end fire" radiation in the direction of the plane of the antenna and thus represent lost energy and spurious directional radiation. Control of surface waves is generally limited to the suppression of the lowest order (TMo) mode by selecting a suitably thin dieletric. An often used rule (James and Henderson [7]), is that for PTFE dielectrics the thickness should be less than 0.09 wavelengths or 5.3 mm. Our choice of dielectric essentially based on availability comfortably meets this criterion.

A final but important and restrictive parameter is the maximum permissable width of the rectangular patches. This is dictated by the necessity to avoid a transverse resonance; the fundamental occurs when the patch is effectively a half wavelength across. For our choice of dielectric, this width is 18 mm. This is a restriction that limits the way in which the release of energy at each patch can be arranged.

Accurate patch characterisation is essential in a series array since any misconception can result in a systematic build-up of error along the array. Two characteristics are of concern, the patch radiation conductance Go and the patch extension or "end effects", Δ_1 and Δ_2.

A standard microstrip junction model is given in Figure 3-3. The aim of element characterisation is to determine Δ_1, Δ_2 and g_o as a function of patch width and mutual coupling. Coupling at 0.6 λo spacings is typically at the -20 dB level for both E and H plane. In the E plane however element spacings can be much less than this in series fed arrays. Consequently characterization is done as a function of E plane spacing but not H plane spacing. The radiation conductance g_o of the patches is difficult to isolate from that of the launching connectors. The best technique for isolating these and that used here is to measure the reflection coefficient from the patch while sliding a short at the output. Recording the maximum reflection coefficient S_1 and the minimum S_2 will give the radiation conductance by:

$$2\, g_o = \frac{S_1 + S_2}{S_1 - S_2}$$

The connecting line extensions Δ are easily obtained by measuring the phase through the patch and comparing to that of a uniform line. Test results were used to develop empirical expressions for use in synthesis programs described in the previous Section 3.1. These results are given in Section 6.0. Note that the line extensions Δ_1 and Δ_2 were not found to be significant functions of patch spacing whereas the radiation conductance g_o was found to be a strong function of spacing over the range of interest. In the case of multi-element test pieces used to determine patch characteristics as a function of spacing, iterative computer techniques are required to derive the parameters of the individual patches.

3.3 Azimuth Design and Corporate Feed

The sidelobe level requirement of -20 dB is met by considering three principal contributions to the sidelobe budget. These are the basic aperture illumination function, errors in the amplitude drive to the elements and phase errors. Figure 3-13 shows graphically the sidelobe level contributions from a random amplitude and phase error superimposed on a basic error-free radiation pattern with a -29 dB maximum sidelobe level. This is a result of a statistical analysis and so the values used are in statistical terms. For 84% of the sidelobes to remain below -20 dB, the total r.m.s. error should be less than 0.3 radians. This error can be variously apportioned between phase and amplitude but the balance chosen for criteria during in-process testing of the corporate feed and array was:

amplitude: defined as ±0.5 dB power
phase: ±11 degrees

A Taylor -30 dB, N=4 distribution was selected to complement the above criteria, this distribution as applied to the 54 elements have values as listed in Table 3-3. The 54 elements and corporate feed output ports are sequentially number 1 to 54 across the face of the array. The distribution is symmetrical with elements 27 and 28 receiving equal maximum RF signal at the center of the array. The data shows an amplitude distribution of 0 dB on these centre elements which decreases to -12.28 dB on the end elements (1 and 54). This is graphically represented in Figure 3-8.

Power division ratios necessary to accomplish the Taylor distribution are achieved by modifying the impedance of different transmission lines in the individual split-tee power dividers. The impedances Z_o1 to Z_o5 were computed using the equations in Figure 3-9. The K numbers (K1 - K27) identify the dividers that are placed in specific locations to determine the right half of the Taylor amplitude distribution (Figure 3-10). Due to symmetry the left half will be a mirror image of the right half.

Table 3-2 contains the impedances of the transmission lines Z_o1 to Z_o5 for the required power division ratios. The impedances Z_o1 to Z_o5 are physically realized by varying the etch widths of the microstrip transmission lines. Figures 3-11 and 3-12 show the required circuit patterns for the split-tee power dividers.

The corporate feed was designed to have a Taylor distribution across its output ports. The specification on tolerance of the amplitude and phase are ±0.5 dB and ±2.5° respectively. (the remaining phase budget being allocated to the cables and the array). Thus a technique for fine tuning the phase as well as the amplitude of the corporate feed was employed. To achieve the phase accuracy across the operating frequency band each output port had the identical transmission line length from the input. This involved extending some lines by use of a trombone. There are numerous discontinuities that the RF signal traversing from the input to each individual output must encounter. These discontinuities tend to alter the phase and hence must be compensated to achieve identical phase across the outputs. A phase trimming stub was inserted at the design stage for the fine tuning within 15°.

Since the MLS antenna was to be tested at boresight and one squint angle, two sets of semi-rigid cables were fabricated for connecting the corporate feed to the elevation arrays. For a boresight beam the cables have equal lengths and thus are relatively easily fabricated. A squint angle of 38.96 degrees was chosen since this results in a 45° interelement phase shift thus reducing the number of cable lengths required to 8 due to the cyclic nature of the phase shifts.

3.4 The Integral Monitor

Reliability demands that there are many checks on the performance of the MLS system and it's components. Correct operation of the azimuth antenna is monitored by external and internal monitors; the external monitor is a small receive antenna placed in the antennas far-field such that the passage of the swept beam can be automatically observed by the system test equipment. The integral monitor described here emulates the behaviour of the external monitor but does so without an intervening propagation path. Small samples of the signals in each of the 54 series elments are summed in a "travelling wave coupler", this summation is comparable to that which occurs at the aperture of the external monitor antenna. Sampling can occur either at the input or at the termination end of the series arrays, in the latter case all phenomena and failures of the elements are observable.

A baseline design for a travelling wave integral monitor is proposed here which is based on microstrip techniques and is compatible with the overall antenna concept. At the end of each series array, figure 3-14, two small holes etched in the ground plane form a directive coupling of approximately -30 dB to a meandering microstrip line on the back of the array. Meanderline lengths can be chosen such that the beam pass can be emulated at any desired angle. The stability of this angle is assured by the use of an air-dielectric between the meanderline and the common ground plane.

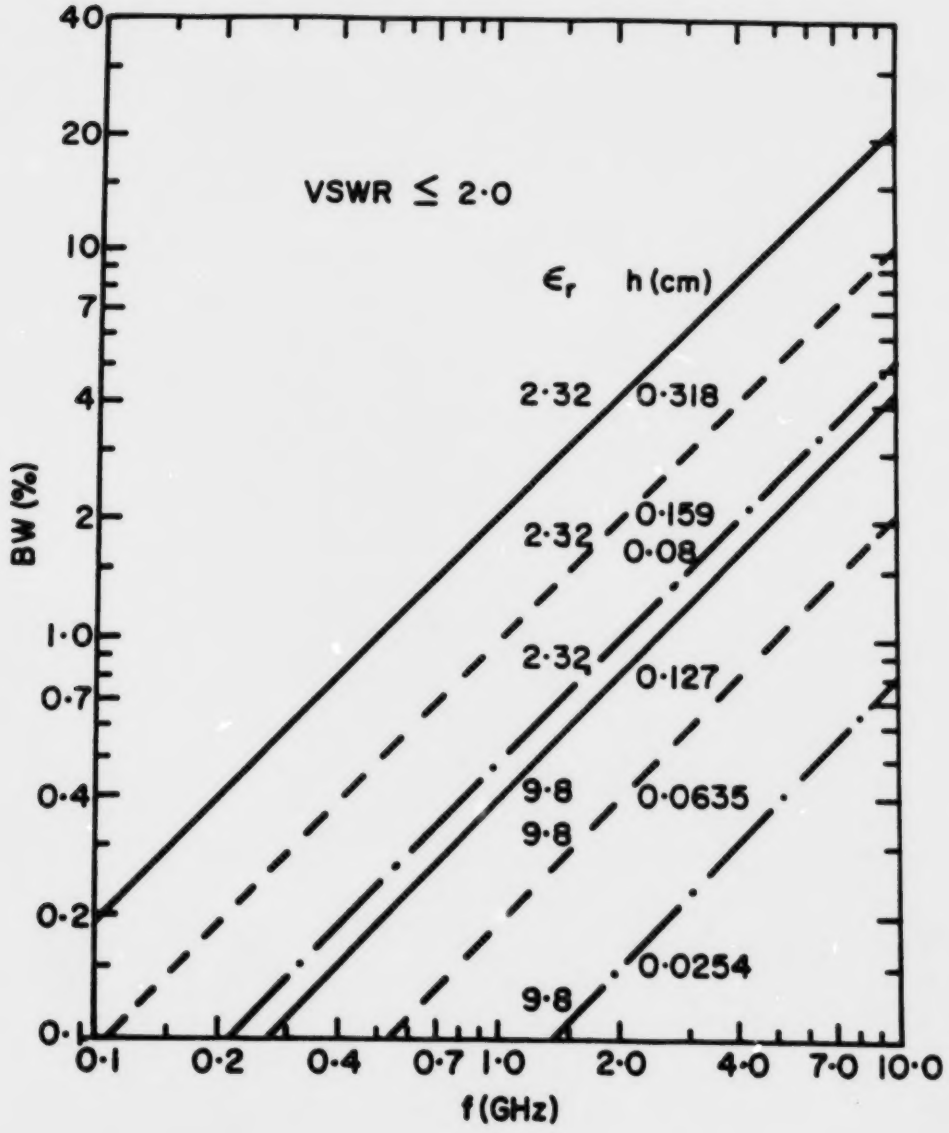

Figure 3-2 Variation of bandwidth with Frequency for Different Dielectric Substrate Parameters

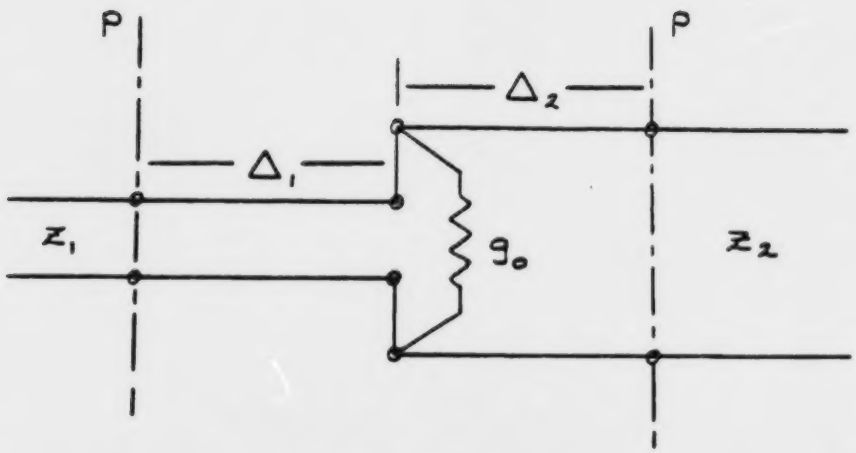

Figure 3-3 Microstrip Junction Patch Model

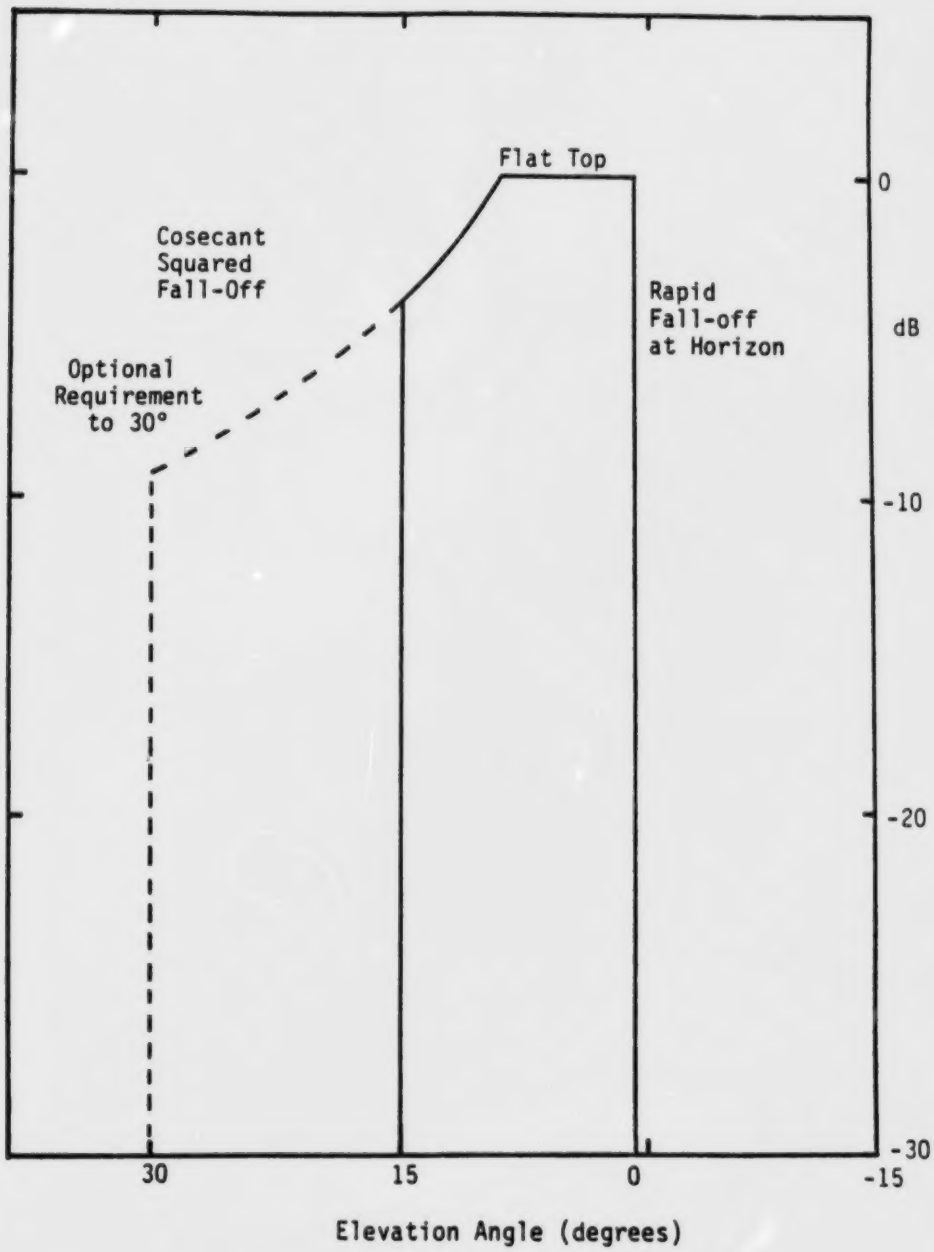

Figure 3-4 Ideal Elevation Array Pattern

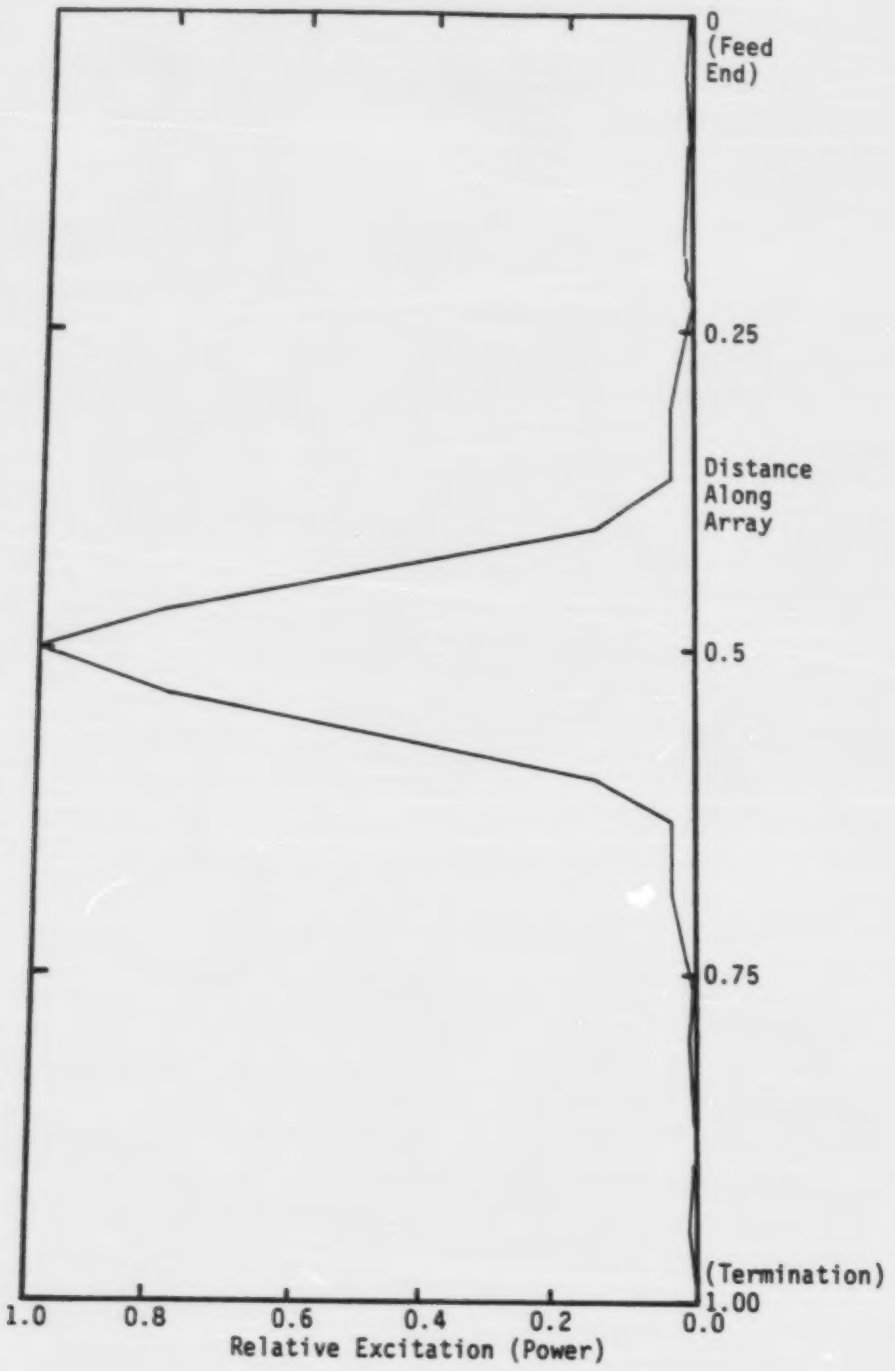

Figure 3-5 Elevation Illumination Function resulting from a Simple Fourier Transform

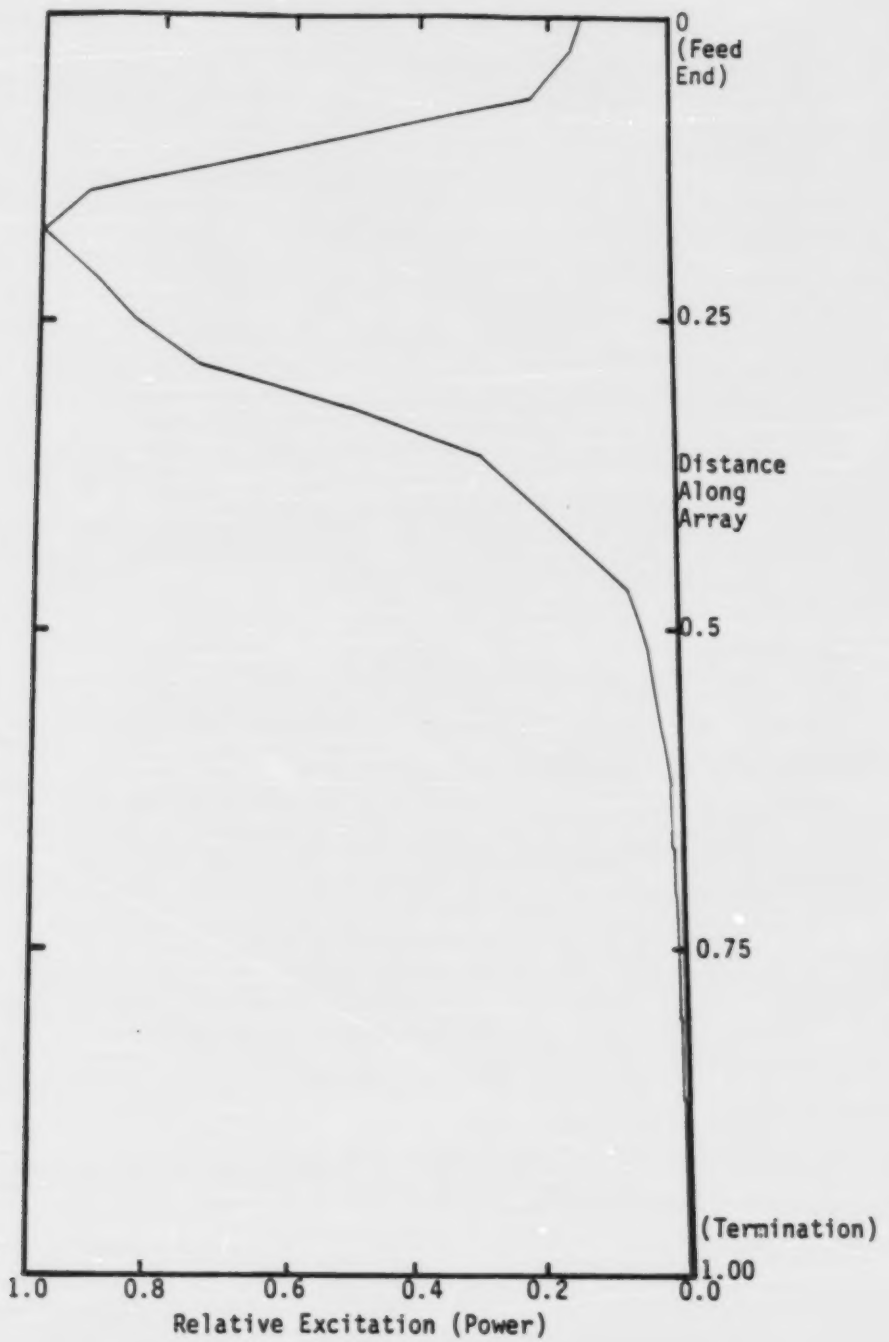

Figure 3-6 Optimized Elevation Illumination Function

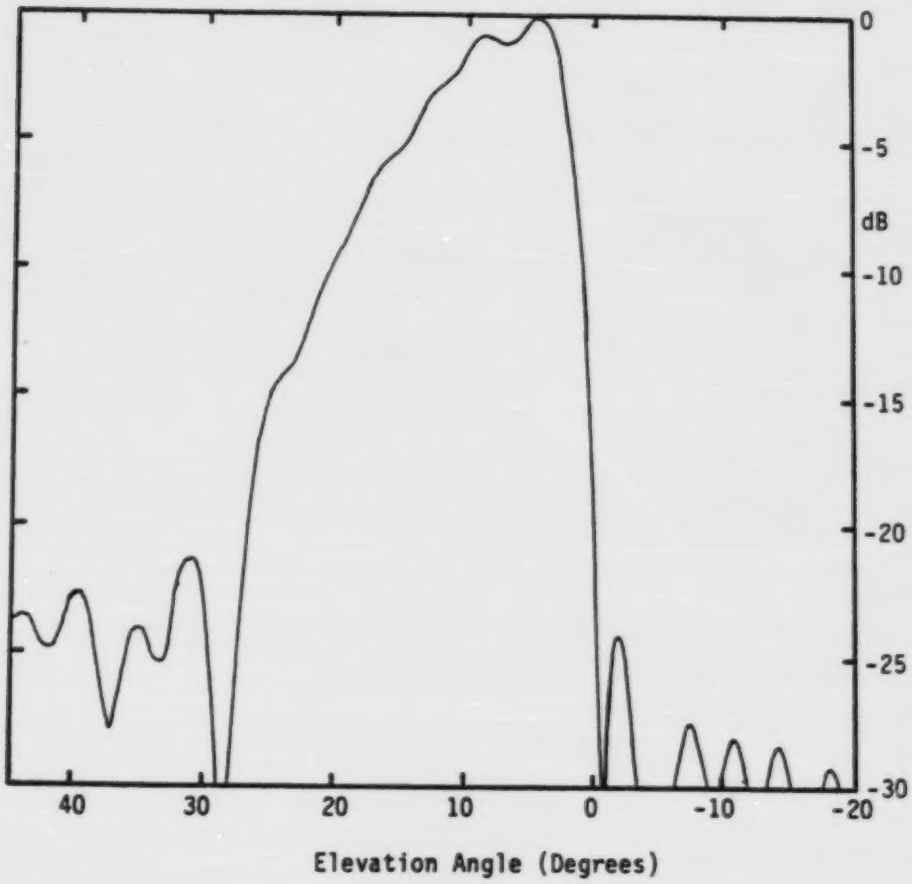

Figure 3-7 Predicted Elevation Array Factor

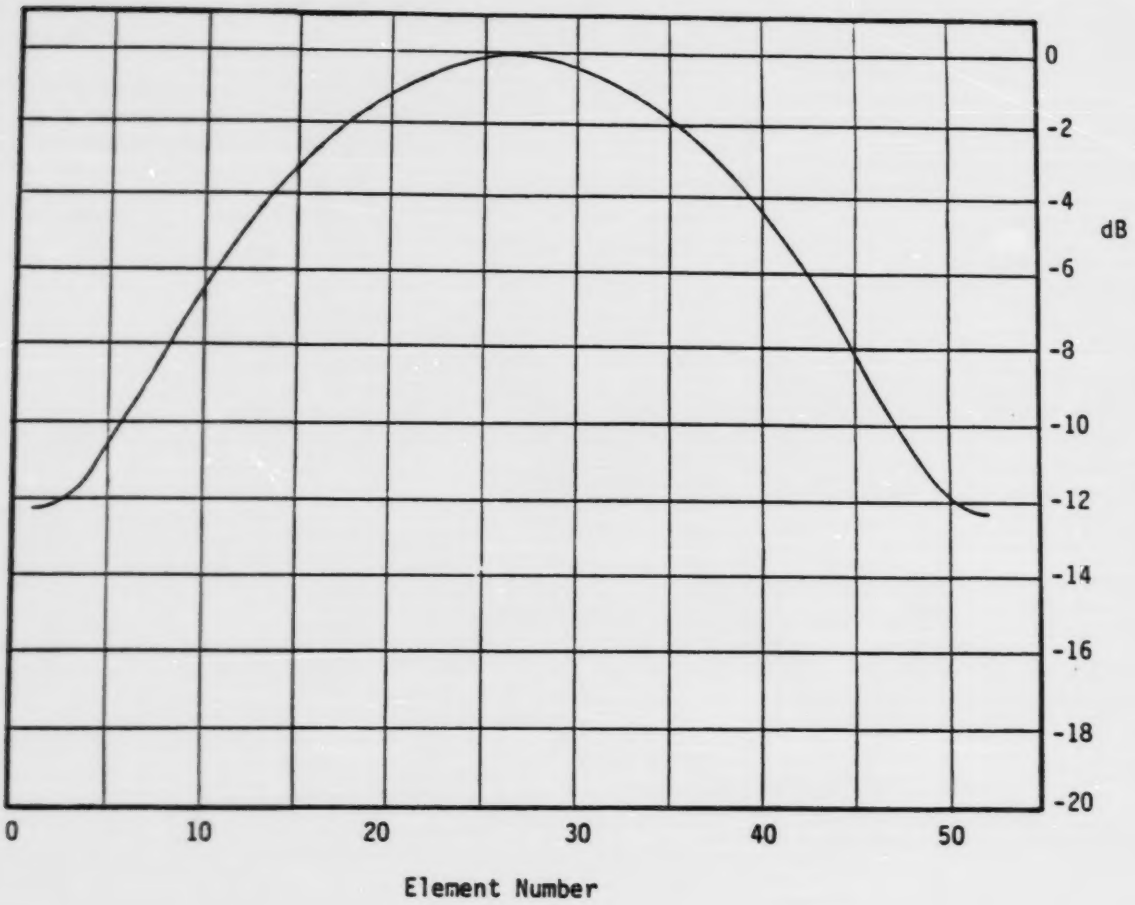

Figure 3-8 Taylor Distribution Function

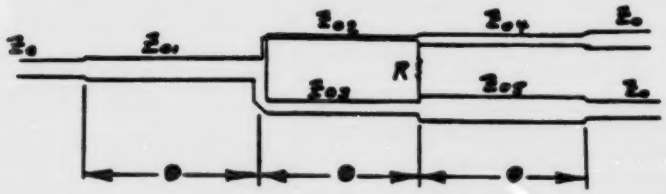

$$\frac{\text{POWER AT PORT 5}}{\text{POWER AT PORT 4}} = K^2$$

CENTER FREQUENCY AT $\theta = 90°$

$$R = Z_0 \frac{1-K^2}{K}$$

$$Z_{01} = \left(\frac{K}{1+K^2}\right)^{1/4} Z_0$$

$$Z_{02} = K^{3/4}(1+K^2)^{1/4}(Z_0)$$

$$Z_{03} = \frac{(1+K^2)^{1/4}}{K^{3/4}}(Z_0)$$

$$Z_{04} = Z_0\sqrt{K}$$

$$Z_{05} = \frac{Z_0}{\sqrt{K}}$$

Figure 3-9 Modified Split-Tee Power Divider

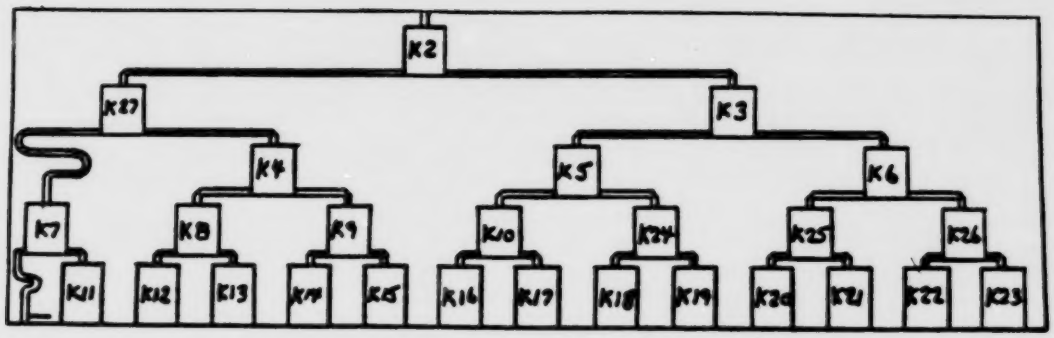

Figure 3-10 Corporate Feed Layout

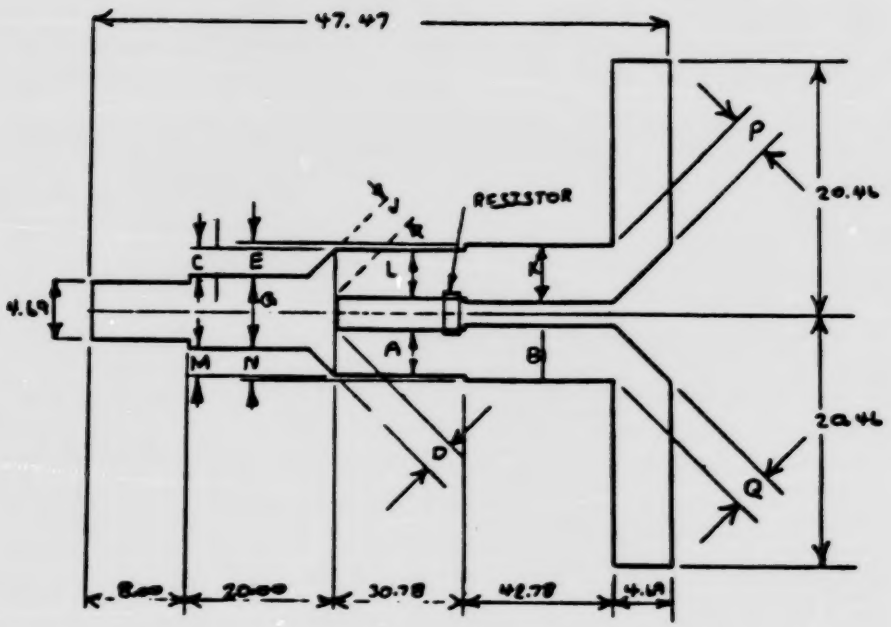

Figure 3-11 Power Divider Layout for K1 to K10 and K24 to K27

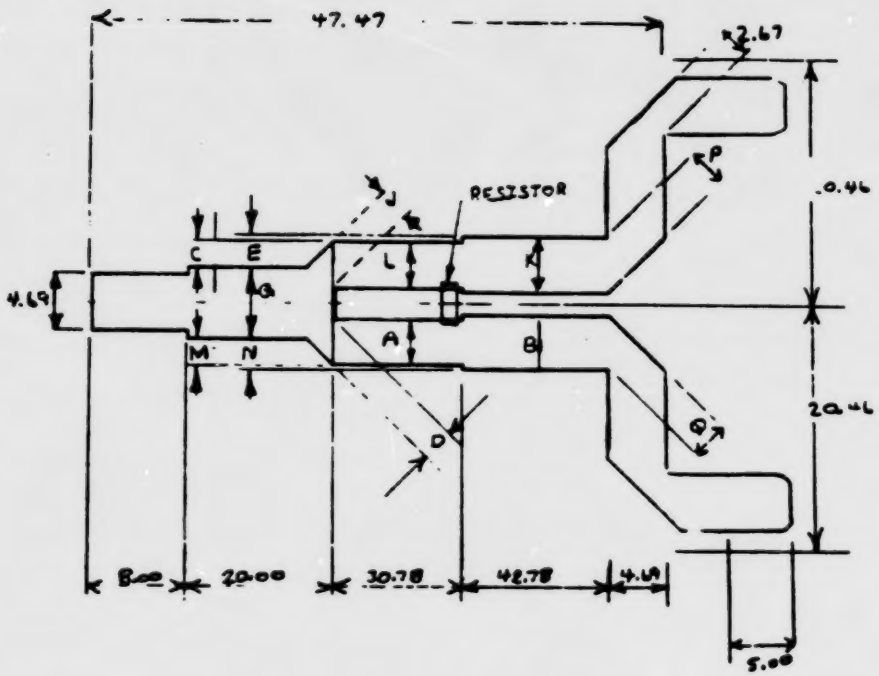

Figure 3-12 Power Divider Layout for K11 to K23

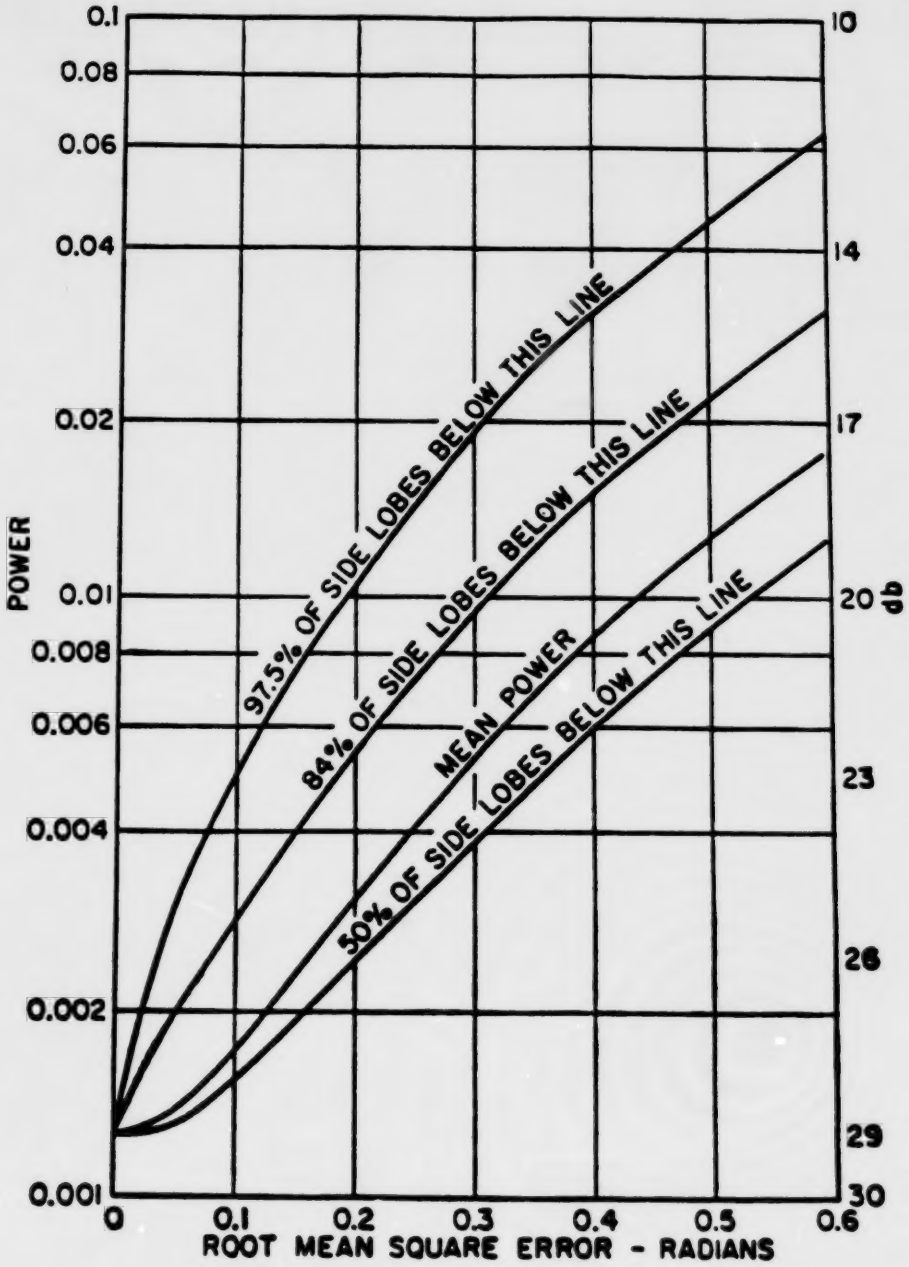

Figure 3-13 Statistical Sidelobe Distribution Resulting from Array Errors

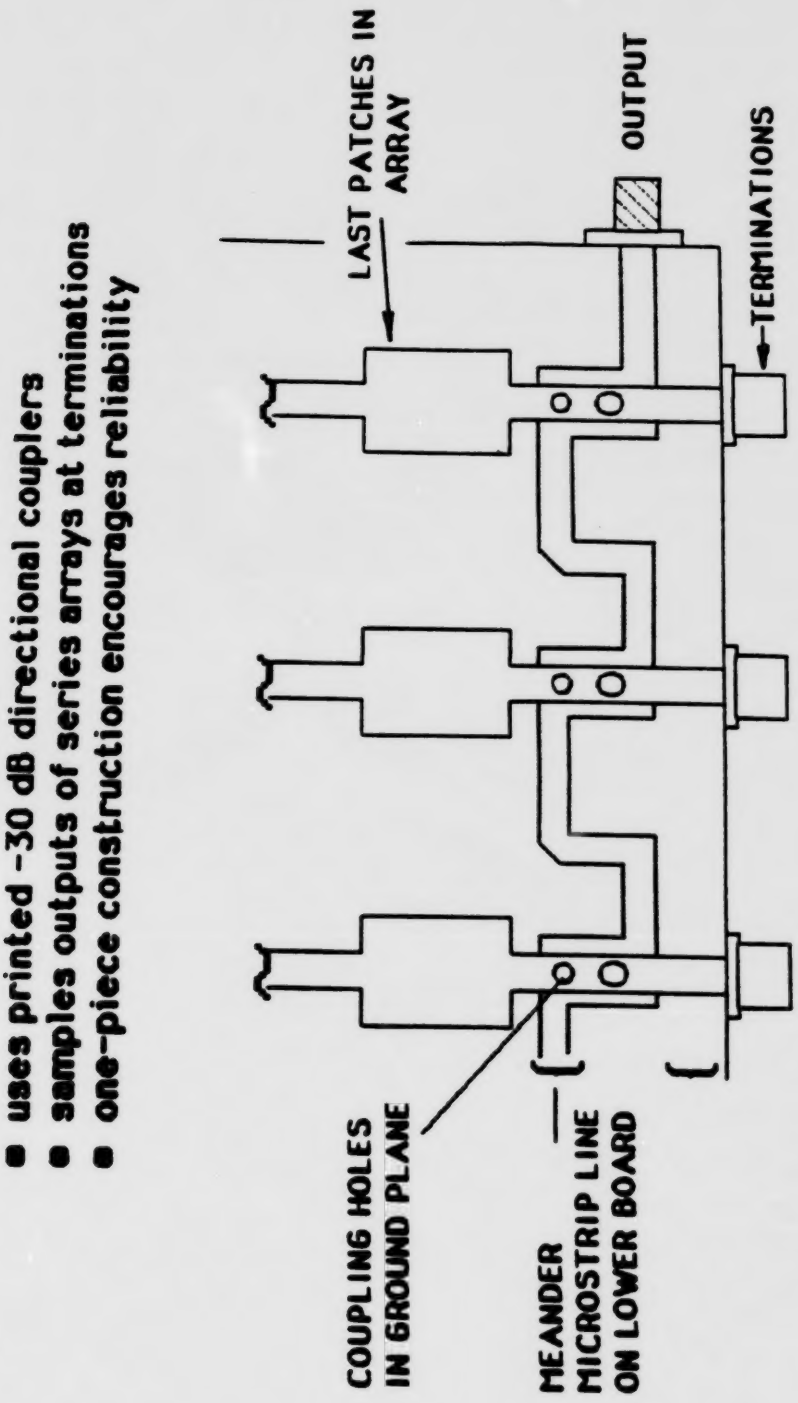
uses printed -30 dB directional couplers
samples outputs of series arrays at terminations
one-piece construction encourages reliability
LAST PATCHES IN ARRAY
OUTPUT
TERMINATIONS
COUPLING HOLES IN GROUND PLANE
MEANDER MICROSTRIP LINE ON LOWER BOARD

Figure 3-14 Proposed Integral Monitor

Element	Excitation Volts	Power dB	Normalized Power dB
27 + 28	1.555	0	7.791
26 + 29	1.548	-0.04	7.721
25 + 30	1.535	-0.12	7.584
24 + 31	1.515	-0.24	7.381
23 + 32	1.490	-0.39	7.120
22 + 33	1.458	-0.59	6.804
21 + 34	1.422	-0.83	6.443
20 + 35	1.380	-1.11	6.042
19 + 36	1.334	-1.43	5.612
18 + 37	1.284	-1.79	5.161
17 + 38	1.230	-2.20	4.695
16 + 39	1.173	-2.66	4.224
15 + 40	1.112	-3.17	3.761
14 + 41	1.048	-3.72	3.307
13 + 42	0.982	-4.34	2.872
12 + 43	0.915	-5.00	2.465
11 + 44	0.848	-5.72	2.090
10 + 45	0.781	-6.48	1.752
9 + 46	0.716	-7.29	1.455
8 + 47	0.654	-8.13	1.200
7 + 48	0.596	-8.98	0.987
6 + 49	0.544	-9.81	0.815
5 + 50	0.498	-10.59	0.680
4 + 51	0.459	-11.28	0.581
3 + 52	0.428	-11.82	0.513
2 + 53	0.406	-12.16	0.474
1 + 54	0.393	-12.28	0.461

Table 3-1 Corporate Feed Distribution

Divider Number	Division Number	Ratio Voltage	Zo_1	Zo_2	Zo_3	Zo_4	Zo_5
K1	1.000	1	42.05	59.46	59.46	50	50
K2	2.618	1.618	40.89	98.93	37.79	63.60	39.31
K3	3.840	1.960	39.88	122.8	31.99	69.99	35.72
K4	1.290	1.136	41.96	67.67	52.46	53.29	46.92
K5	1.825	1.351	41.58	81.23	44.51	58.16	43.02
K6	1.815	1.347	41.59	80.99	44.62	58.04	43.08
K7	1.964	1.401	41.46	84.50	43.03	59.19	42.24
K8	1.095	1.046	42.03	62.24	56.84	51.15	48.88
K9	1.182	1.087	42.01	64.70	54.74	52.13	47.95
K10	1.292	1.137	41.96	67.73	52.42	53.31	46.90
K11	1.018	1.009	42.04	59.99	58.93	50.22	49.78
K12	1.037	1.018	42.04	60.55	58.39	50.46	49.55
K13	1.056	1.028	42.04	61.12	57.87	50.69	49.32
K14	1.077	1.038	42.04	61.72	57.31	50.94	49.08
K15	1.099	1.048	42.03	62.35	56.74	51.19	48.83
K16	1.123	1.060	42.03	63.04	56.13	51.47	48.57
K17	1.151	1.073	42.02	63.83	55.46	51.79	48.27
K18	1.179	1.086	42.01	64.62	54.81	52.10	47.98
K19	1.204	1.097	42.00	65.31	54.25	52.38	47.73
K20	1.216	1.103	41.99	65.65	53.99	52.51	47.61
K21	1.198	1.095	42.00	65.15	54.38	52.31	47.79
K22	1.132	1.064	42.03	63.29	55.91	51.57	48.47
K23	1.028	1.014	42.04	60.29	58.65	50.35	49.66
K24	1.420	1.192	41.88	71.13	50.09	54.58	45.80
K25	1.463	1.210	41.86	72.24	49.38	54.99	45.46
K26	1.171	1.082	42.01	64.39	54.99	52.01	48.07
K27	.469	.685	41.32	41.44	88.37	41.38	60.42

Table 3-2 Split-Tee Power Dividers Design Values

4.0 MECHANICAL DESIGN

4.1 Breadboard Antenna

Mechanical design aspects for the breadboard antenna were limited to the array support structure and test range interfaces. Two features were considered of paramount importance; to provide an accurate and rigid support for the printed arrays and corporate feeds and to permit the possibility of further expansion.

The basis of the support structure is a welded aluminum tube space frame, this has mounting pads on front, back and bottom for connection to arrays, corporate feeds and test range positioner. The pads were machined after welding to lie in planes with an accuracy of ±0.010". Three printed circuit boards form the radiating arrays, each with 18 elevation arrays. These are mounted on weight-relieved ¼" alloy plates which in turn bolt to the front pads. Two corporate feed networks are housed in two screened boxes which screw to the back pads. The bottom pads effect a connection with the test range positioner via a simple interface fixture which can be seen in Figure 5-4.

To permit the possibility of further work with the inclusion of phase shifters, machined areas are provided in appropriate positions to the rear of the structure, above the corporate feeds.

All microstrip test pieces and the arrays were fabricated by a conventional photographic-resist and etch process and used OAK-605 material. This laminate is available in sheets up to 1219 mm x 914 mm and has the following properties.

- woven glass and PTFE dielectric
- 1 oz copper clad both sides
- dielectric constant 2.33
- dielectric thickness 1.57 ± 0.05 mm
- loss tangent 0.0015 at 10 GHz

4.2 Study of Mechanical, Thermal and Structural Design

Antenna mechanical requirements are stringent and a very high reliability is necessary. Environmental conditions encompass a full range of precipitation, temperature and jet-blast. In common with all equipment which stands close to a runway, the property of frangibility is critical.

There are two structural forms which are currently used to build microstrip antennas, these are illustrated in Figure 4-1. In the first the microstrip antenna is printed on to one side of a double sided copper-clad laminate. The reverse side forms the antenna's ground plane. This laminate is then supported by a separate mechanical stiffener which may be one of many forms. In figure 4-1a it is shown as a classic composite sandwich which is the approach suggested in the case of the MLS antenna. Other variants are simple metallic supports or unfurlable structures such as the tetrahedral truss for use with spacecraft antennas. In many cases, the mechanical support may be part of an aircraft of ground vehicle where the antenna requirements are often subservient to those of the carrier.

The second variant, Figure 4-1b is one favoured for spacecraft use, but is only useful at compartively low frequencies, perhaps up to 2 GHz where the antenna's dielectric layer is sufficiently thick to be of structural use in a sandwich configuration. A material of low dielectric constant is used such as polyimide honeycomb or a low density foam. This, in conjunction with carefully chosen face-skins can provide excellent electrical and mechanical properties. Further sandwich layers of transmission line can be built behind the radiating section to provide power distribution, separation of polarization or the division of power into element sub-arrays. These layers can be used to form the mechanical backbone of the antenna and the resulting structure can be highly optimized from both electrical and mechanical viewpoints, With current technology however, this method is expensive to construct and is not considered viable for MLS.

To build an antenna of the size required (1150 mm high and 1950 mm wide) with a reasonably small number of printed panels, large sheets are required which are currently only available in PTFE based laminate. PTFE is widely used as a dielectric in microstrip applications, at 5 GHz it's electrical loss is reasonably low (even for transmission line lengths in the order of 1m as dictated by the MLS application). This material has two undesirable properties which affect both electrical and mechanical design aspects.

i) a "glitch" in the otherwise reasonably linear, negative, slope in the dielectric constant-temperature characteristic;

ii) a tendency to flow or "creep" under stress.

Normally, both of these characteristics are controlled by laminate manufacturers by incorporating glass-fibres into a PTFE matrix. Alternative materials are now becoming available such as fluoropolymers which do not have glitch but which also require stabilization. Currently, two basic forms of glass are used - woven and random fibres - and each imparts different characteristics to the laminate. Measured dielectric constant versus temperature is plotted for a number of samples in Figure 4-2. It appears that the manufacturers claim that random fibres in PTFE do reduce variations with temperature and the magnitude of the "glitch" is justified.

Mechanical characteristics of the PTFE are apparently "improved" by the glass reinforcing, that is, the modulus and stability are increased and the thermal coefficient of expansion is reduced. Manufacturing techniques and quality control procedures are such that very stringent specifications on dielectric constant are available; for example, on a typical value of between 2.3 and 2.8 (depending on type), tolerances of ±0.1 are offered. There are no equivalent guarantees on the mechanical properties and the onus is with the user to ensure that worst case conditions have been forseen.

With large antennas and particularly with series arrays which are sensitive to dielectric and dimensional changes and which have relatively narrow RF bandwidths, it is vital to control all influences or to limit their effects. RF design techniques can consider such variables as dielectric constant and dimensional changes with temperature, provided they are known. For the structural type of Figure 4-1a, comprising a printed antenna on a supporting substrate, there is an elegant and cost-effective solution which makes the best use of commercially available materials, their properties and fabrication techniques. The supporting substrate, for example, must have the following properties:

- known coefficients of expansion in azimuth and elevation directions;
- low coefficients of expansion;
- modulus of elasticity much greater than that of the laminate.

It is evident that a sandwich structure using Graphite Fibre Epoxy Composites (GFEC) fulfils these requirements.

Construction details of the proposed MLS azimuth antenna are illustrated in Figure 4-3. As suggested above, the printed antenna board is bonded to a GFEC-honeycomb-GFEC sandwich; the honeycomb material is aluminum to enhance front-to-back thermal conductivity.

A choice of GFEC face skins is available, in this case, a dual layer of woven and unidirectional fibres have been chosen. Woven fibres can impart a small positive Thermal Coefficient of Expansion (TCE) to the composite while unidirectional fibres can be arranged to have a near-zero TCE. It can be shown that, in the elevation direction, a small positive TCE can assist in compensating for the negative slope of dielectric constant versus temperature and this feature (structural compensation) can be used in the RF design and synthesis procedure.

In the azimuth or scan direction, a zero TCE is demanded by the strict requirements on beam angle and this is provided by a parallel lay of unidirectional fibres. This is similar in concept to the practice of using INVAR ties along the back of a conventional waveguide antenna but the GFEC is significantly less massive.

The antenna is exposed to the full range of outdoor ambient conditions, temperatures from -50°C to +50°C (+65°C in some specifications). While the radome affords some basic protection, antenna heating is implictly forbidden by civil MLS specifications since the antenna's reliability must be considered to include the heater failure rate and modes. The antenna, therefore, sees the full ambient through the radome with the certainty of very different inputs between front and back. Because of the small, but non-zero TCE of the face skins, their temperatures should remain similar, the conductivity of the aluminum honeycomb is assisted by front and back layers of thermal control insulation. Additional "half-sandwiches" of polyimide and KAPTON as shown in Figure 4-3 may perform this function, but alternatively a closed cell foam can be used.

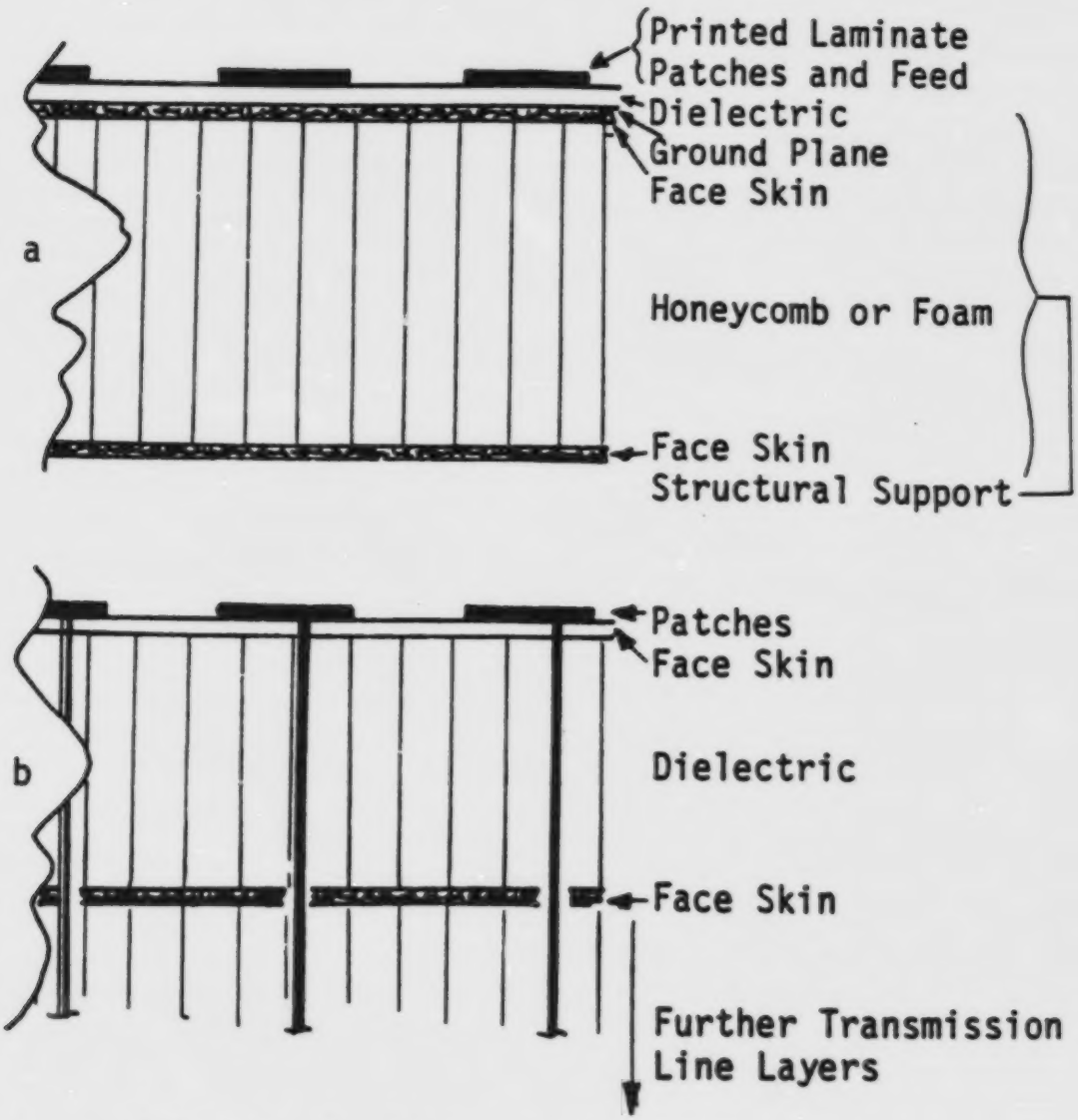

a. printed laminate supported by a structural substrate
b. sandwich structure with common electrical-mechanical central dielectric

Figure 4-1 Two Structural Types

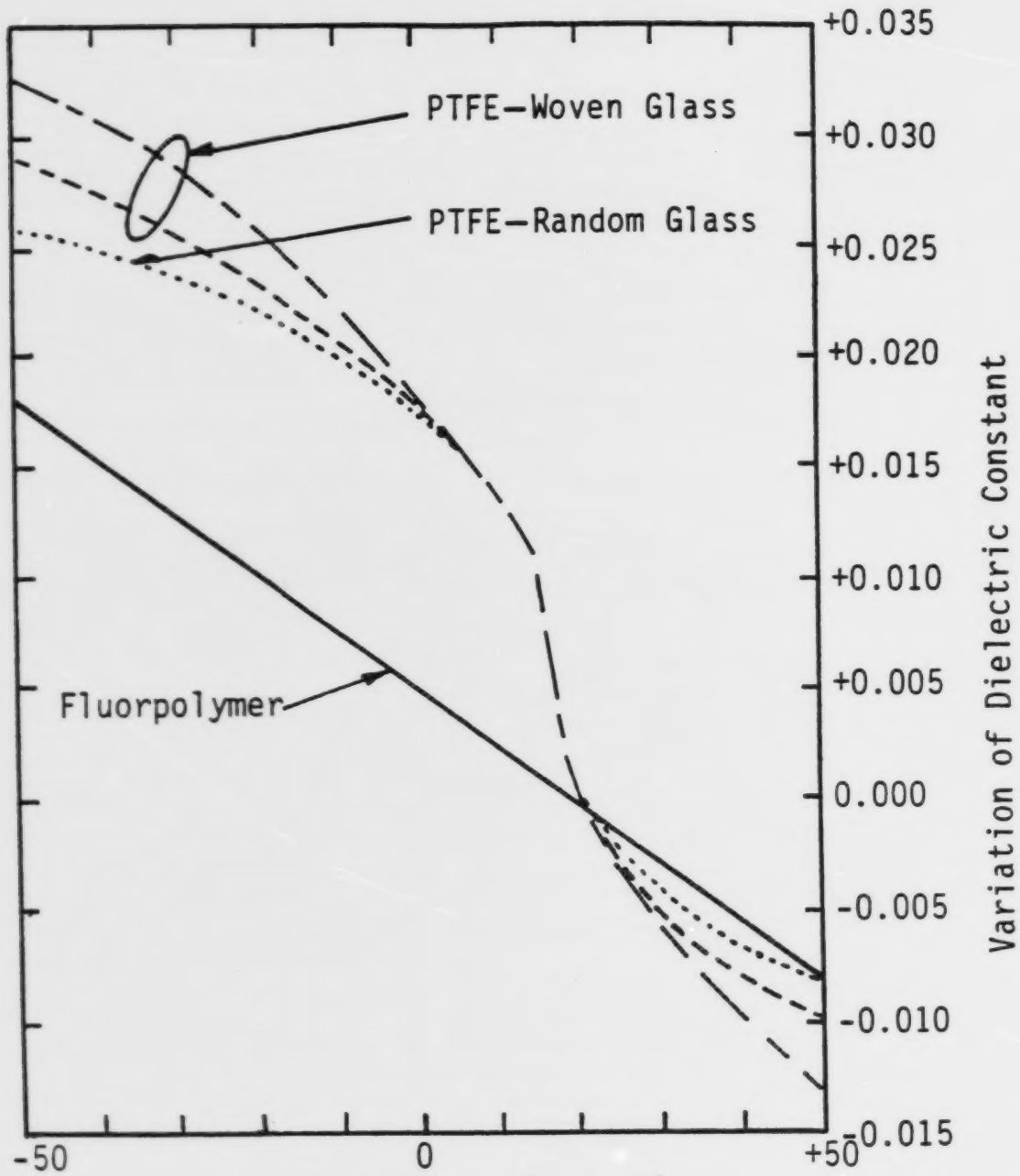

Figure 4-2 Variation of Laminate Dielectric Constant with Temperature

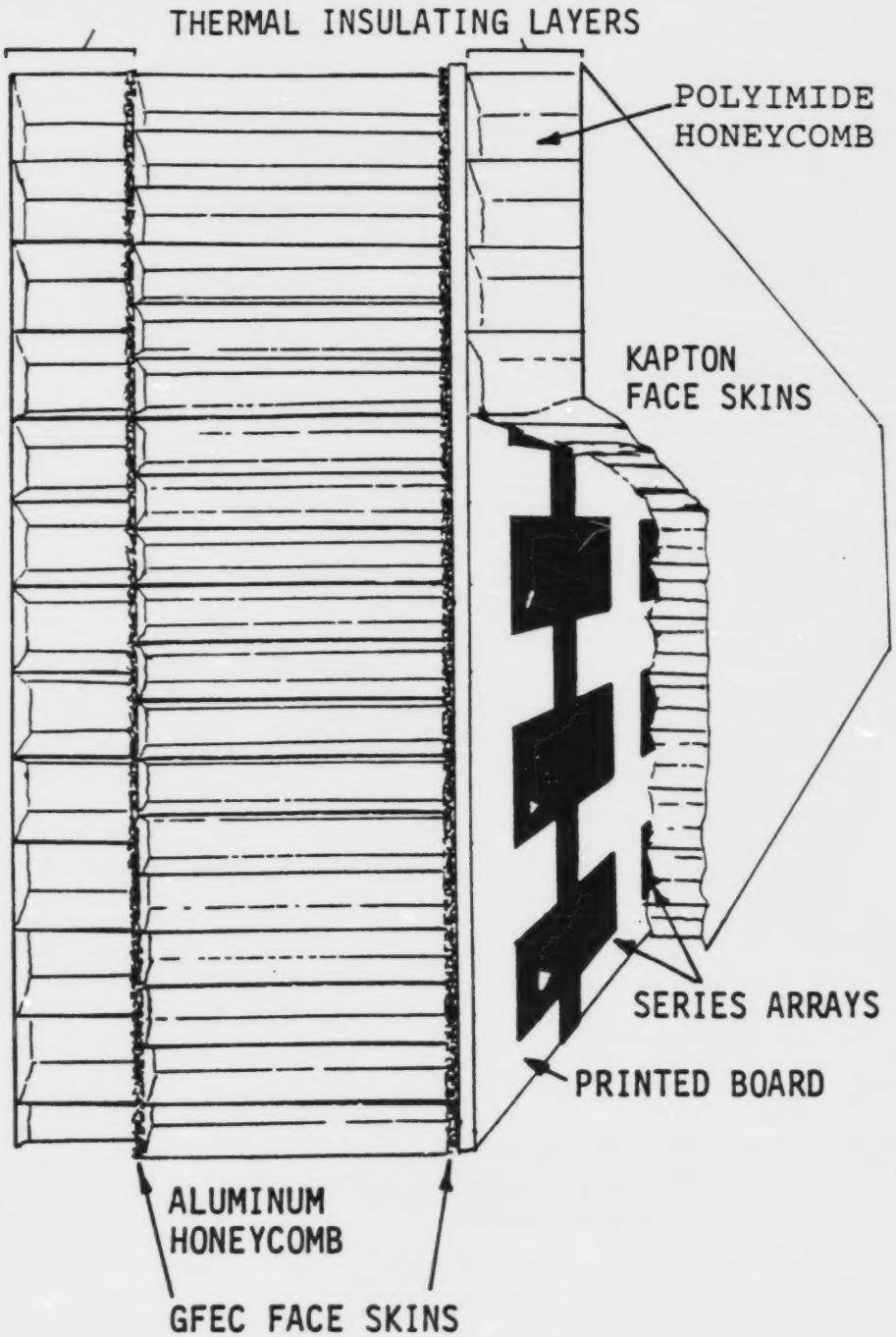

Figure 4-3 Proposed Construction of MLS Azimuth Antenna

5.0 TEST PLAN

No formal test plan or procedure was required by this program, to engender a better understanding of the results the test articles; components, array and corporate feed and the test arrangements used are summarized in the sub-sections below. The sequence of tests conducted throughout the programme is illustrated in Figure 5-1, which shows the tests in the actual order in which they were conducted.

Single patches with a range of patch dimensions were first characterized to determine the patch extensions or "end effects".

Short arrays of six patches in a series configuration were then measured to confirm the calculated propagation velocity and patch impedances.

A full length single linear array was then constructed and tested for insertion loss and insertion phase. Elevation radiation patterns were measured at mid-band and band edges, 5.03, 5.06 and 5.09 GHz.

A set of four arrays were then constructed, at the design azimuth spacing and impedance, mutual coupling, insertion loss and phase and elevation radiation patterns were checked.

As a preliminary to integrating the complete antenna, the 54-way microstrip corporate feed was manufactured and tested. Some select-on-test adjustment was performed to equalise the phase and amplitude distribution of the output ports.

The antenna array which comprises three identical printed arrays was then assembled and subjected to impedance and transmission measurements. During the phase transmission tests it was discovered that there was some variation in terminal phase. To accommodate the test schedule and to ensure that the antenna had azimuth sidelobes within specification, the series elements were patched with varnish to arrive at a more uniform terminal phase. Full radiation pattern and gain tests then followed integration with the corporate feed.

Finally a further complete antenna was assembled incorporating arrays printed on laminate with a more controlled dielectric constant. No "patching" was employed and the antenna was subject to a full set of tests.

A test procedure was issued for this final test, this was used in draft form during the tests and red-lined where appropriate.

5.1 Test Articles

The following items were subject to various RF tests both as part of the design process and as tests on the finished antenna. They are shown on the figures tabled below.

	ITEM	FIGURE NO.
a	single microstrip patches	5-2
b	short linear array pairs	5-2
c	single linear array	5-2
d	quad linear array	5-2
e	corporate feed	5-3
f	antenna array	5-4
g	MLS antennas 001 and 002	5-4

Table 5-1 Test Articles

All microstrip test pieces and the arrays were fabricated by a conventional photographic-resist and etch process and used OAK-605 material.

5.1.1 Configuration of the MLS Antenna

For final performance tests of radiation pattern and gain the antenna arrays 001 and then 002 were integrated with the corporate feed and support frame. Antenna 002 is depicted in Figure 5-4.

Since the MLS antenna was to be tested with its azimuth beam at both the straight-ahead (boresight) and at one squint angle, two sets of rigid cables were fabricated for connecting the corporate feed to the series arrays. For the boresight beam, the cables are all of equal length. A squint angle of 38.96 degrees was chosen as being close to the maximum required (±40°) and needing incremental phase shifts of 45° between adjacent elevation arrays. This way only eight different lengths are required which simplified cable fabrication and test.

5.1.2 Configuration of Intermediate Test Pieces

Figure 5-2 shows the layout of the microstrip test pieces used to determine patch characteristics and for measurements on reduced size arrays. The corporate feed circuitry is shown pictorially in Figure 5-3, note that the full, 54 way, power splitter used in the final configuration employs two such corporate feeds and a commercial two way coaxial divider.

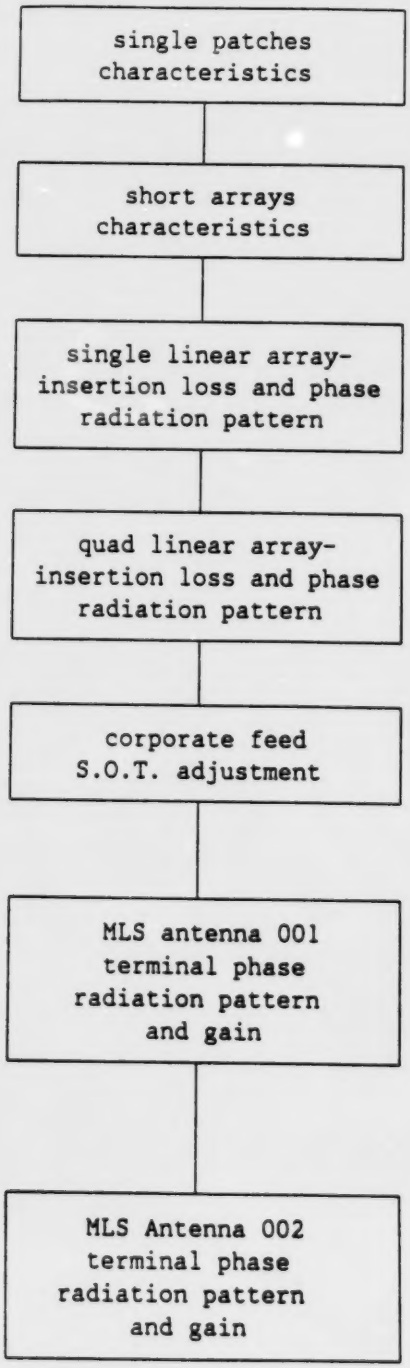
single patches characteristics
short arrays characteristics
single linear array-insertion loss and phase radiation pattern
quad linear array-insertion loss and phase radiation pattern
corporate feed S.O.T. adjustment
MLS antenna 001 terminal phase radiation pattern and gain
MLS Antenna 002 terminal phase radiation pattern and gain

Figure 5-1 Test Sequence

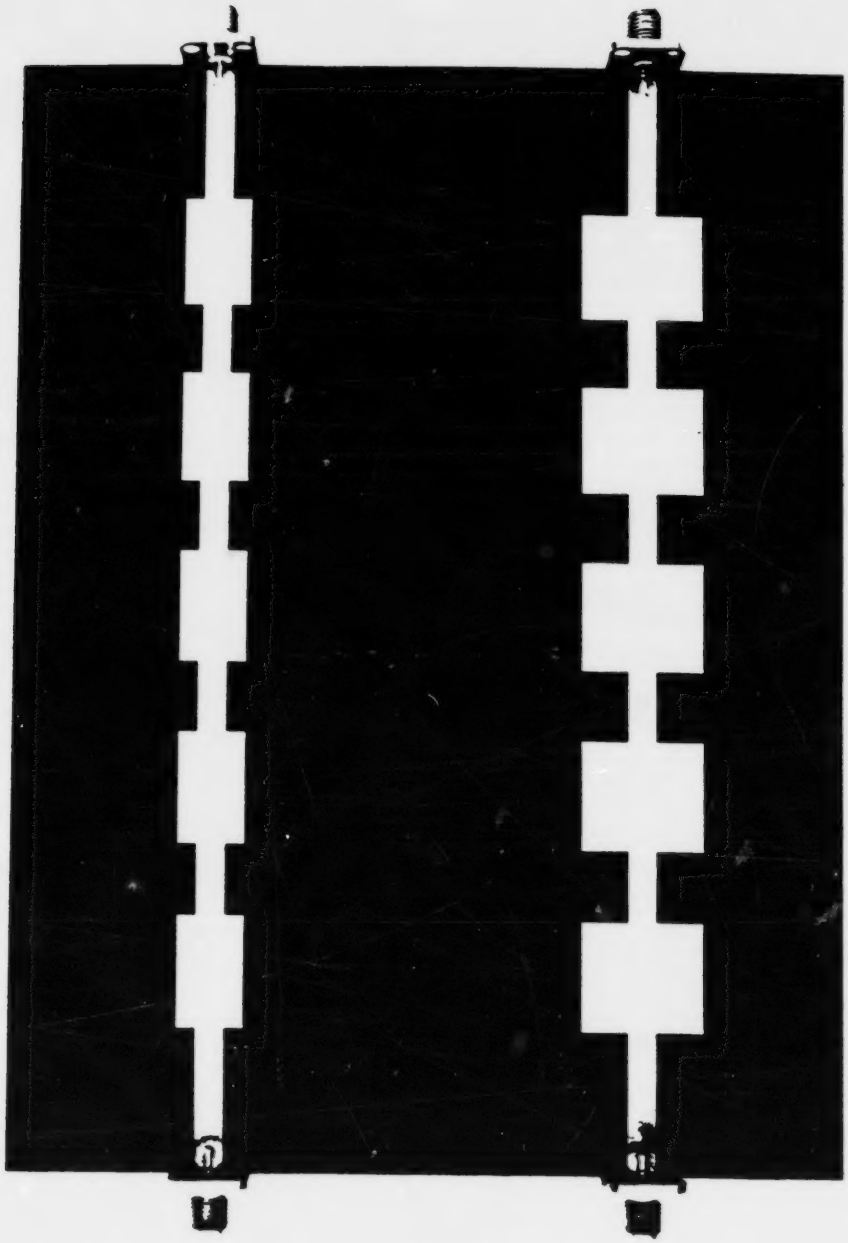

Figure 5-2 Early Test Pieces

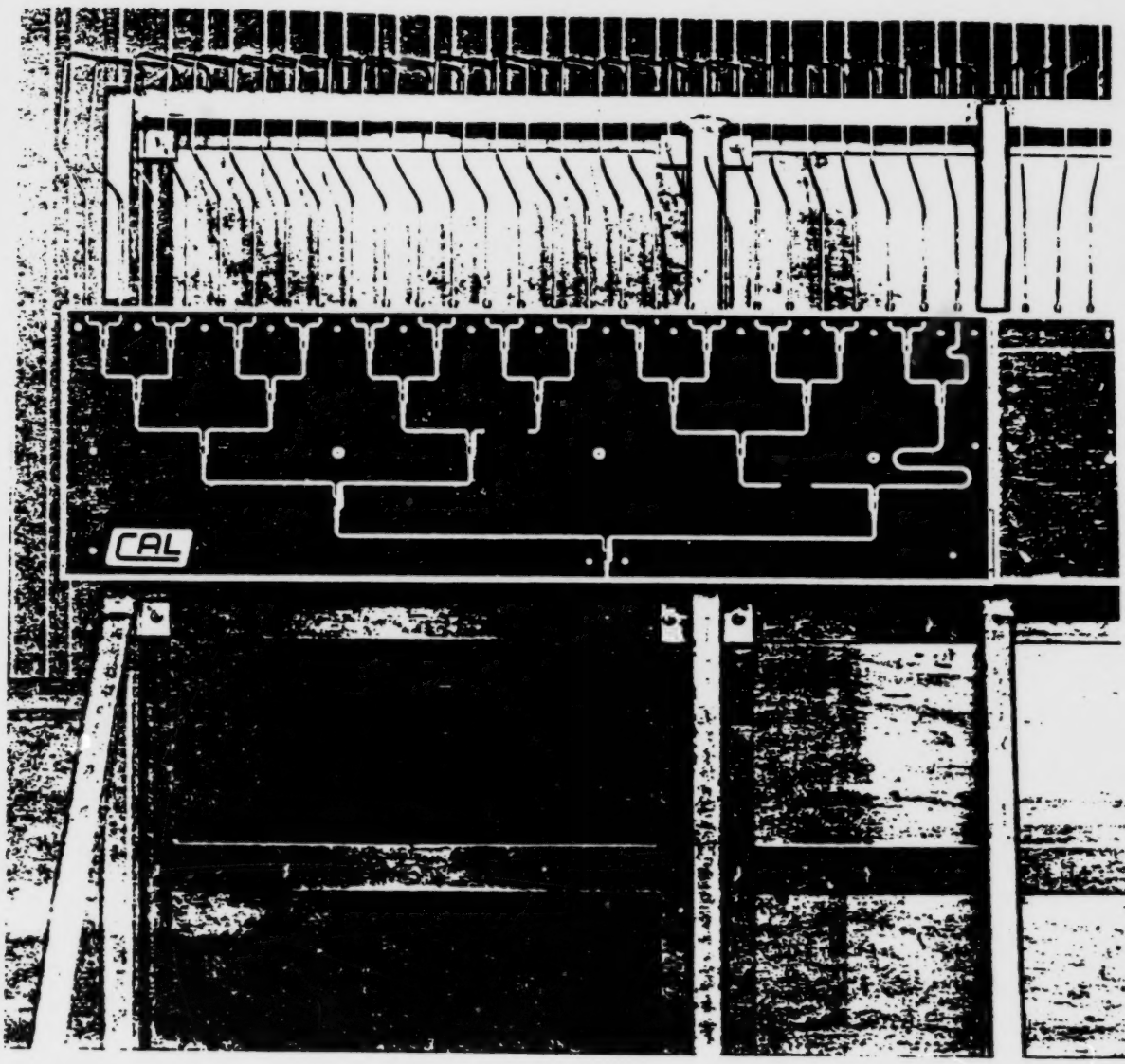

Figure 5-3 Corporate Feed

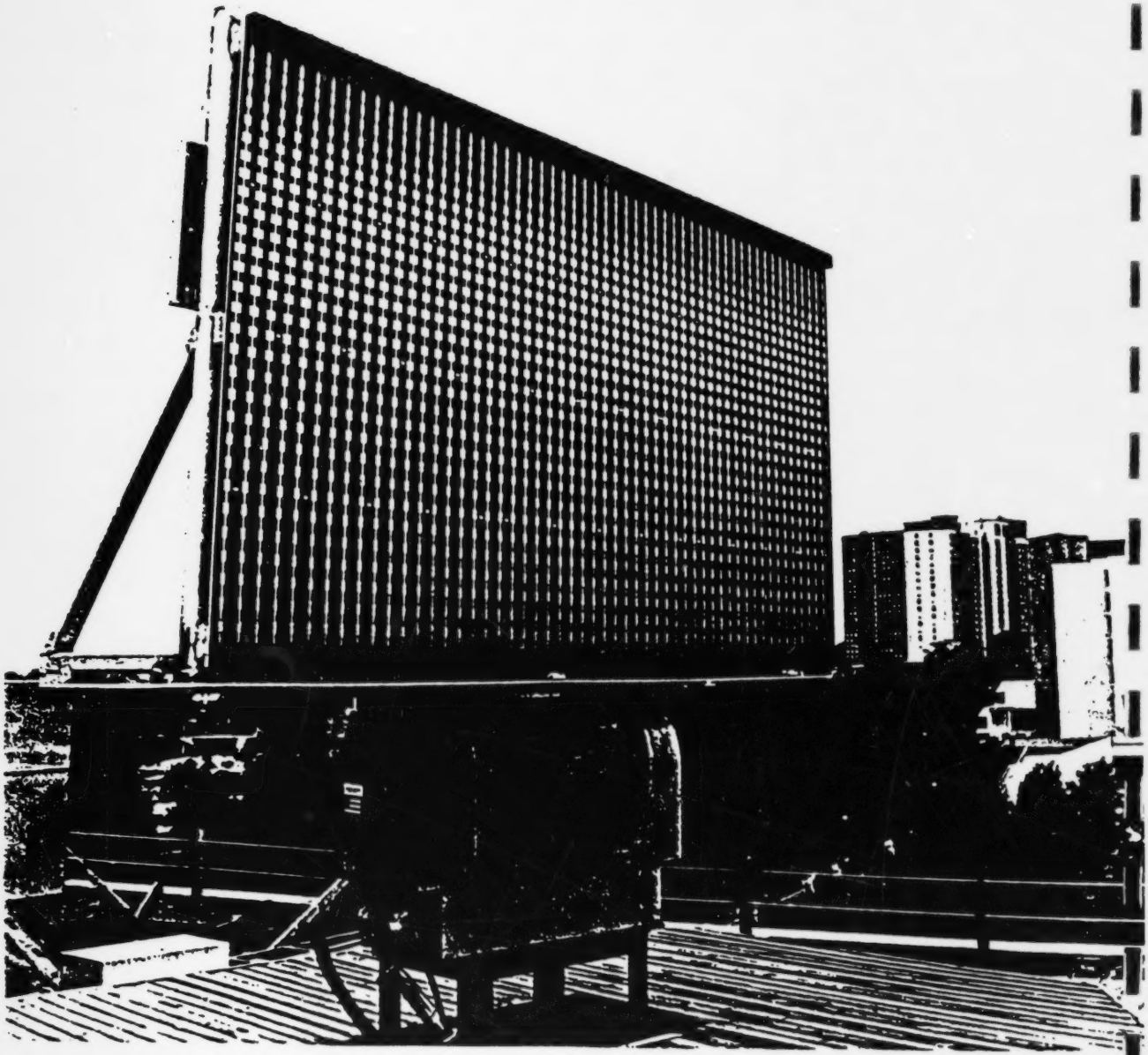

Figure 5-4 Complete MLS Antenna on NRC Test Range

5.2 Test Equipment

Two types of test were made, bench tests on transmission and reflection properties and radiation pattern and gain. For bench tests, a Hewlett Packard 8409C Automatic Network Analyzer (ANA) was used at CAL. Radiation pattern and gain of antenna 001 were measured at the Communications Research Centre (CRC) test facility known as the David Florida Laboratory (DFL) at Shirley Bay, Ottawa.

Radiation pattern and gain of antenna 002 was measured at the National Research Council NRC, Ottawa, test range. This range has recently been commissioned and is fully automated with a desktop computer controller. It has a 300 yard length and a good vertical section. A functional diagram and layout of the range is presented in Figure 5-5.

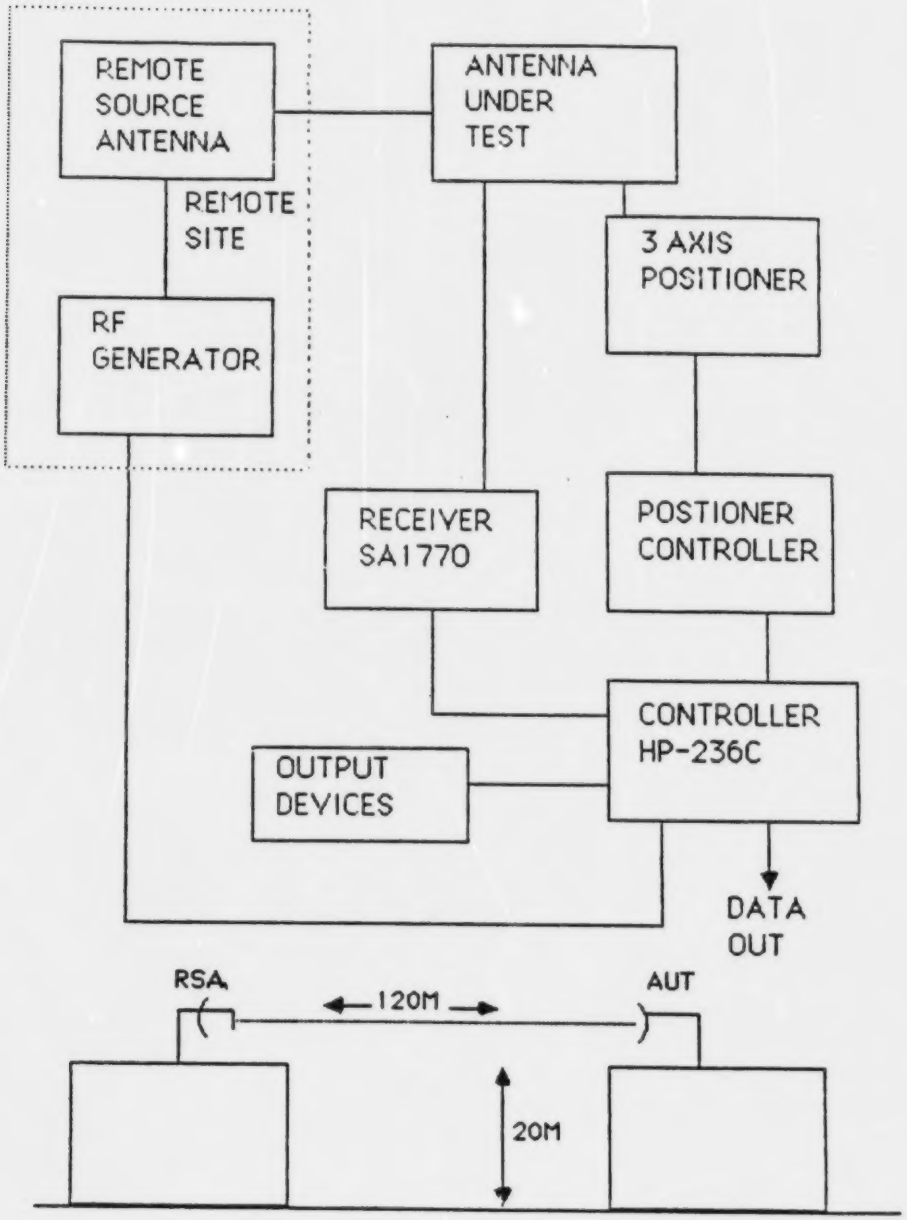

Figure 5-5 Equipment and Physical Layout of NRC Facility

6.0 TEST RESULTS AND DISCUSSION

Following the evolution of the antenna design and test, the following test results are presented and discussed.

- radiation conductance and extensions of single patches
- tests on quadruple array
- corporate feed tests
- measurements on antenna 001
- measurements on antenna 002

A considerable number of radiation patterns were acquired for antennas 001 and 002 and these are contained in an appendix at the end of this report.

6.1 Characteristics of Single Patches

Transmission line extension for a range of patch widths from 7.8 mm to 20.5 mm are shown graphically in Figure 6-1. These extensions are in effect, how much extra line appears electrically, in excess of the physical length. Accurate determination of these extensions is critical since they directly influence the phase characteristics and thus the radiation pattern of a series array. As may be expected, the extensions Δ_1 and Δ_2 at the source end and load end respectively are not influenced by patch spacing but only by patch width. The widest patch creates a total extension of around 1.5 mm which represents a phase of nearly 10° at the MLS frequency.

Radiation conductance g is shown in Figure 6-2 as a function of patch width and with patch spacing as a parameter. Here both variables have a significant effect, conductance varies over a 100:1 range with a 3:1 change in width. A sharp change in conductance is also evident between the case of a single patch, identified as having infinite spacing and patches with typical spacings.

6.2 Quadruple Array

Test on this article were especially important since the verification of two principles was at stake, these being the accuracy of the single patch characteristics and the underlying assumption that the influence of coupling between the series arrays was negligible. Additionally, this test validates the design process and design software.

Figure 6-3 is an elevation radiation pattern at centre frequency, 5.06 GHz, of the quad array. Superimposed on this is the predicted elevation array factor, the general similarity down to the -20 dB level indicates the success of the design process. Most importantly, since this was the most difficult parameter to meet, is the match of the predicted and measured slopes in the vicinity of the horizon. The horizon angle would normally be chosen after full analysis of the measured results but it will normally lie between the -5 dB and -10 dB points on the right hand side of the pattern.

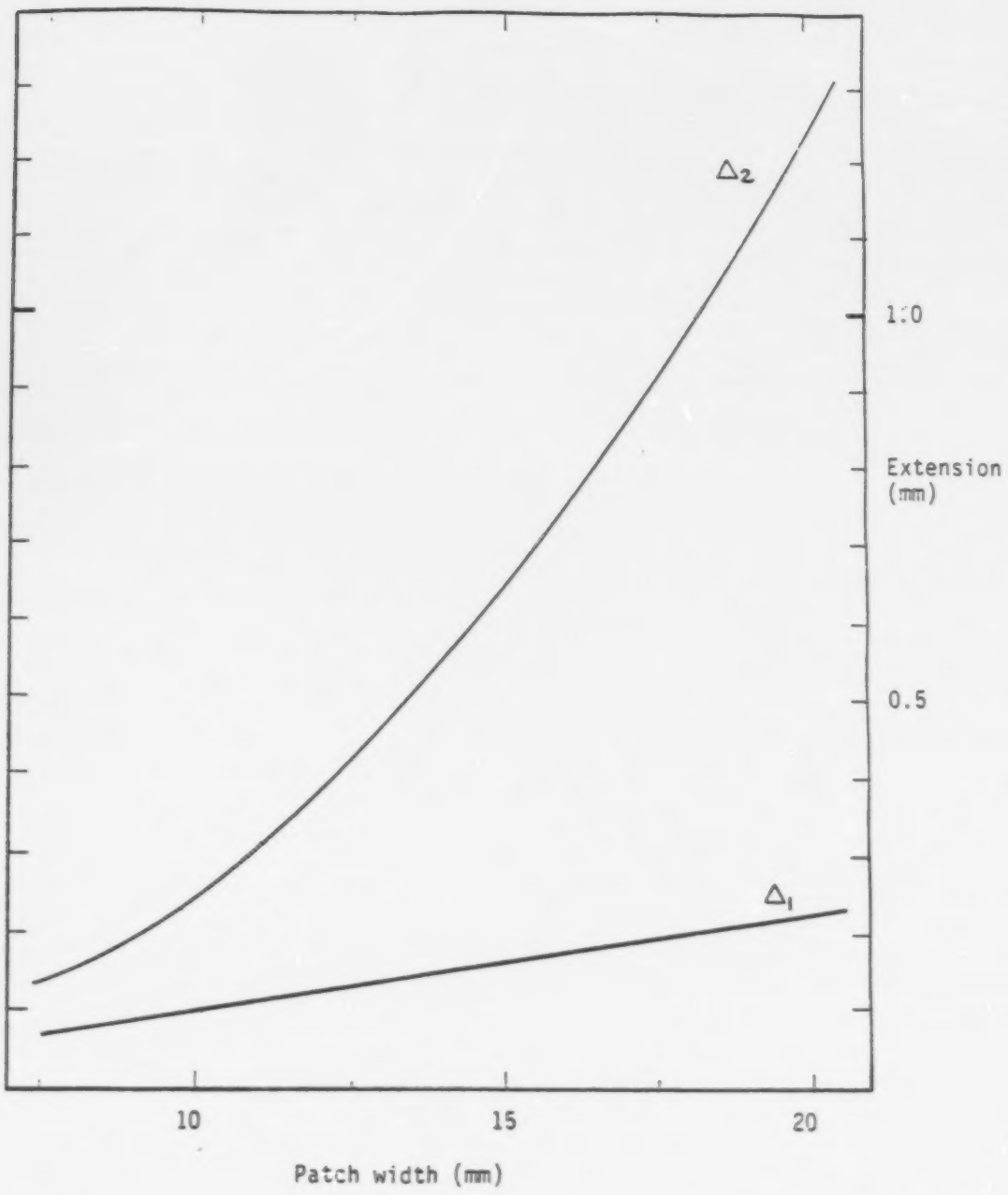

Figure 6-1 Transmission Line Extension

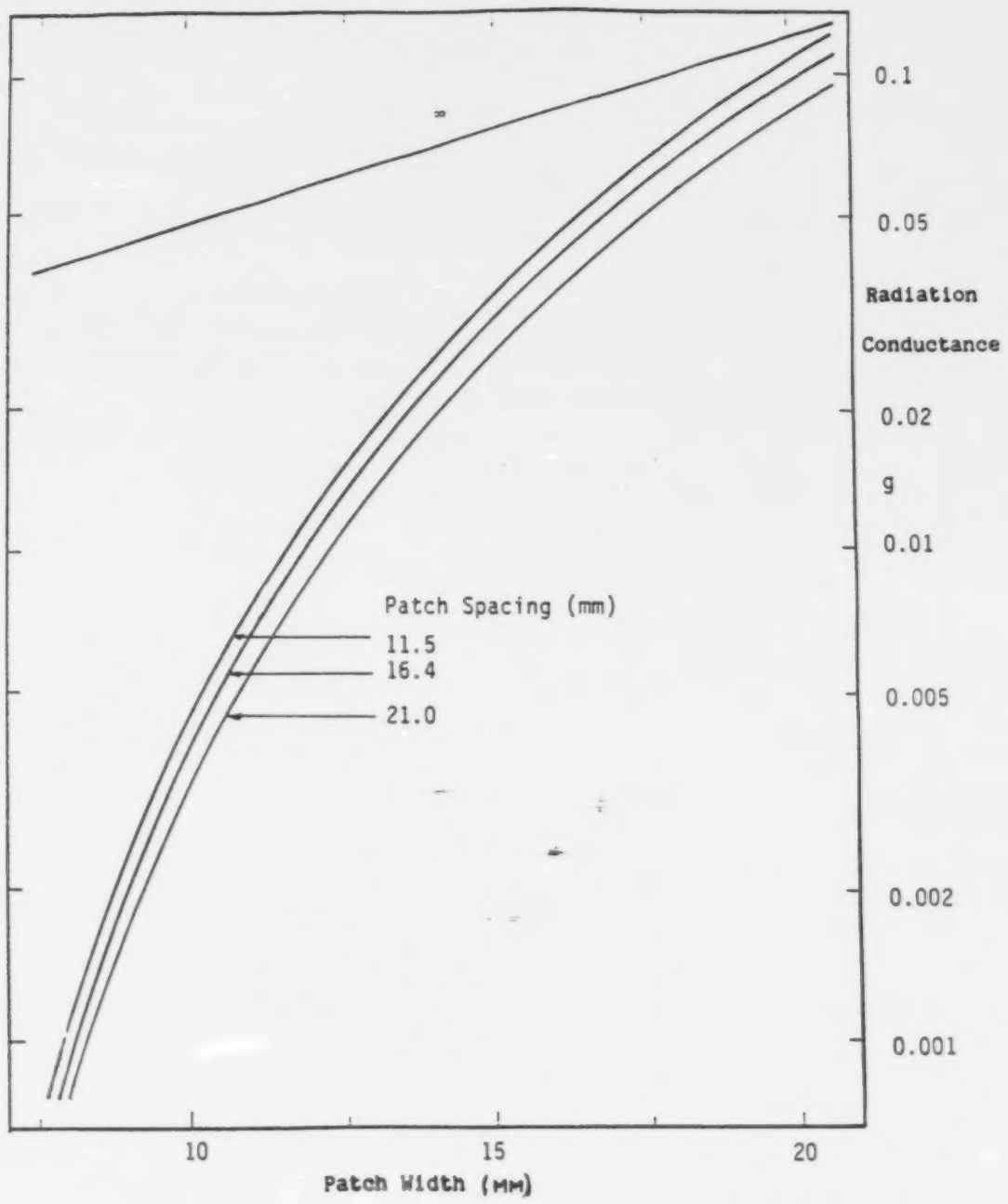

Figure 6-2 Radiation Conductance as a Function of Patch Width and Spacing

Some narrowing of the measured pattern can be seen in comparison to the predicted array factor. One of the unknowns in array design is the radiation pattern of an "immersed" element. In isolation the pattern of most element types can be calculated to a high degree of accuracy, the act of placing an element in an array of identical elements usually places the calculation of its immersed properties beyond the scope of current antenna technology. This is particularly true of microstrip elements. Generally, an immersed element will couple to adjacent elements and its impedance and radiation properties will be affected. With microstrip elements this coupling occurs via the following paths:

- through the interconnecting transmission lines
- radiation mode coupling in the front hemisphere
- in surface waves trapped in the dielectric

Only the first item is accounted for by measurements of radiation conductance as described in the previous section. Coupling via radiative and surface modes are best investigated by measurements of radiation performance. The principal noticeable effect in Figure 6-3 is in a narrowing of the elevation pattern; this may be safely attributed to a significant increase in element directivity when immersed in the array. Such an increase has the effect of narrowing the apparent element beamwidth which in turn narrows the array pattern.

6.3 The Corporate Feed

This comprises two 27 way microstrip power divides which are joined with a commercial 2:1 splitter. It is the results of the tests on the two 27 way dividers both before and after phase trimming that are the subject of this section. Results are in terms of the 54 outputs divided into two sections which represent the "mirror image" left and right hand dividers.

Table 6-1 lists the measured output phases and amplitudes before and after phase adjustment by means of the trimming stubs (Section 3.3). These stubs were included to enable the 54 outputs to be phase equalised in the presence of irregularities within the dividers. In a real system such a procedure would be unnecessary as phase differences would be measured during equipment tests and taken out by the phase shifter settings. This experiment did not include phase shifters and so trimming was essential but detrimental to the amplitude accuracy.

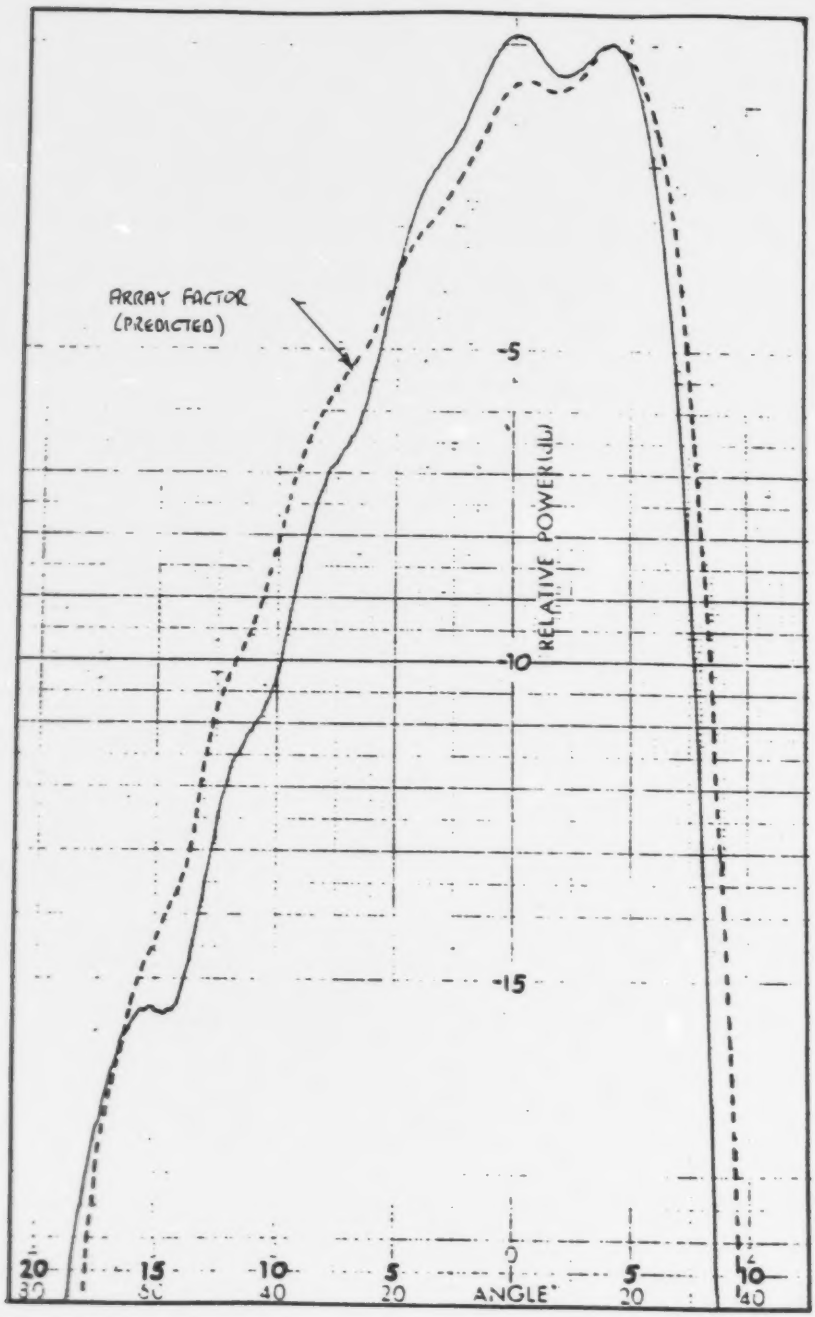

Figure 6-3 Radiation Pattern in Elevation Plane of Quadruple Series Array

	DIVIDER NO 1			DIVIDER NO 2		
Port Number	Phase< Before Tuning (deg)	Phase< After Tuning (deg)	Amp After Tuning (deg)	Phase< Before Tuning (deg)	Phase< After Tuning (deg)	Amp After Tuning (dB)
1	41	0	-11.7	0.	0.	-13.0
2	28	0	-11.6	- 9.5	4.	-12.7
3	28	0	-11.4	- 4.5	2.5	-12.5
4	26	0	-11.0	- 0.5	0.5	-12.0
5	59	-3	-10.1	- 2.	-1.5	-10.6
6	51	0	- 9.6	-10.	-0.5	-10.1
7	52	0	- 8.4	- 3.5	1.	-10.4
8	28	0	- 7.7	- 6	-3.4	- 9.5
9	44	0	- 8.0	- 6	-3.5	- 7.5
10	45	0	- 7.1	-18.2	-4.5	- 6.4
11	33	0	- 7.0	-12.	-1.	- 6.4
12	35	0	- 5.9	-18.	-5.	- 4.8
13	34	0	- 4.8	-20.	-5.5	- 5.7
14	40	0	- 4.4	-14.	-1.5	- 5.6
15	30	0	- 3.2	-11.	-7.	- 4.2
16	18	0	- 2.9	-10.5	-3.5	- 3.9
17	29	0	- 2.1	- 6.5	-2.	- 1.7
18	27	0	- 1.8	-11.5	-2.	- 1.2
19	28	0	- 1.7	- 2.	-2.5	- 1.9
20	31	+1	- 1.4	- 6.	-2.5	- 1.6
21	25	0	- 1.1	- 7.	-4.5	- 1.1
22	28	0	- 1.1	3.	-2.5	- 1.0
23	-8	0	- 0.5	12.5	-6.5	- 0.0
24	35	0	- 0.5	-15.5	-3.5	+ 0.15
25	26	0	- 0.3	-19.2	0.5	0. 0
26	30	0	+ 0.15	- 9.	2.5	- 0. 25
27	30	0	0.0	- 1.5	1.	0.0

Table 6-1 Corporate Feed, Phase and Amplitude

6.4 Antenna 001

This antenna was trimmed to obtain a more uniform phase transmission, table 6-2 summarises the results before and after trimming.

Antenna radiation patterns measured at the DFL test range are reproduced in Figures A-1 to A-21. Generally measurements were made at three frequencies, 5.03, 5.06 and 5.09 GHz with a range of angular scales and in azimuth and elevation directions. A limited set of azimuth plane patterns were taken with the beam squinted to approximately 40°.

6.5 Antenna 002

The use of a closer tolerance dielectric resulted in significantly greater uniformity of transmission phase, Table 6-4.

Radiation patterns, this time measured at the NRC test range are presented in Figures A1-25 to A1-36. Notably fewer patterns resulted from this test since data has been recorded digitally and plots of any scale may be produced as required or the data may be analysed by software.

This antenna was very successful, the azimuth and elevation patterns exhibit significantly improved sidelobe performance over antenna 001. The azimuth first sidelobes in particular are well below the -20 dB specification level thus giving a substantial margin for the effects of phase shifters bit quantization errors and temperature extremes.

Qualitative performance of this antenna can be assessed by means of the contour plot, figure 6-4. In particular, the azimuth sidelobes are regular and there is no evidence of spurious or grating lobes.

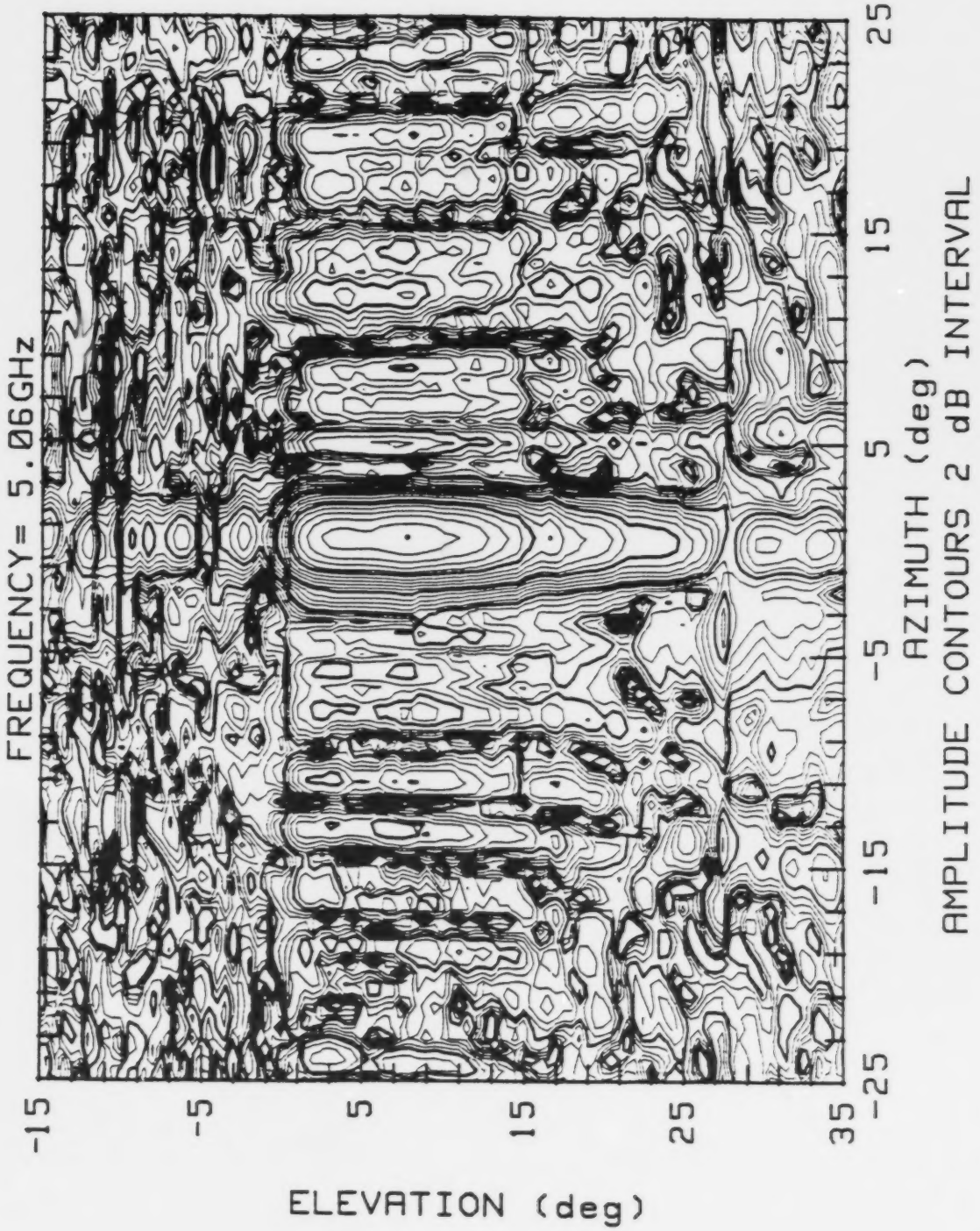

Figure 6-4 Contour Plot Radiation Pattern of Antenna 002, 5.06 GHz with beam on boresight

	BOARD NO.1		BOARD NO. 2		BOARD NO. 3	
ELEMENT	PHASE BEFORE	PHASE AFTER	PHASE BEFORE	PHASE AFTER	PHASE BEFORE	PHASE AFTER
1	0	0	0	-1.5	-1.5	- 2
2	-18	- 3	8	8	8.5	- 3
3	-35	- 2	4	3.5	- 2.5	- 2.5
4	-38	- 7	7.5	7	- 5.5	- 5
5	-23	- 2.5	- 7.5	-10.5	-10	-10
6	-39	- 5.5	20	9.5	24.5	9
7	-38	- 3.5	33.5	15	32.5	15.5
8	-17.5	- 3.5	0	0	1.5	3
9	-45	-12	24	10.5	30	13
10	-24	- 2	9	9.5	8	10
11	-46	-11	26.5	14	30	10.5
12	-13	- 2.5	13.5	9.5	14.5	7
13	- 8	- 4.5	6.5	6	11.5	10
14	-49	-15	15	10	20	11
15	-53	-20.5	3.5	3.5	7.5	9
16	-44	- 9	9	8.5	10	13.5
17	-49	-18	24.5	13	26	13
18	-48.5	-15.5	40	20	41.5	19

Table 6-2 Antenna 001 Transmission Phases Before and After Trimming 5.06 GHz

PORT	PHASE	AMP.	PORT	PHASE	AMP.	PORT	PHASE	AMP.
1	67°	1.0	19	75°	1.4	37	67°	1.3
2	72	1.0	20	83	1.5	38	78	1.3
3	73	1.0	21	91	1.5	39	88	1.2
4	73	0.6	22	83	1.3	40	85	1.3
5	78	0.9	23	77	1.3	41	83	1.3
6	87	0.7	24	75	1.6	42	84	1.1
7	82	1.0	25	78	1.6	43	81	1.2
8	77	1.0	26	77	1.6	44	75	1.5
9	67	1.1	27	74	1.6	45	65	1.6
10	64	1.8	28	80	1.6	46	69	1.4
11	70	1.7	29	76	1.55	47	76	1.2
12	78	1.4	30	82	1.55	48	83	1.4
13	84	1.2	31	83	1.5	49	87	1.4
14	88	1.4	32	82	1.4	50	77	1.35
15	88	1.2	33	76	1.6	51	82	1.3
16	86	1.4	34	63	1.7	52	73	1.4
17	76	1.4	35	66	1.7	53	72	1.8
18	71	1.2	36	74	1.3	54	73	1.4

note: amplitudes are in dB and are in terms relative to 1.0 dB of port 1

Table 6-3 Antenna 002 Transmission Phases and Amplitudes

7.0 CONCLUSIONS AND RECOMMENDATIONS

This development of a microstrip MLS azimuth antenna has been remarkably successful. No significant difficulties in the RF design have been encountered and an RF design process has been developed and proven which accounts for non-calculable effects.

The program objective, which was to develop the design tools and to make and test an antenna which met the MLS azimuth RF requirements, has been achieved. Since the objective was limited to meeting the RF performance parameters and not mechanical, physical and environmental specifications the antenna was essentially an RF breadboard.

An important outcome of this work has been the development and proving the RF design process. This has implications outside of MLS; wherever series arrays are employed. The particular difficulty of the series array is that small systematic errors in the assumed characteristics of the elements can result in large cumulative errors as the array proceeds. At the present time the method used here is the only feasible way of determining element characteristics. Many attempts are being made to generate accurate mathematical models of groups of patches, often based on finite element-method of moments techniques. A group at MIT has taken the step of developing a completely new branch of mathematics to assist in the solution of coupled patches. So far no purely analytical method has succeeded and it remains essential to carry out immersed element characterisation by measurement. Fortunately the advent of automated self calibrating RF test equipment, the automatic network analyser, has made the task reasonably simple. The accuracy of patch characterisation, radiation conductance and "end effects" has been demonstrated by the correct operation of the series arrays.

A single hitch occurred with antenna 001 which highlighted the importance of careful procurement control of the dielectric material. This was resolved within the program by the purchase of additional material at an off-the-shelf but more stringent dielectric constant tolerance. Whereas this episode was expensive in program terms, it had the advantage of highlighting a difficulty that may have arisen at a worse time in a subsequent development. Further, it encouraged a survey of material availability and performance that would otherwise not have been done.

Owing to the success of this program in the technical realm and the large export and domestic market opportunities, it is recommended that the MLS antenna program be continued. The next and final development phase should be started immediately and should comprise the construction and test of an "engineering model" antenna. This would incorporate comprehensive structural and thermal design and a survey and analysis of materials and processes. Full environmental testing would support claims that the antenna was compliant to all requirements.

8.0 REFERENCES

1. Maillouse, R.J., McIlvenna, J.F. and Kernweis, N.P; "Microstrip Array Technology", IEEE Transactions on Antennas and Propagation, Vol. AP-29, No. 1, January 1981, pp. 25-37.

2. Hall, P.S. and James, J.R.; "A Survey of Flat Profile Microwave Antennas", Royal Military College of Science, U.K., Technical Note 103, April 1977.

3. Hexcell Corporation, "Mechanical Properties of Hexcell Honeycomb Material", Publication No. TSB 120, Hexcell Corporation, Dublin, California, USA.

4. Griffen, J.M and Cowles, P.R.,; "Modelling of Microstrip Disc Antennas", Fourth International Conference on Antennas and Propagation, ICAP 85, IEE Publication No. 248.

5. MOSIG, J.R. and GARDIOL, F.E.; "A General Integral Equation Formulation for Microstrip Antennas and Scatterers"; Private Communication but to be published in Proceedings of the IEE London, Part H.

6. Bailey, S; "MLS Microstrip Study" Transporation Development Centre publication TP 5438E, April 1984.

7. James, J.R. and Henderson, A.; "High Frequency Behaviour of Microstrip Open-Circuit Termination", IEE J Microwaves, Optics and Acoustics, Vol. 3, 1979, pp. 205-218.

APPENDIX

Radiation Patterns of MLS Antennas.

Full sets of radiation acquired for antennas 001 and 002 are contained within this appendix. Summary tables relating acquisition parameters to figure number are presented overleaf.

Frequency GHz	Source Polarization	Pattern Cut	Angular Scale	Squint	Figure Number
5.03	V	AZ	±180°	0	A-1
5.03	V	AZ	± 45°	0	A-2
5.03	V	AZ	± 9°	0	A-3
5.06	V	AZ	±180°	0	A-4
5.06	V	AZ	± 45°	0	A-5
5.06	V	AZ	± 9°	0	A-6
5.09	V	AZ	±180°	0	A-7
5.09	V	AZ	± 45°	0	A-8
5.09	V	AZ	± 9°	0	A-9
5.03	H	EL	±180°	0	A-10
5.03	H	EL	± 45°	0	A-11
5.06	H	EL	±180°	0	A-12
5.06	H	EL	± 45°	0	A-13
5.09	H	EL	±180°	0	A-14
5.09	H	EL	± 45°	0	A-15
5.06	H	EL	± 45°	0	A-16*
5.03	H	EL	± 45°	0	A-17
5.06	H	EL	±180°	0	A-18
5.06	V	AZ	± 45°	0	A-19
5.09	V	AZ	± 45°	0	A-20
5.09	V	AZ	±180°	0	A-21

* gain measurement

Table A1-1 Summary of Radiation Patterns, Antenna 001

Frequency GHz	Pattern Cut	Angular Scale	Squint	Figure Number
5.03	AZ	±150	0	A-22
5.03	EL	-40 +20	0	A-23
5.06	AZ	±150	0	A-24
5.06	EL	-40 +20	0	A-25
5.09	AZ	±150	0	A-26
5.09	EL	-40 +20	0	A-27
5.03	AZ	±150	39	A-28
5.03	EL	-40 +20	39	A-29
5.06	AZ	±150	39	A-30
5.06	EL	-40 +20	39	A-31
5.09	AZ	±150	39	A-32
5.09	EL	-40 +20		A-32

Table A1-2 Summary of Radiation Patterns, Antenna 002

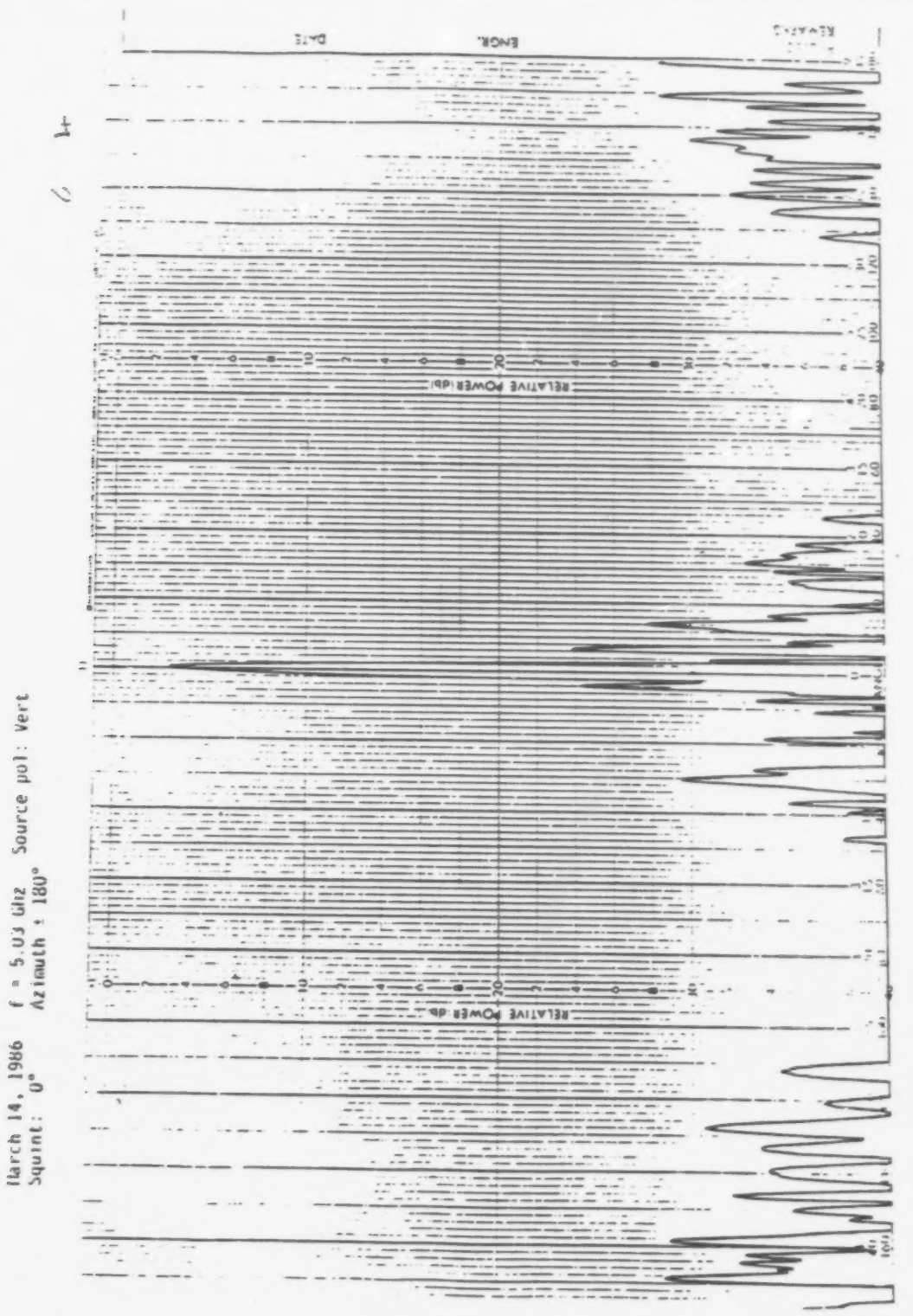

Figure A1-1 Azimuth Radiation Pattern of Antenna 001, 5.03 GHz

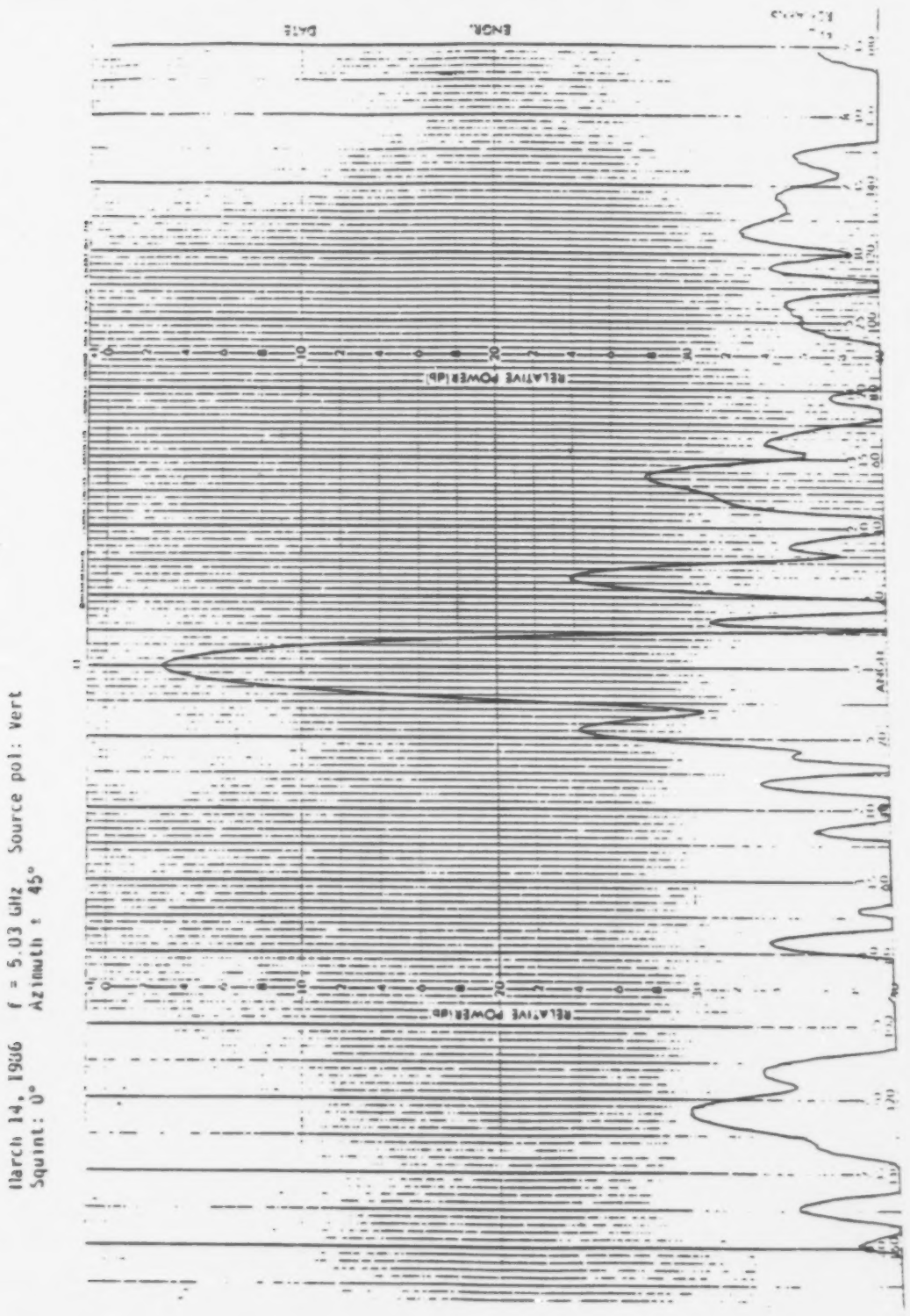

Figure A1-2 Azimuth Radiation Pattern of Antenna 001, 5.03 GHz

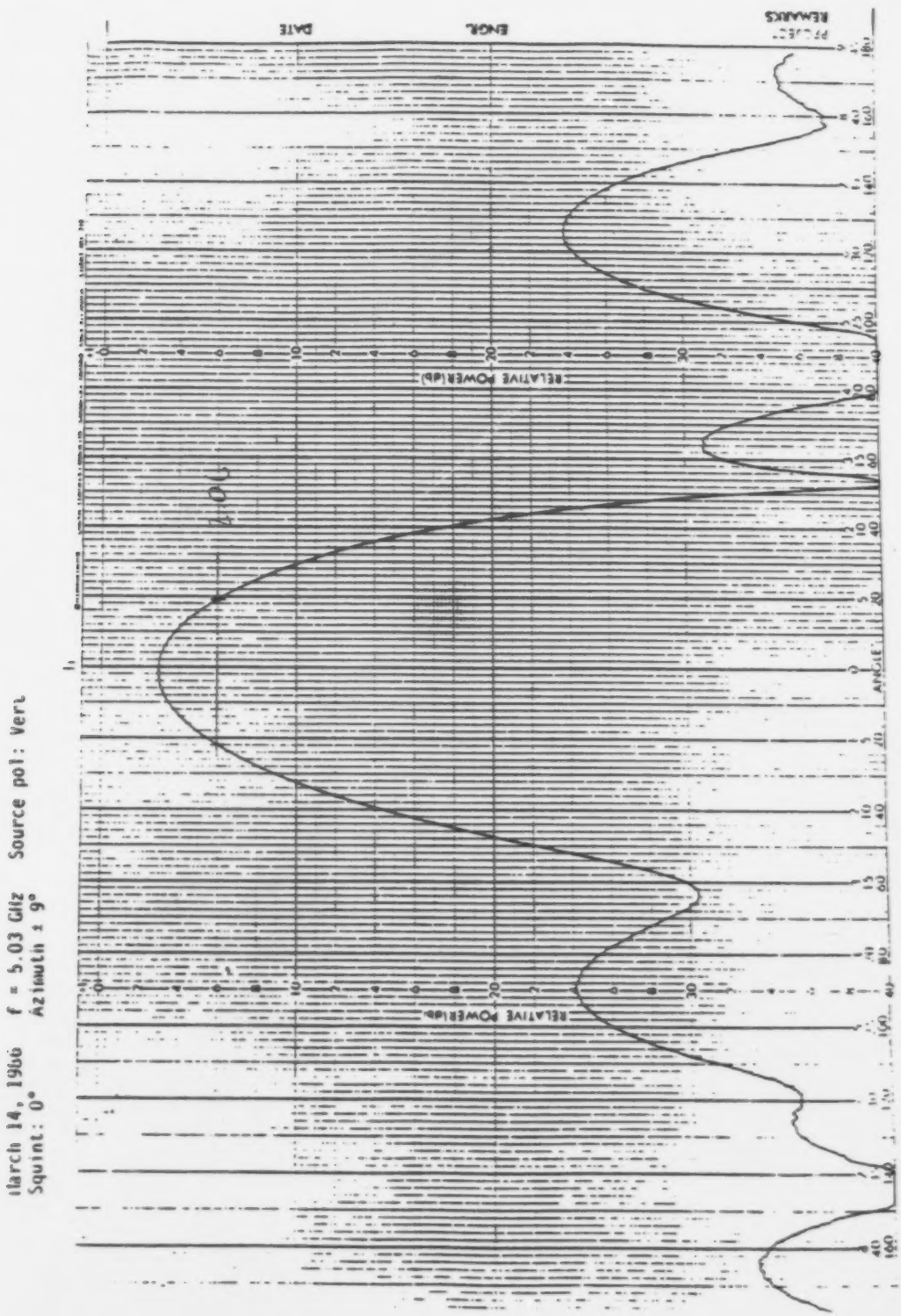

Figure A1-3 Azimuth Radiation Pattern of Antenna 001, 5.03 GHz

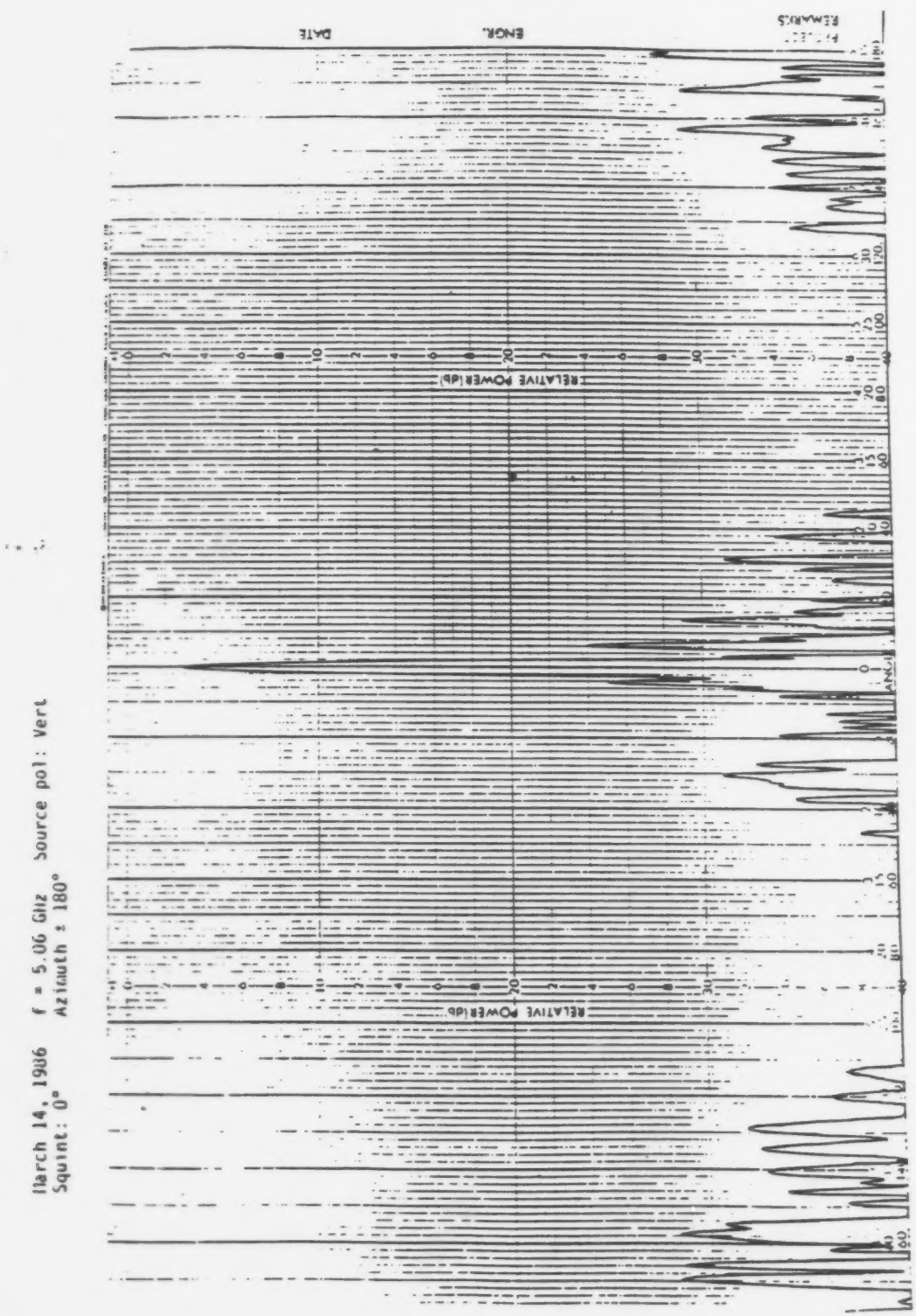

Figure A1-4 Azimuth Radiation Pattern of Antenna 001, 5.06 GHz

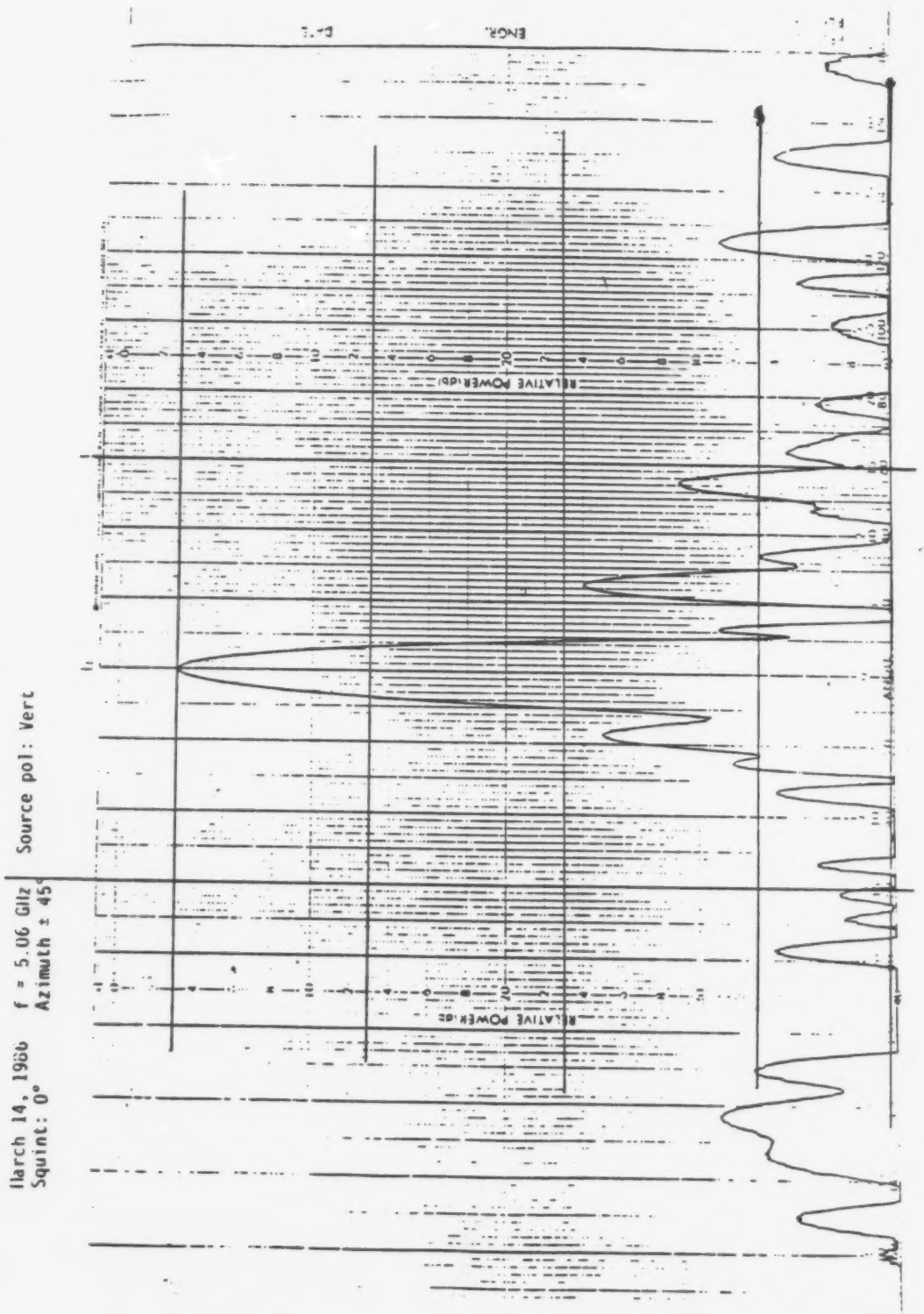

Figure A1-5 Azimuth Radiation Pattern of Antenna 001, 5.06 GHz

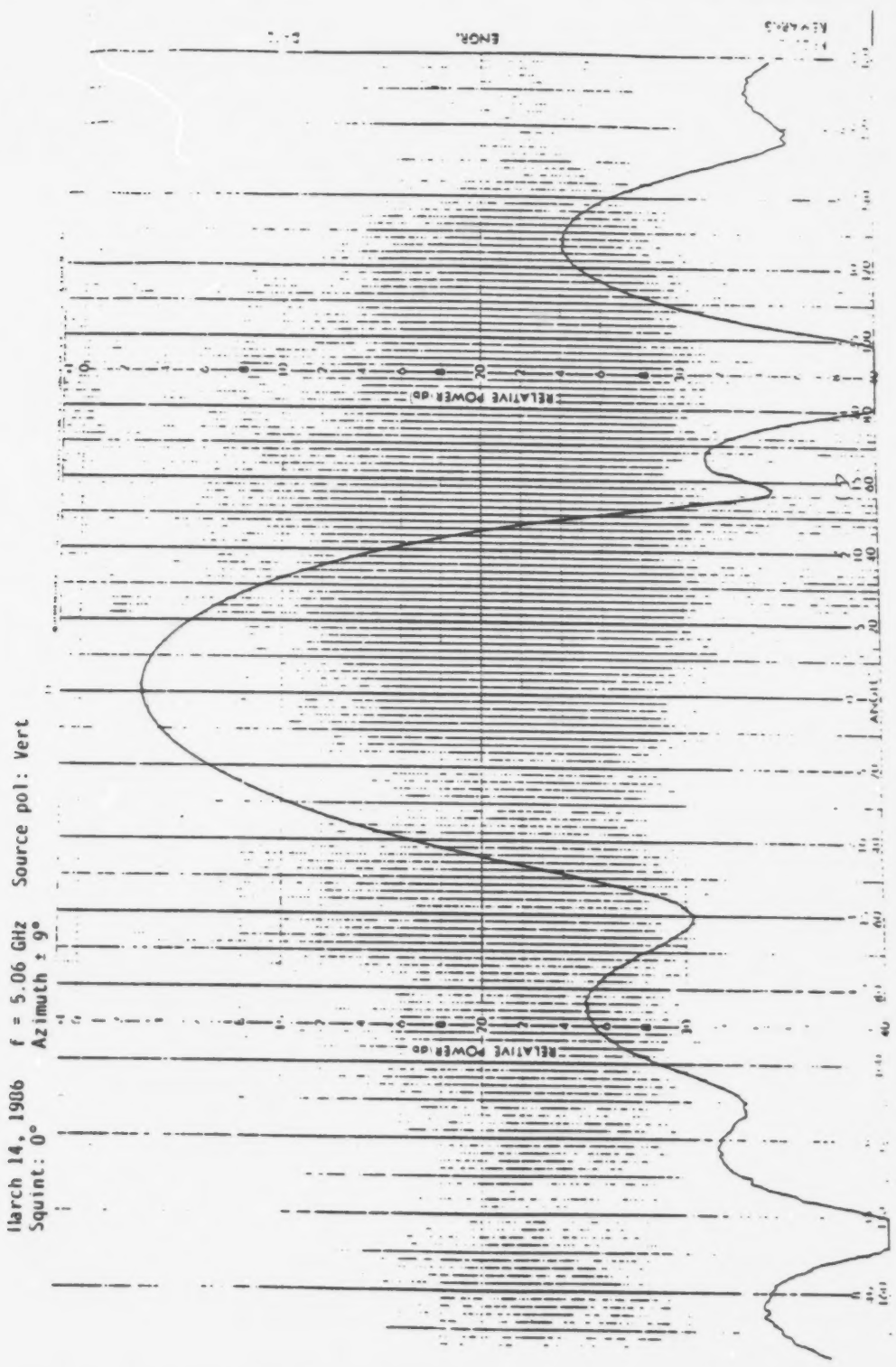

Figure A1-6 Azimuth Radiation Pattern of Antenna 001, 5.06 GHz

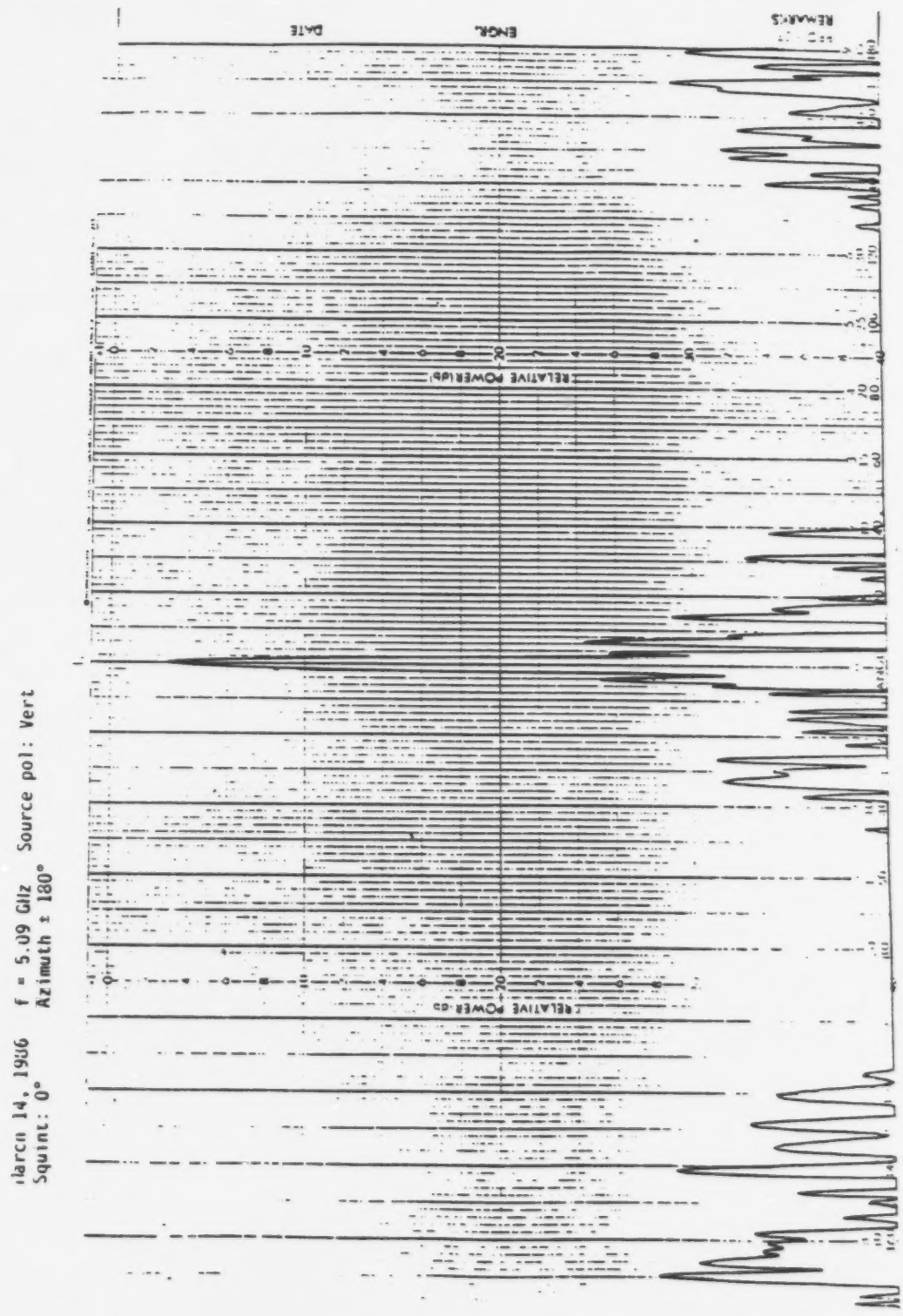

Figure A1-7 Azimuth Radiation Pattern of Antenna 001, 5.09 GHz

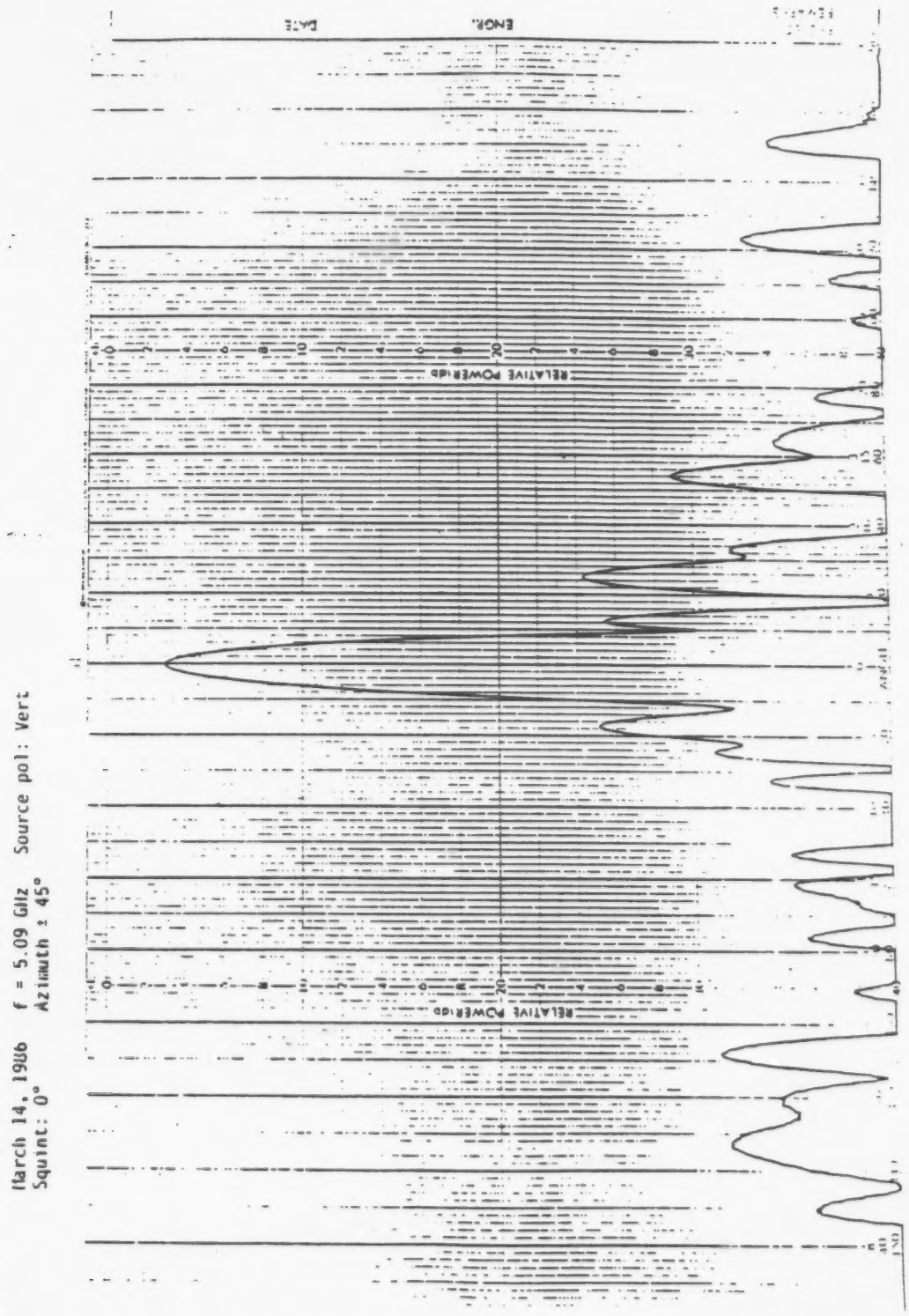

Figure A1-8 Azimuth Radiation Pattern of Antenna 001, 5.09 GHz

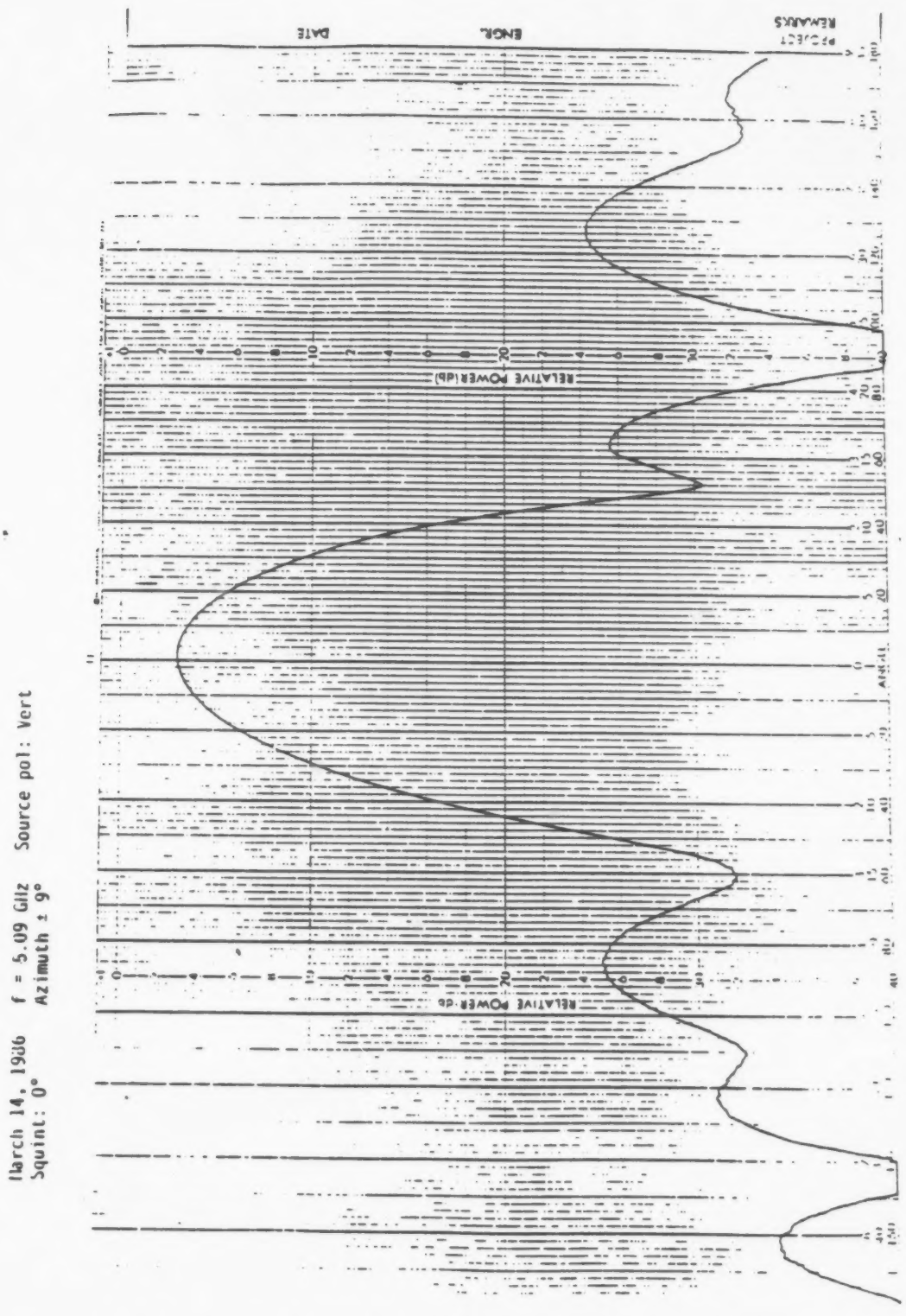

Figure A1-9 Azimuth Radiation Pattern of Antenna 001, 5.09 GHz

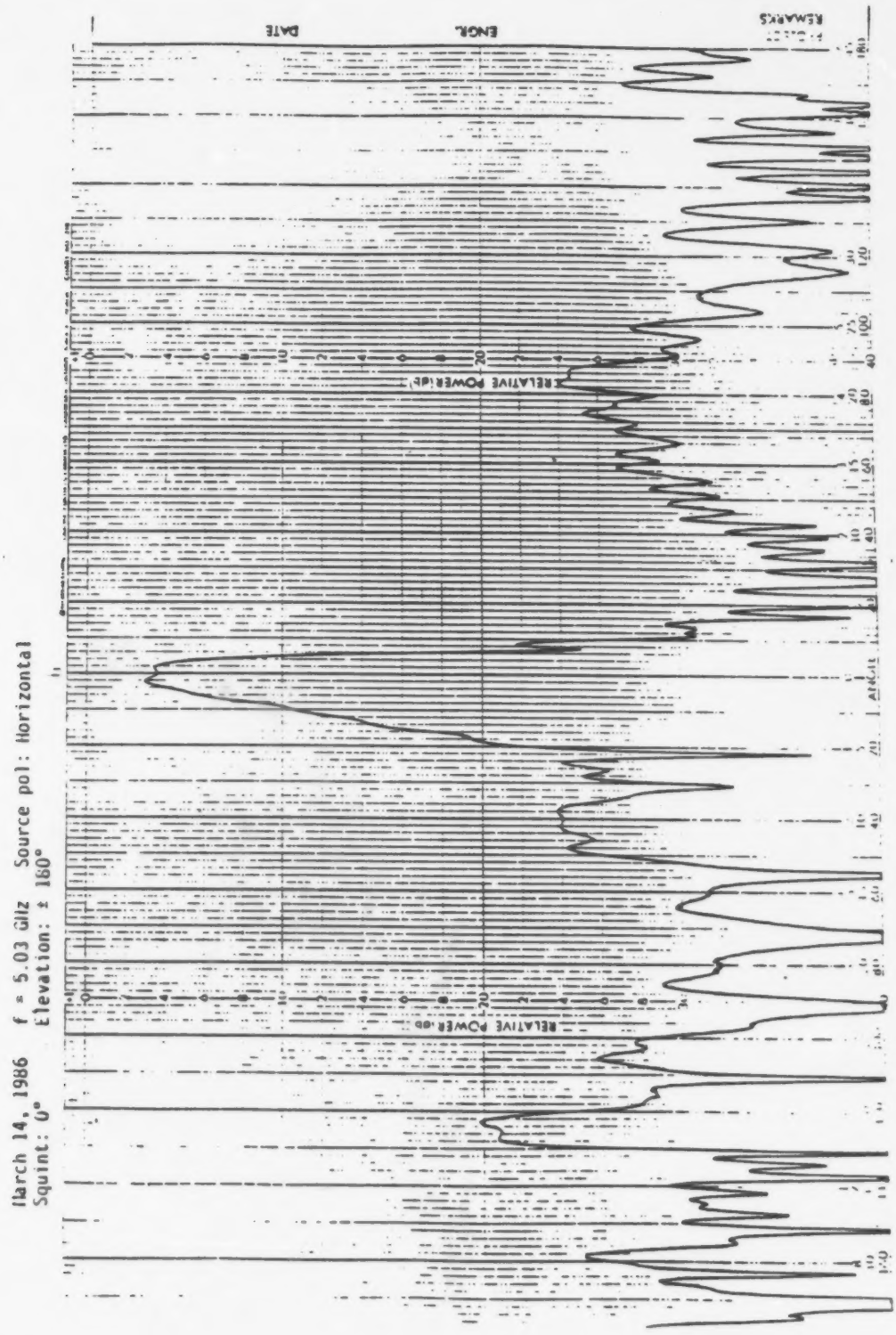

Figure A1-10 Elevation Radiation Pattern of Antenna 001, 5.03 GHz

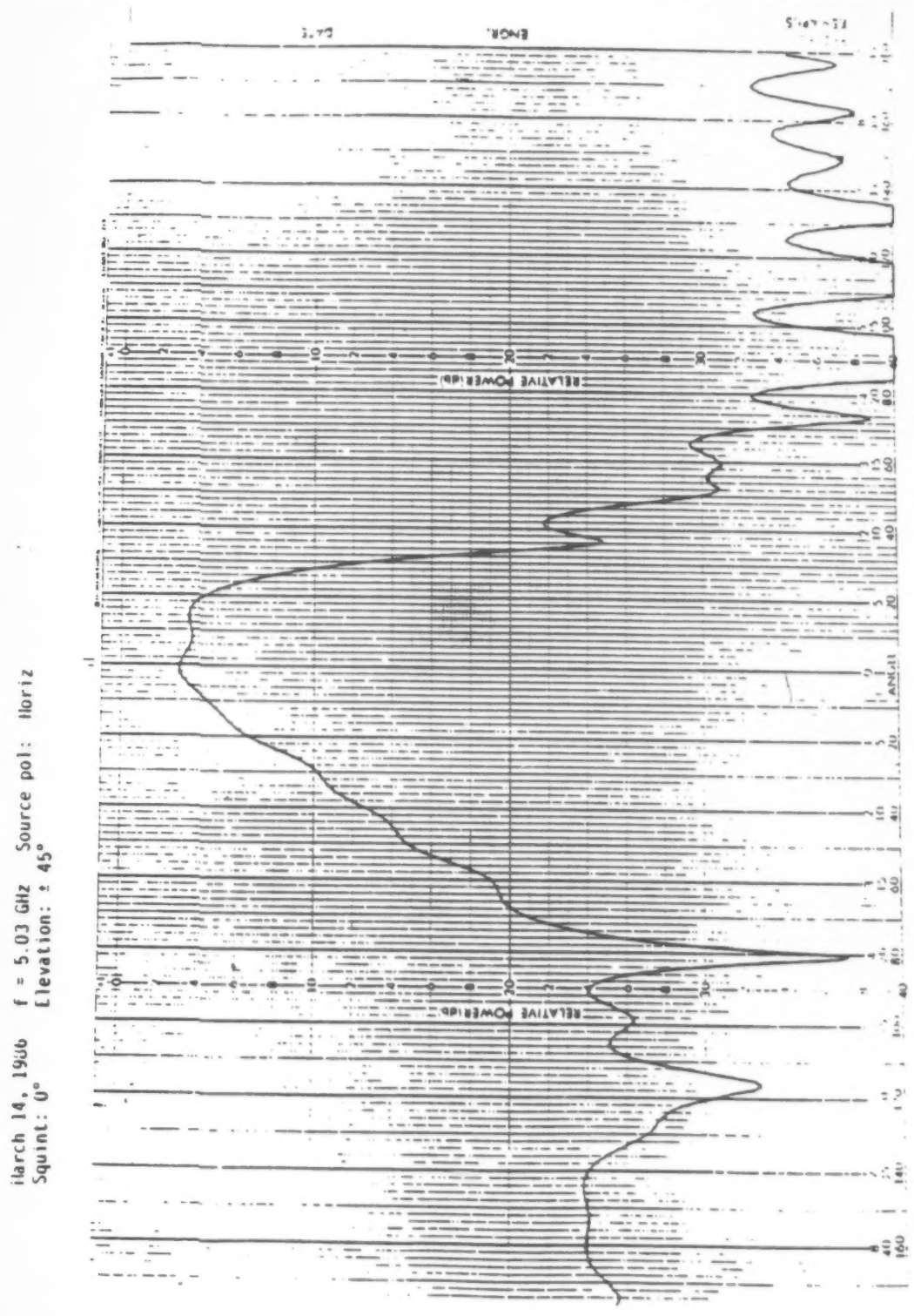

Figure A1-11 Elevation Radiation Pattern of Antenna 001, 5.03 GHz

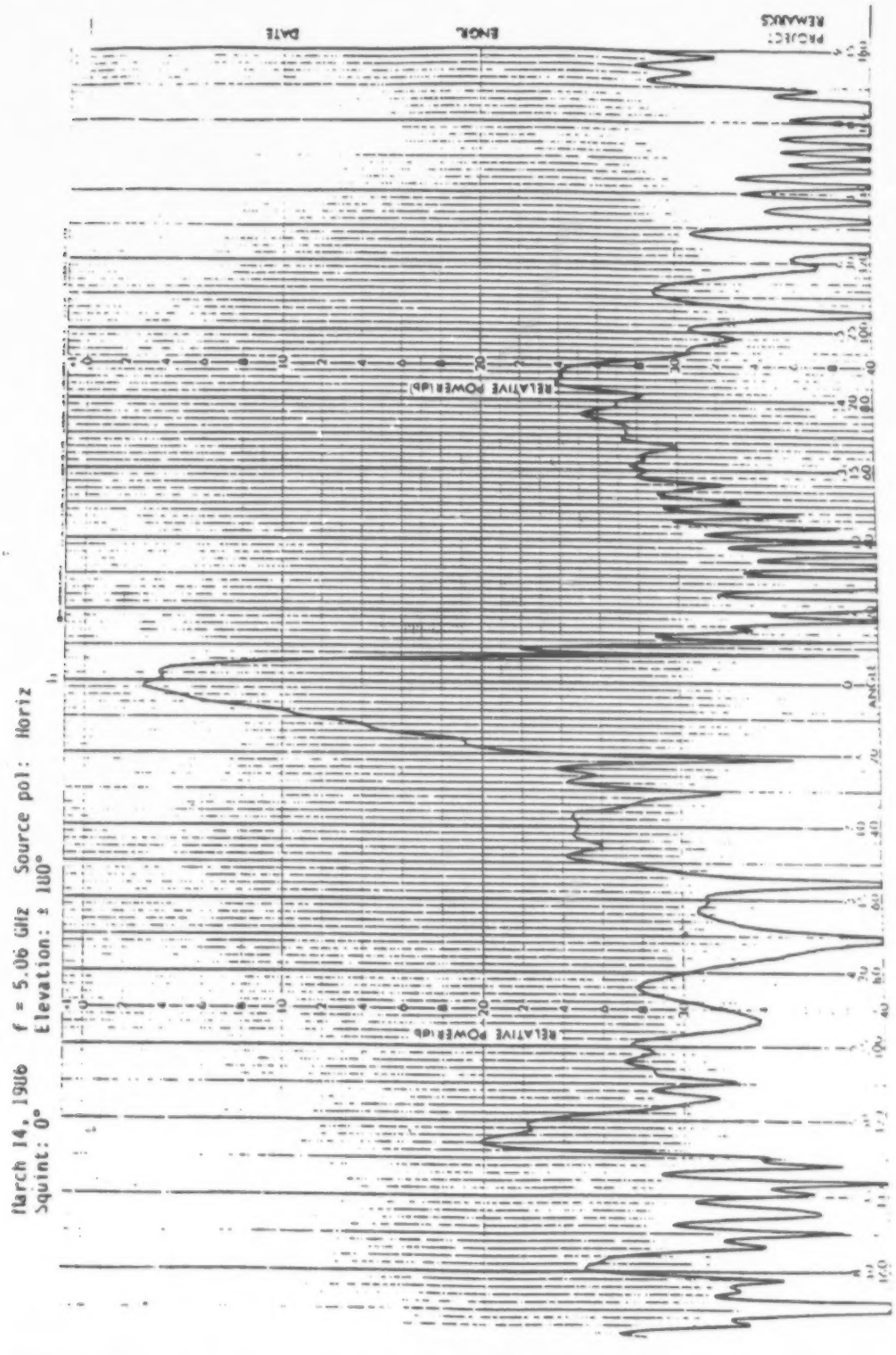

Figure A1-12 Elevation Radiation Pattern of Antenna 001, 5.06 GHz

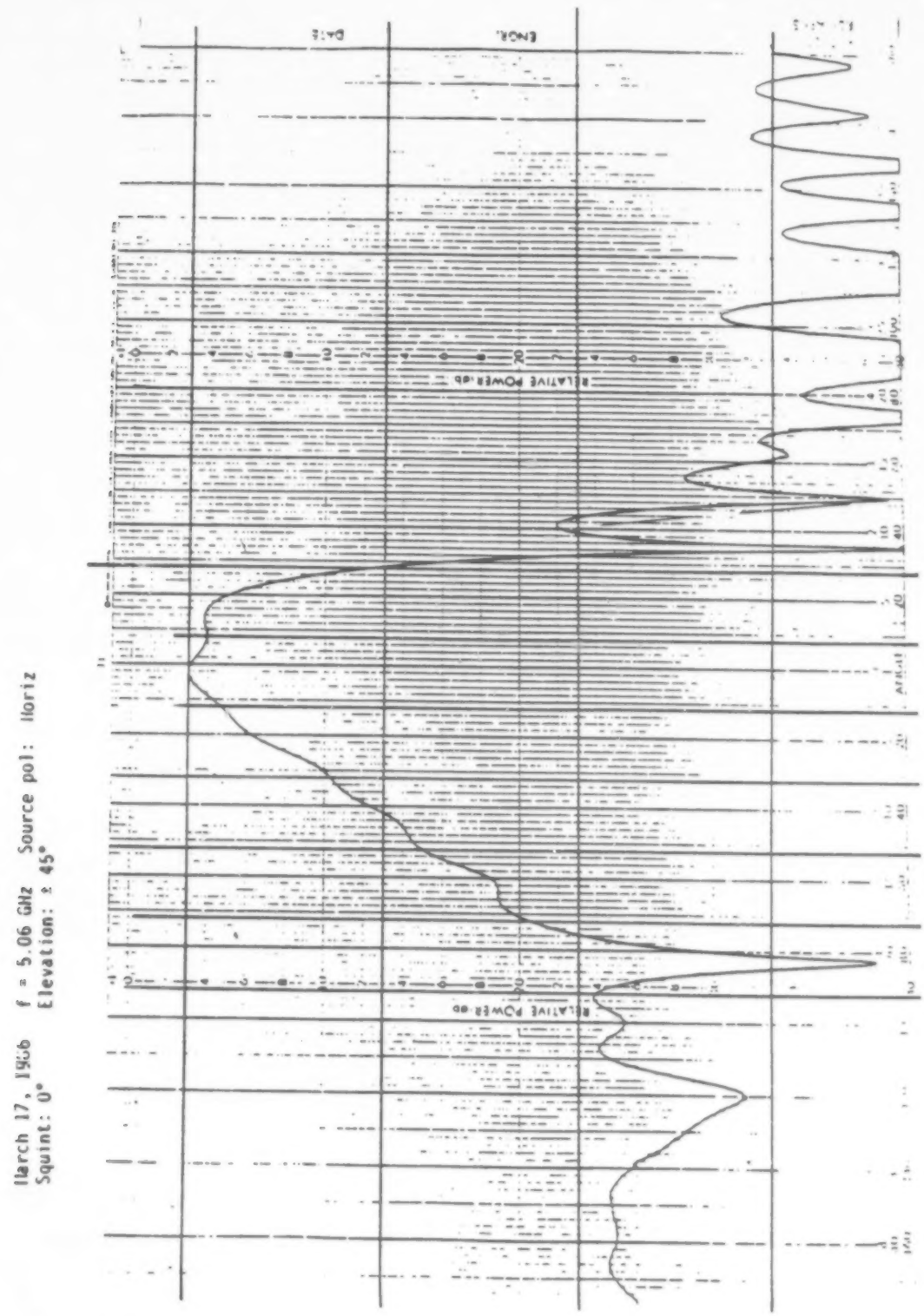

Figure A1-13 Elevation Radiation Pattern of Antenna 001, 5.06 GHz

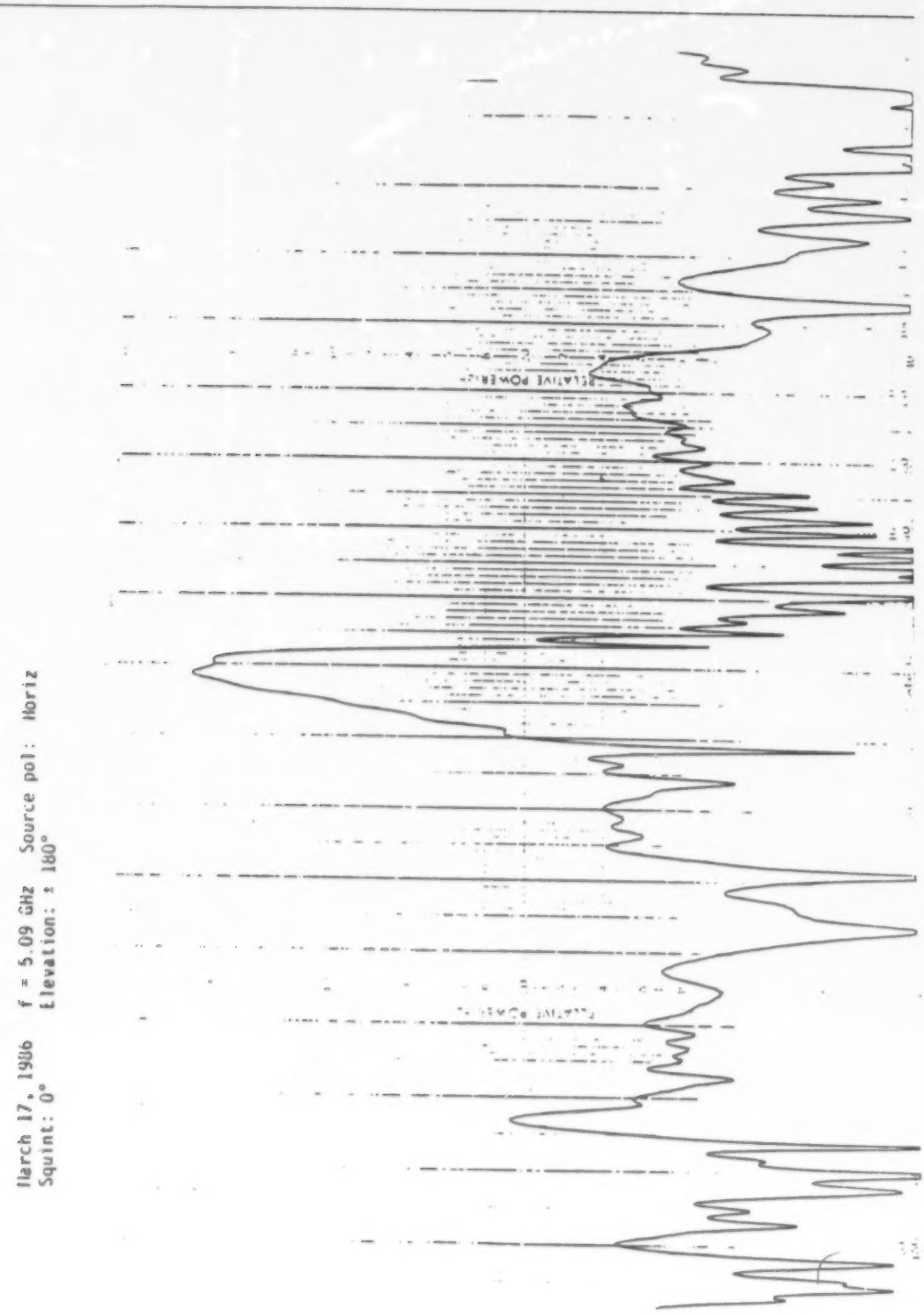

Figure A1-14 Elevation Radiation Pattern of Antenna 001, 5.09 GHz

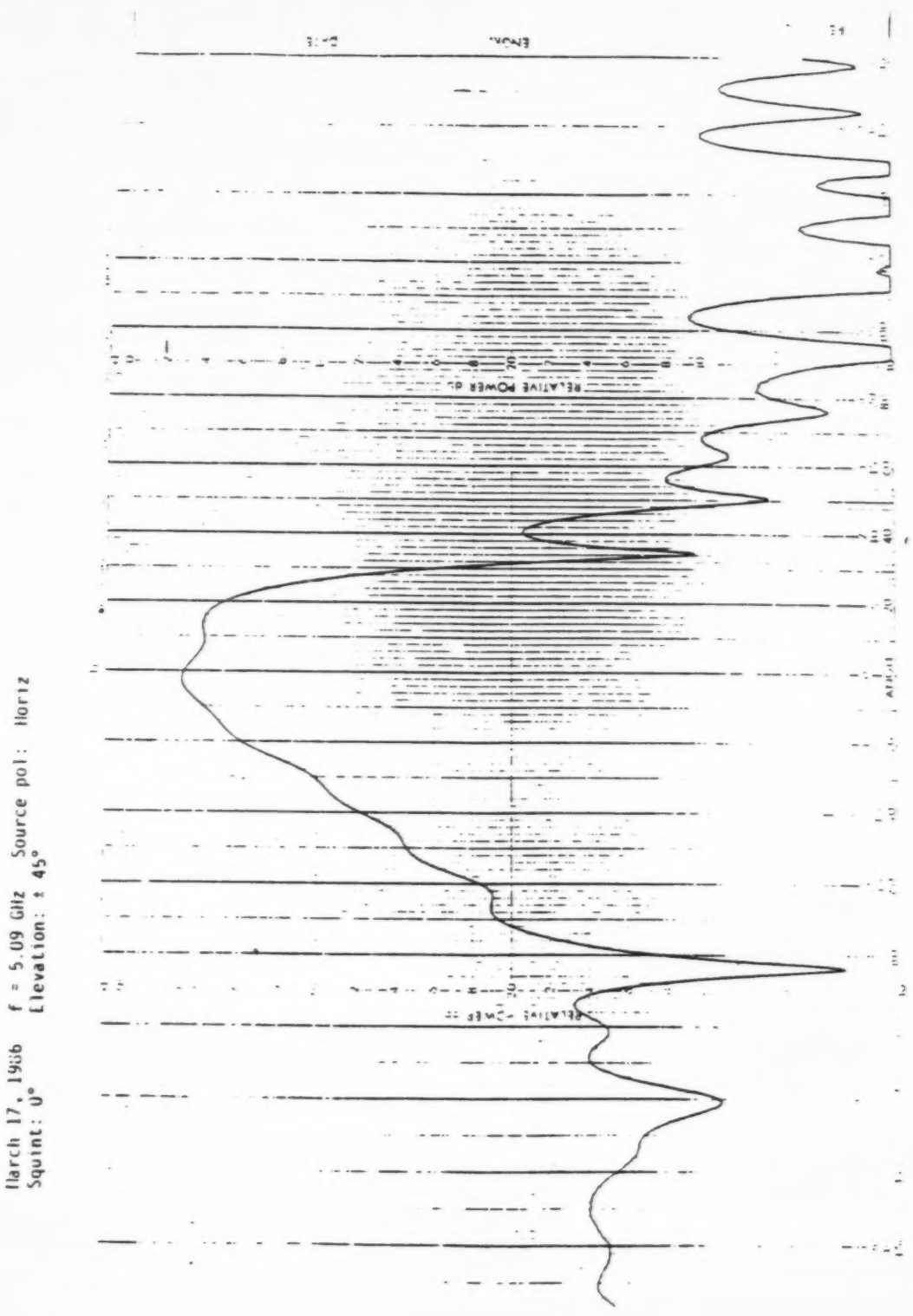

Figure A1-15 Elevation Radiation Pattern of Antenna 001, 5.09 GHz

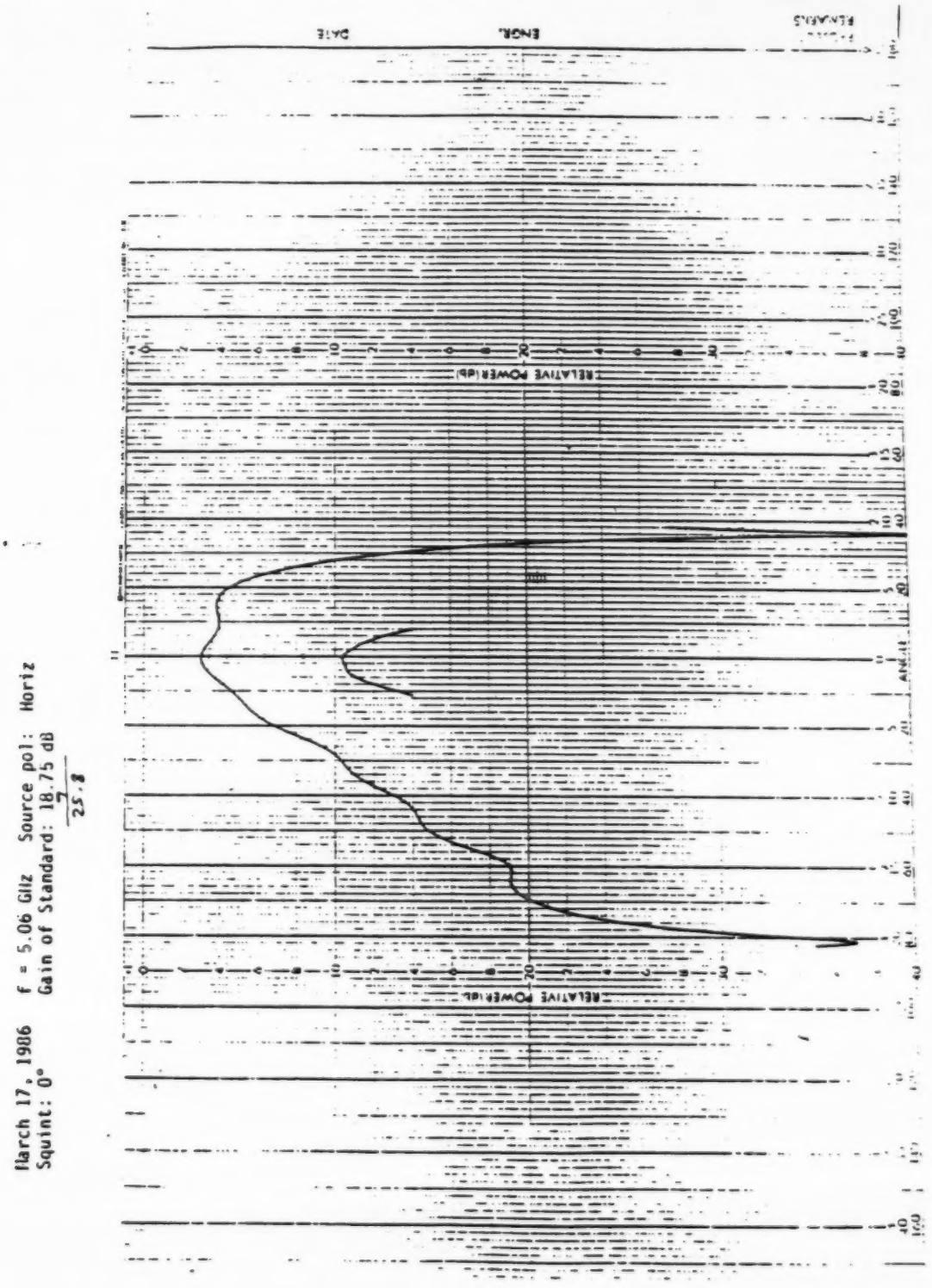

Figure A1-16 Elevation Radiation Pattern of Antenna 001, 5.06 GHz Used to Record Gain Measurement

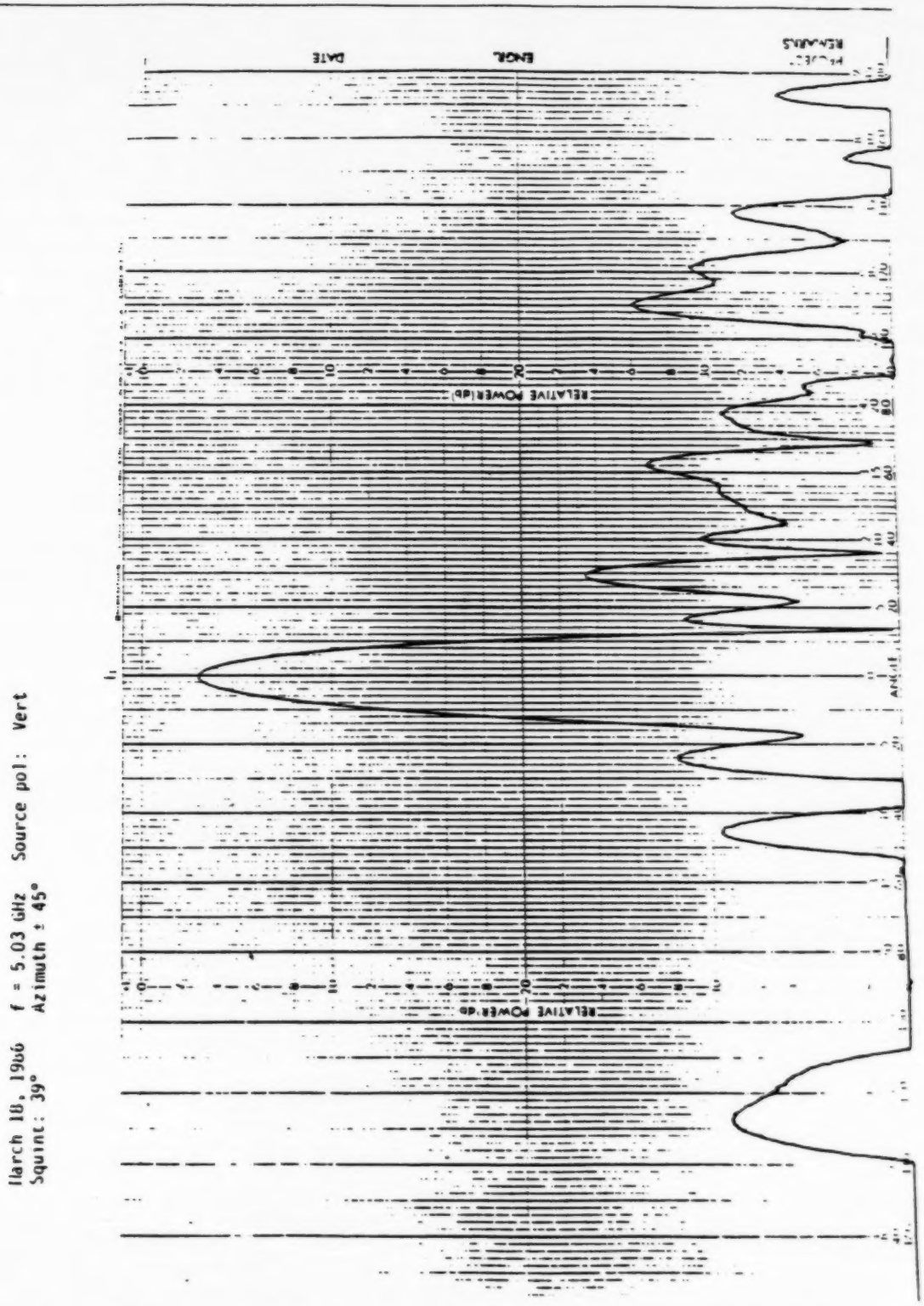

Figure A1-17 Azimuth Radiation Pattern of Antenna 001, 5.03 GHz With Squinted Beam

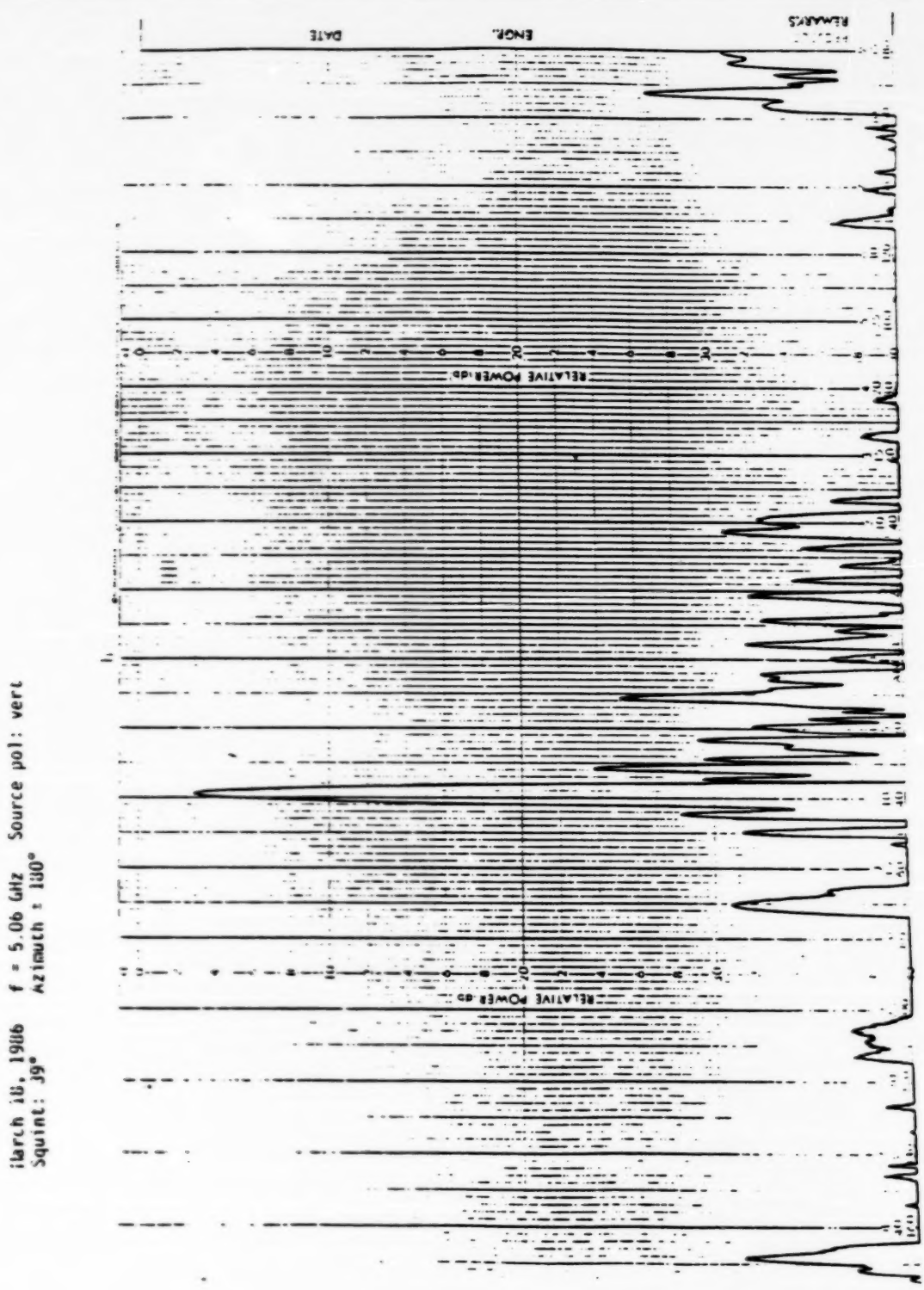

Figure A1-18 Azimuth Radiation Pattern of Antenna 001, 5.06 GHz With Squinted Beam

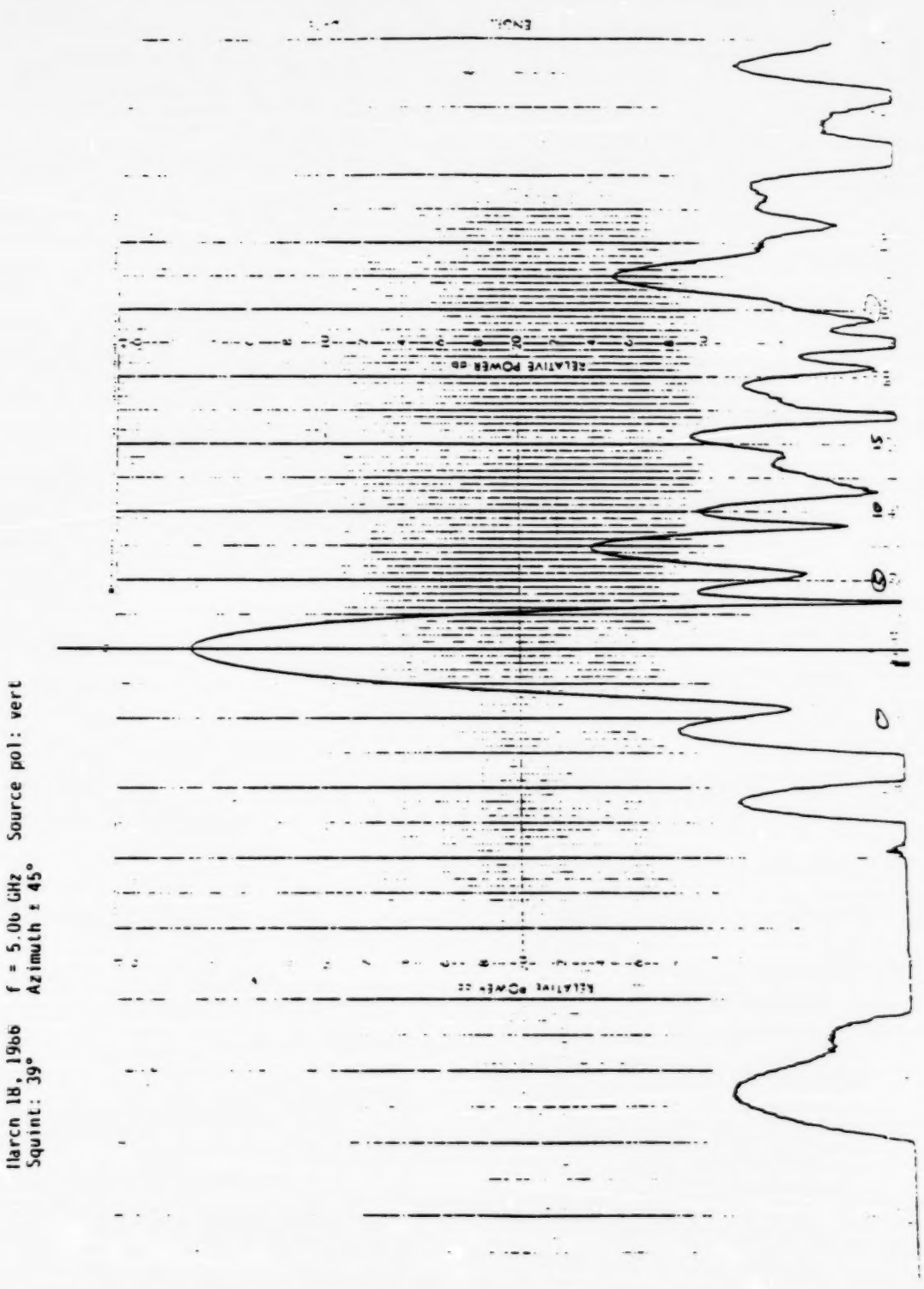

Figure A1-19 Azimuth Radiation Pattern of Antenna 001, 5.06 GHz With Squinted Beam

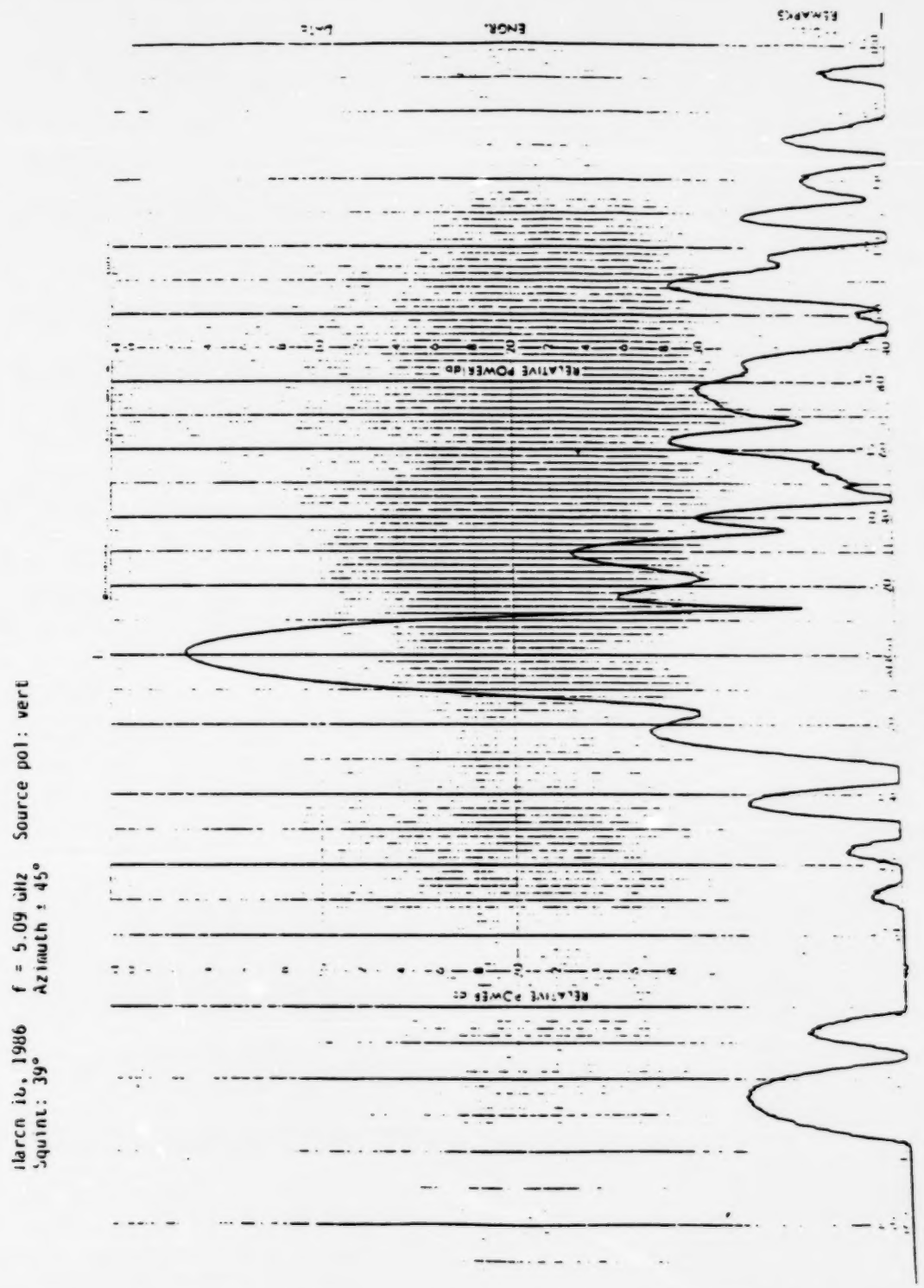

Figure A1-20 Azimuth Radiation Pattern of Antenna 001, 5.09 GHz With Squinted Beam

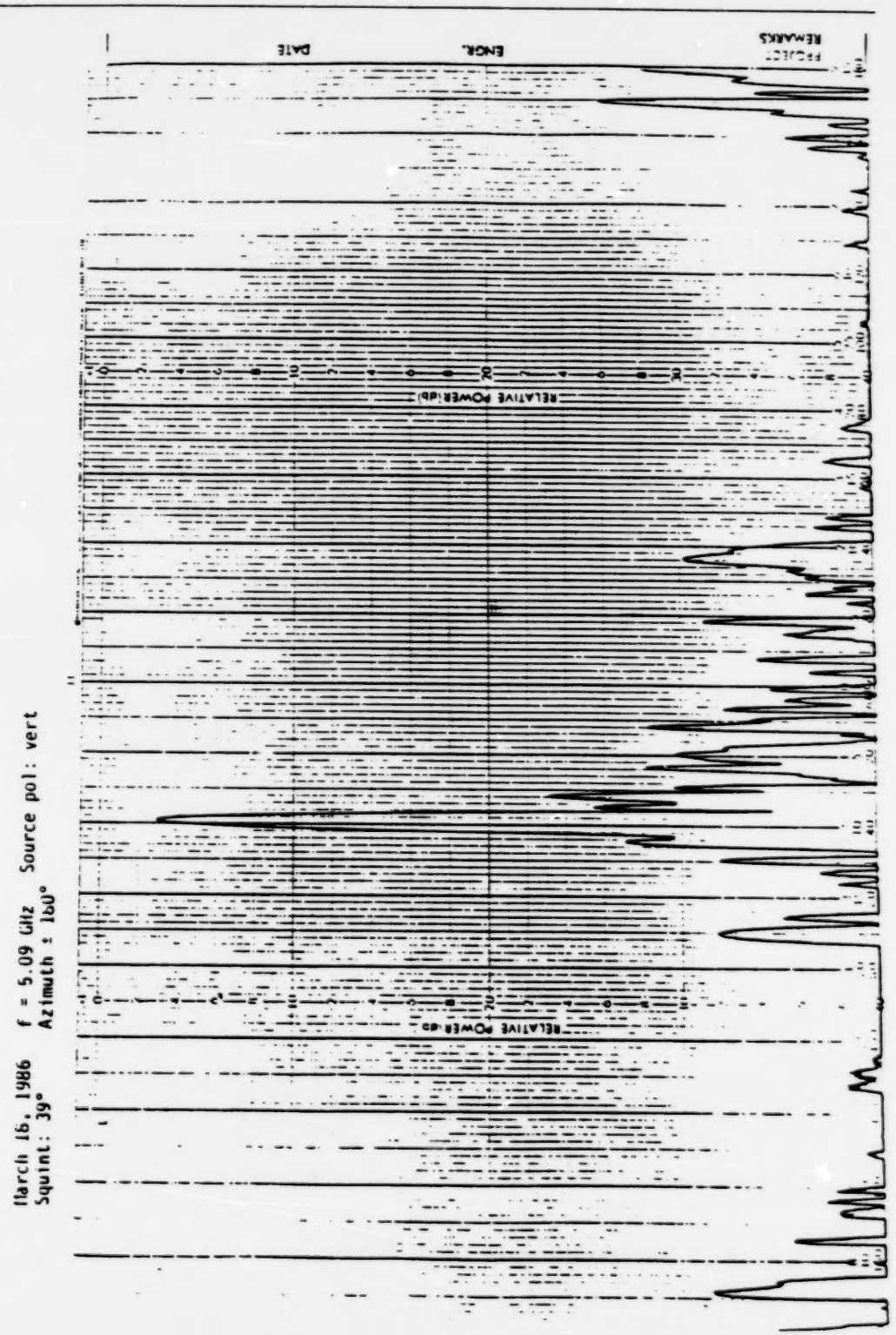

Figure A1-21 Azimuth Radiation Pattern of Antenna 001, 5.09 GHz With Squinted Beam

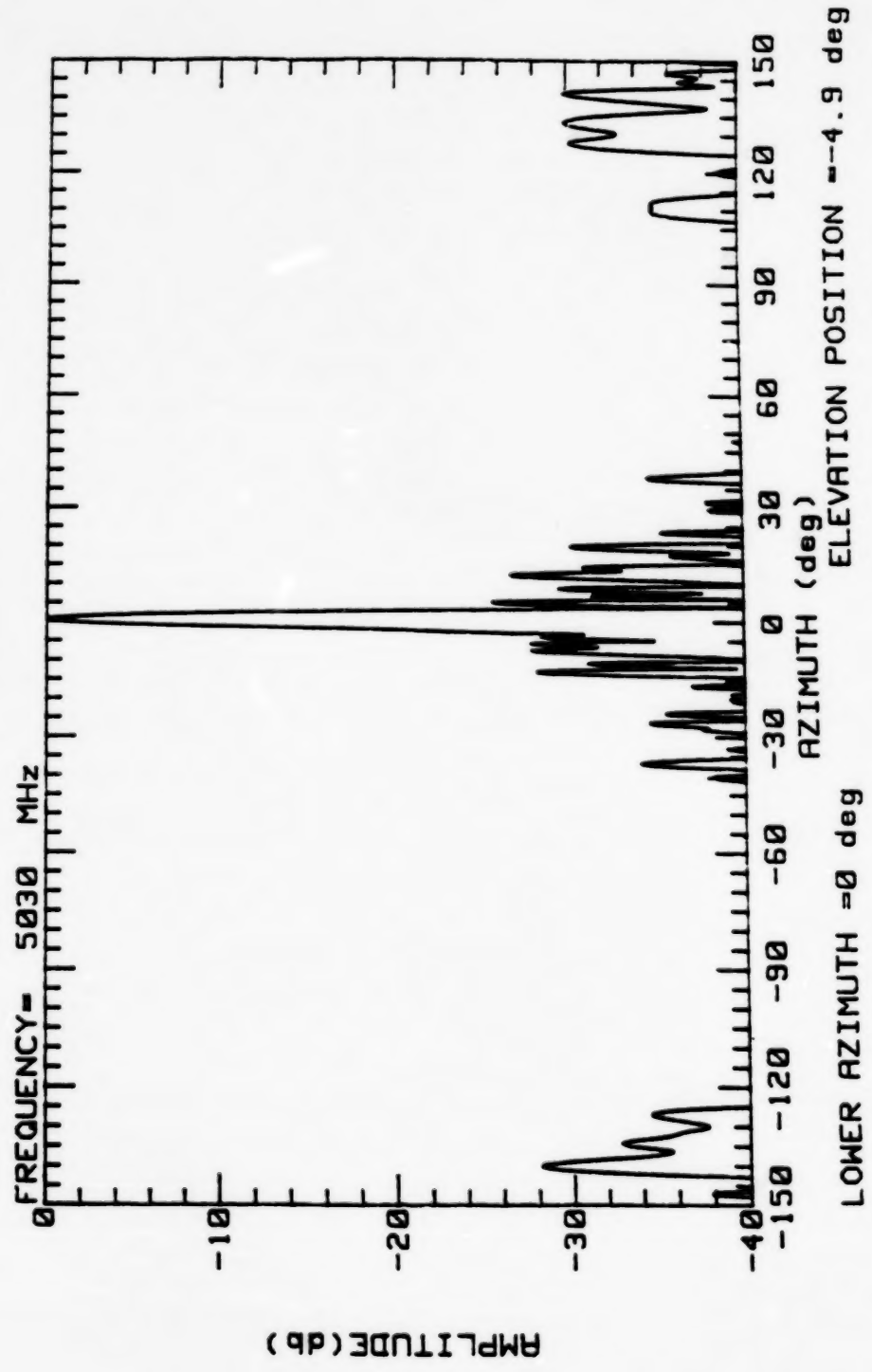

Figure A1-22 Azimuth Radiation Pattern of Antenna 002, 5.03 GHz

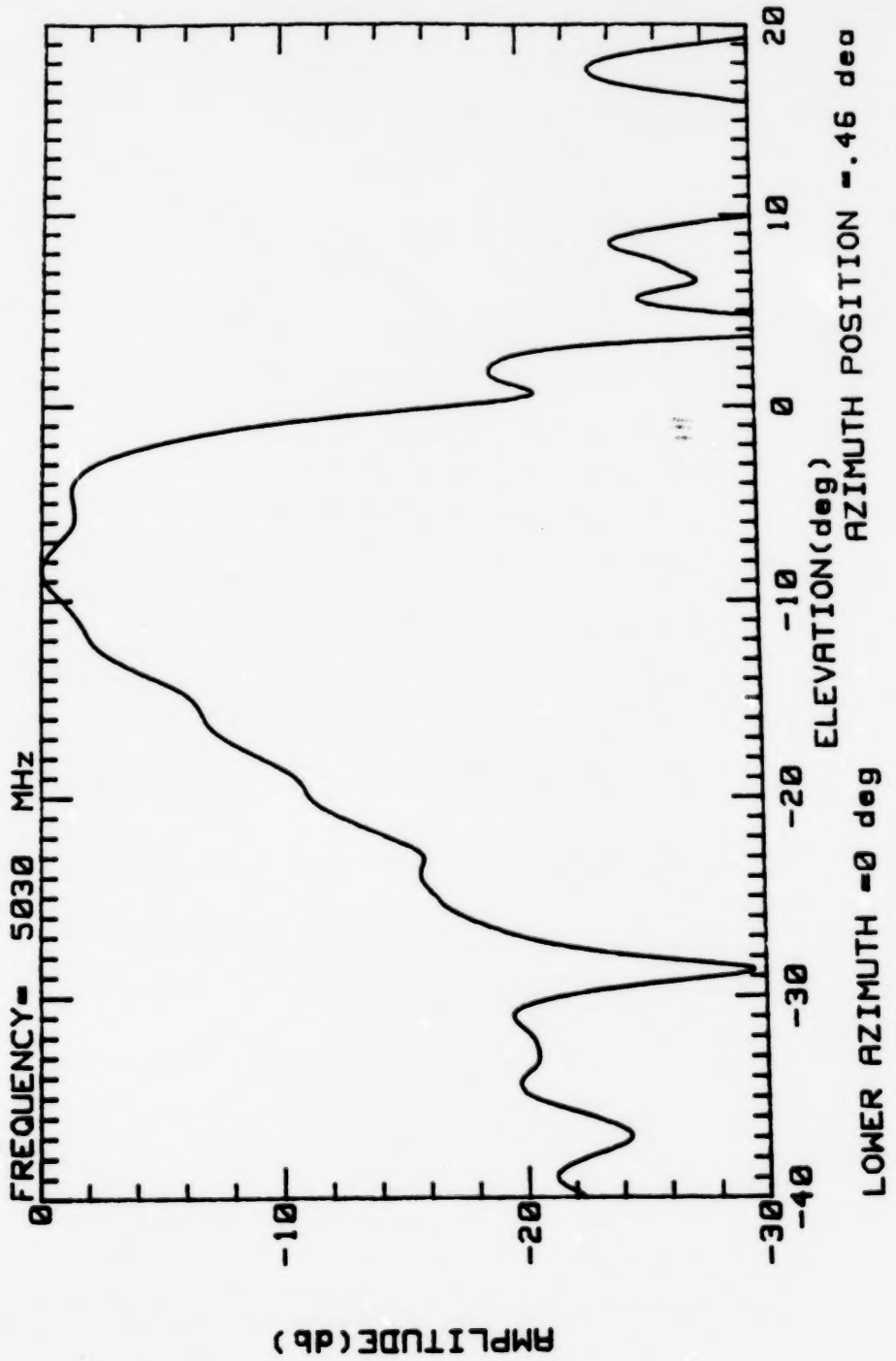

Figure A1-23 Elevation Radiation Pattern of Antenna 002, 5.03 GHz

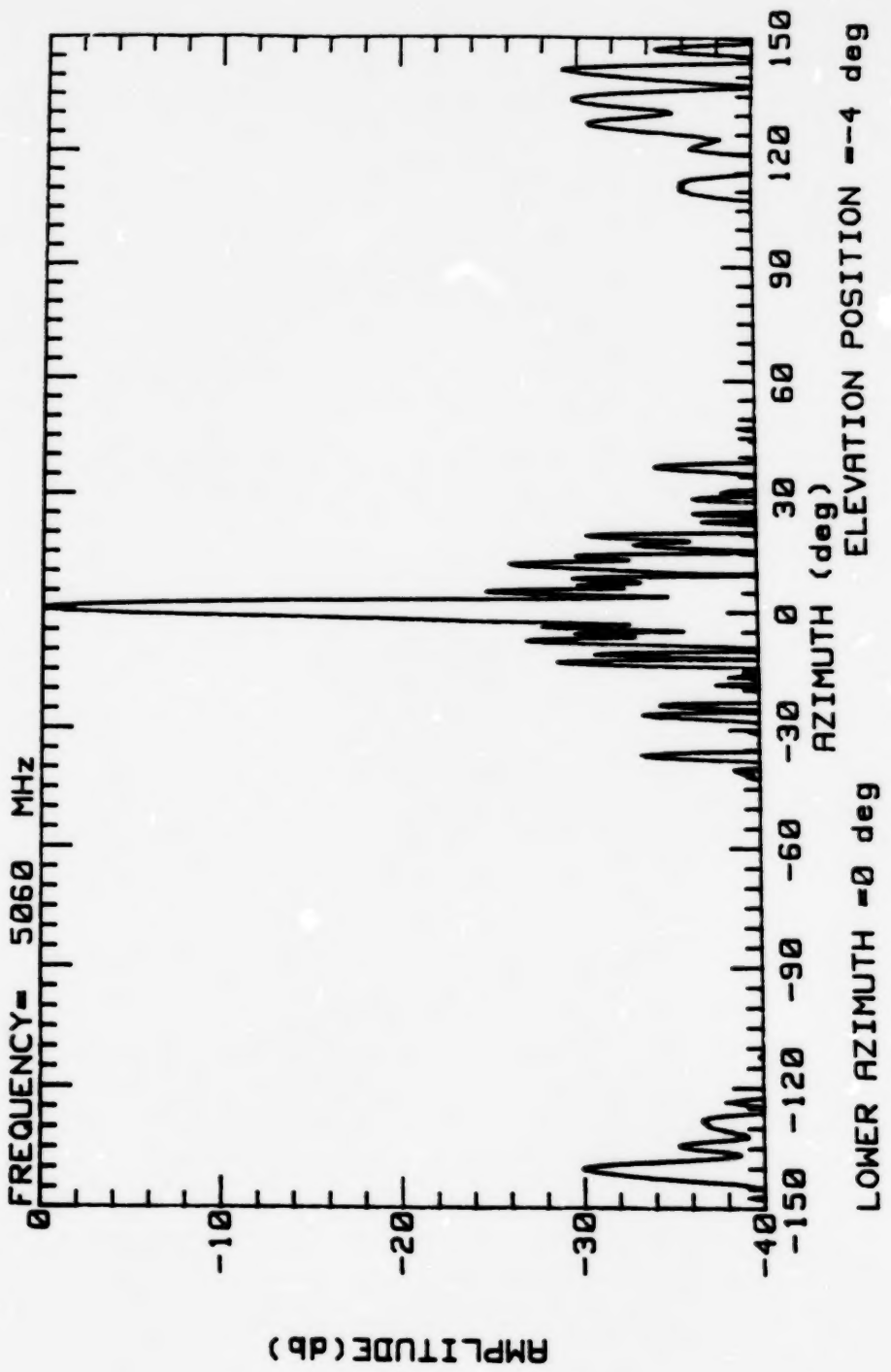

Figure A1-24 Azimuth Radiation Pattern of Antenna 002, 5.06 GHz

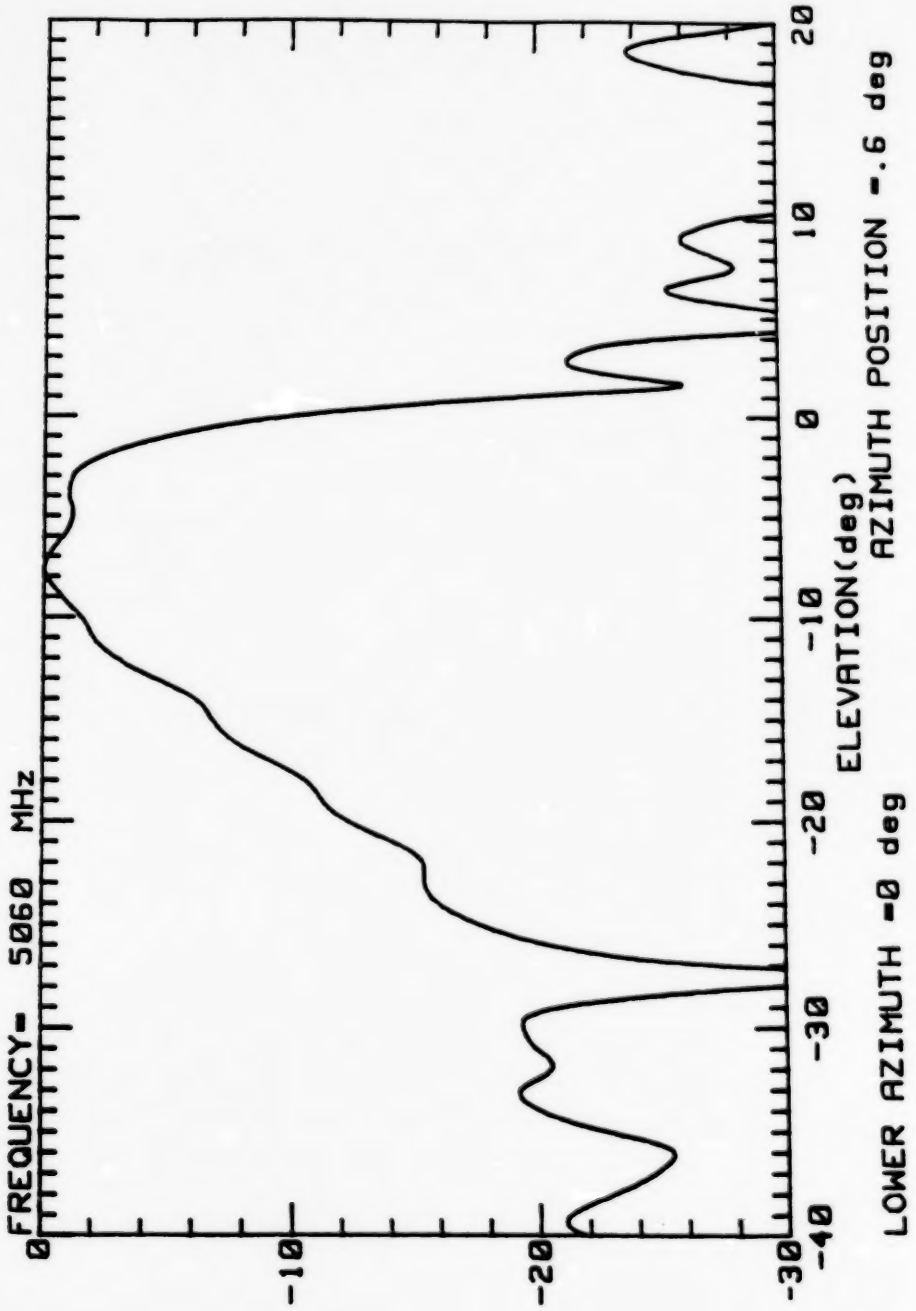

Figure A1-25 Elevation Radiation Pattern of Antenna 002, 5.06 GHz

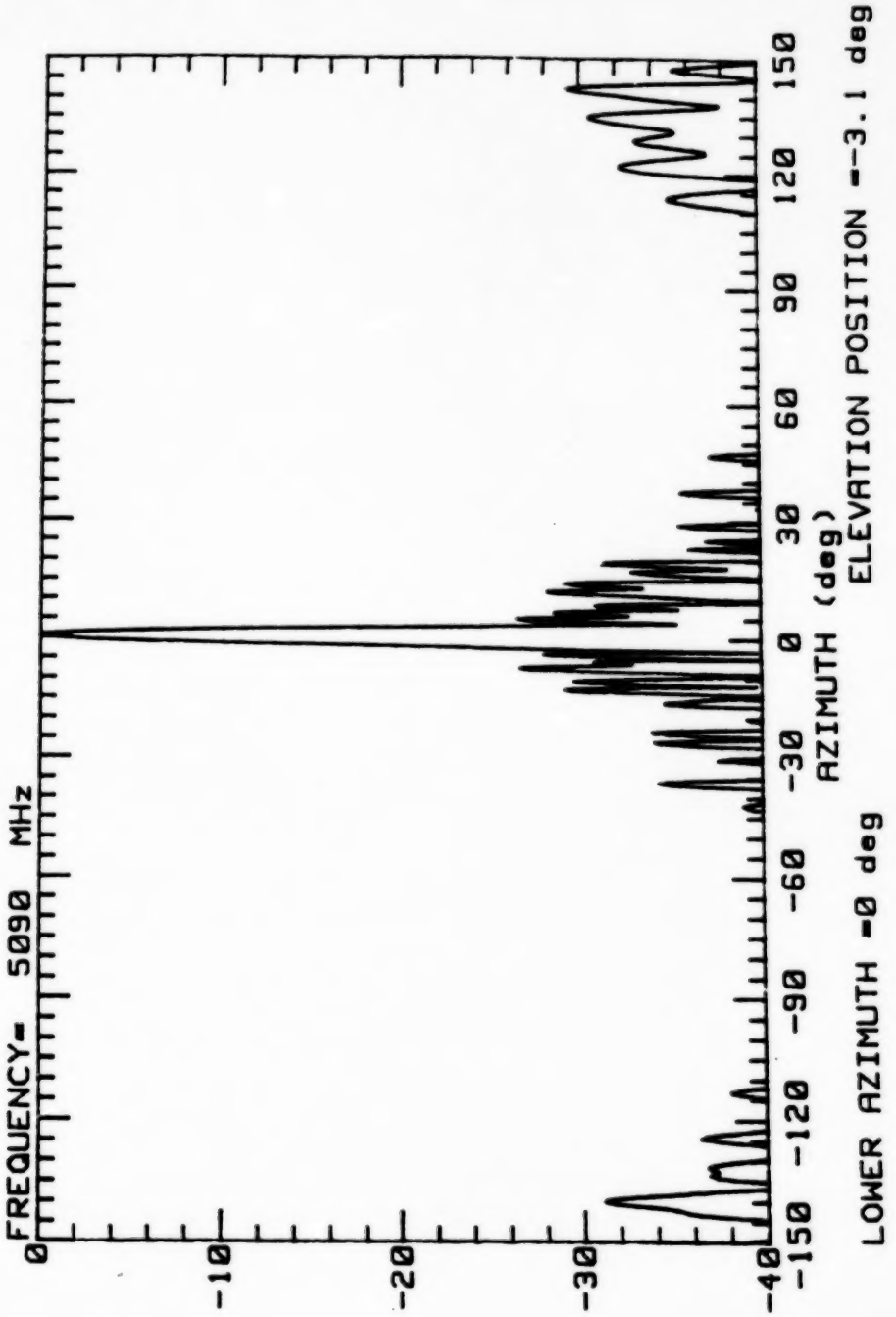

Figure A1-26 Azimuth Radiation Pattern of Antenna 002, 5.09 GHz

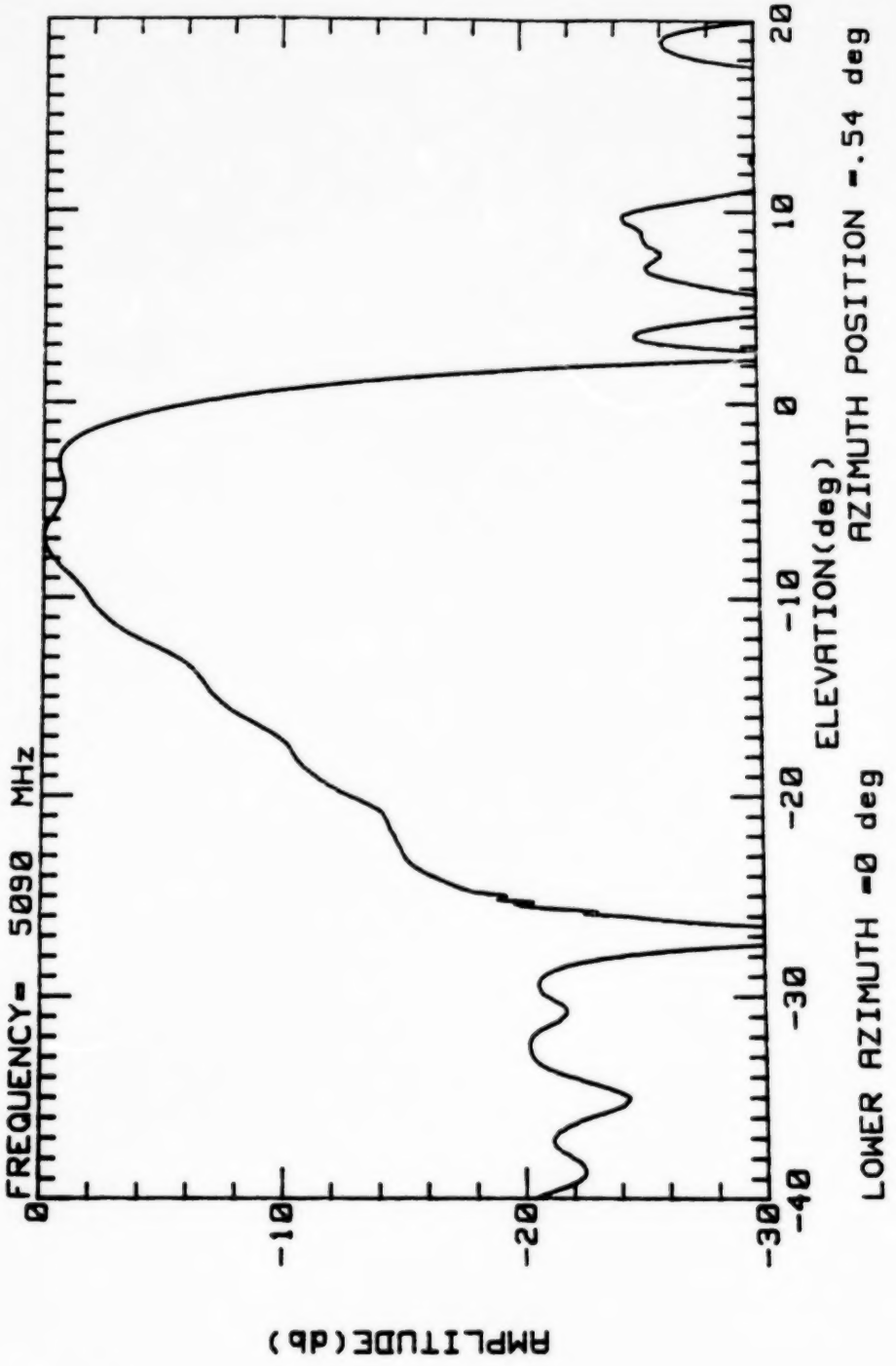

Figure A1-27 Elevation Radiation Pattern of Antenna 002, 5.09 GHz

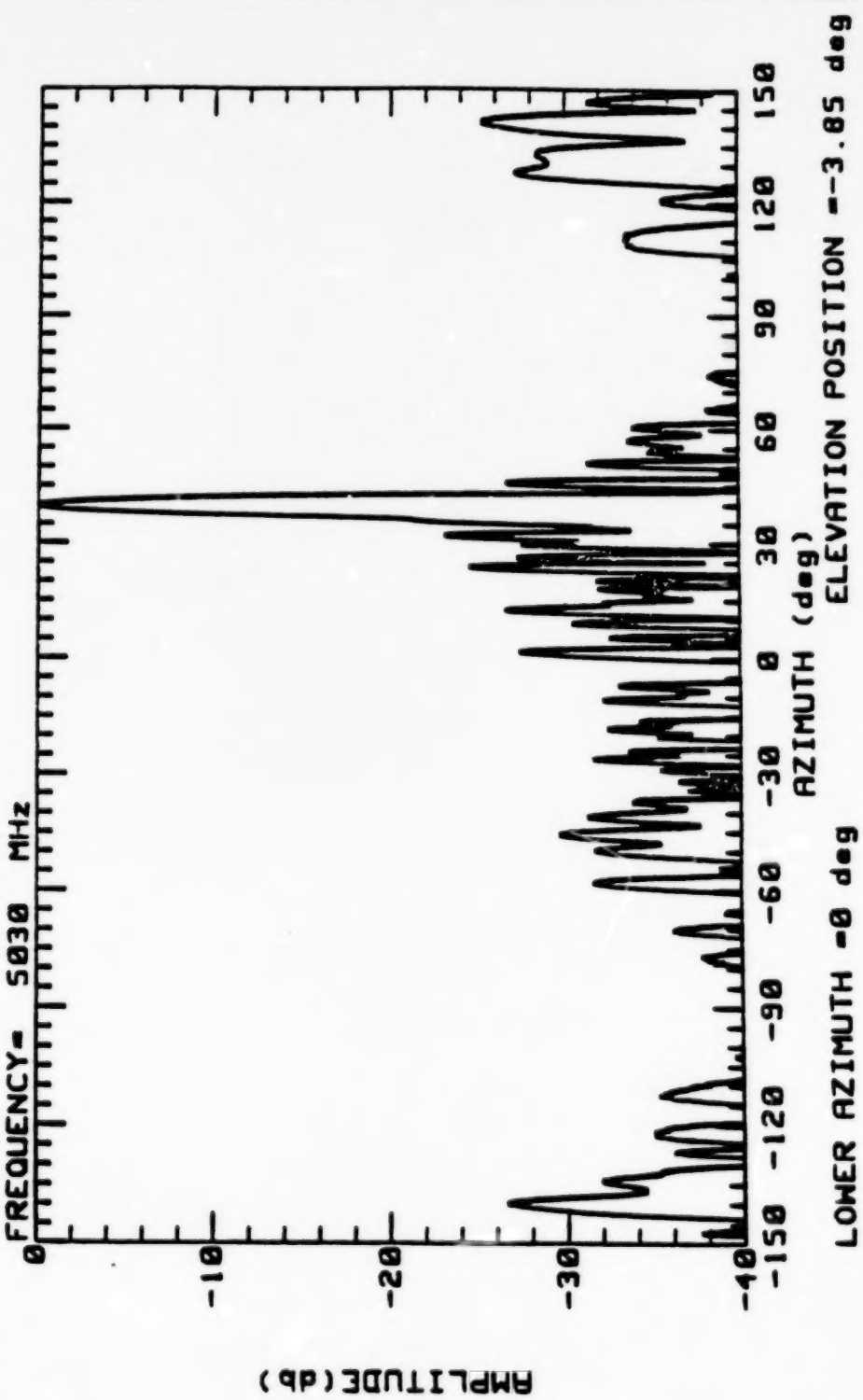

Figure A1-28 Azimuth Radiation Pattern of Antenna 002, 5.03 GHz With Squinted Beam

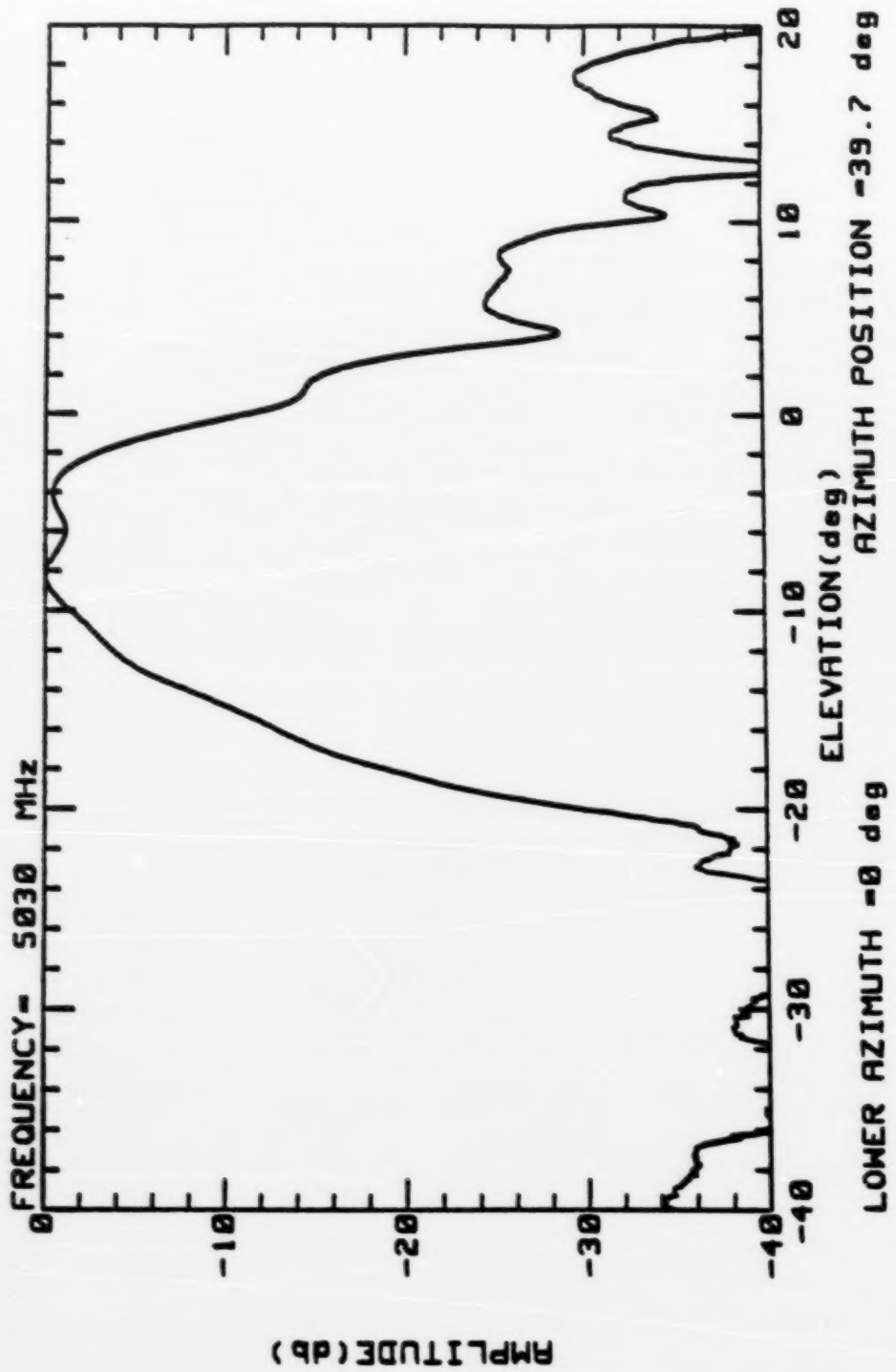

Figure A1-29 Elevation Radiation Pattern of Antenna 002, 5.03 GHz With Squinted Beam

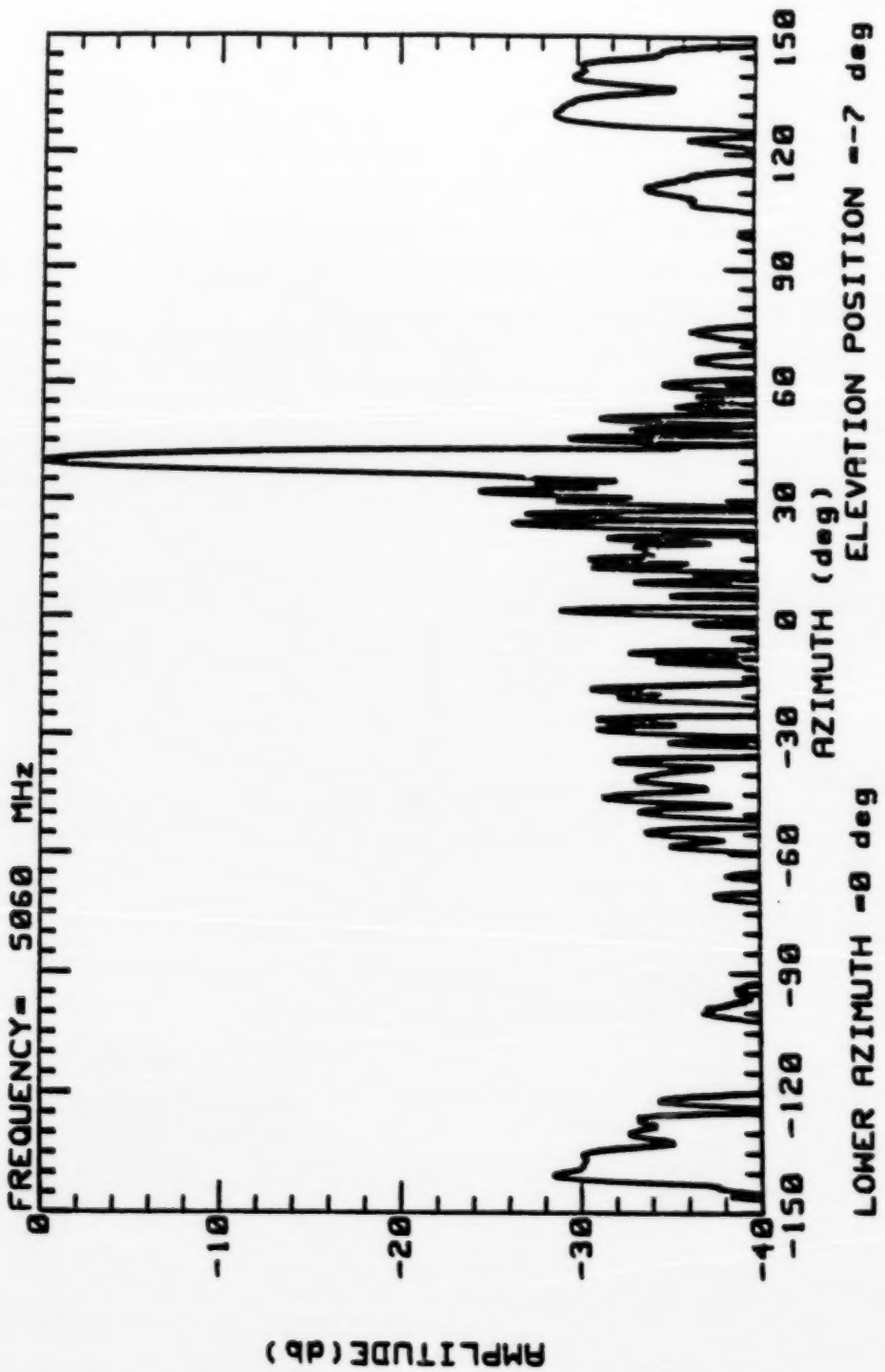

Figure A1-30 Azimuth Radiation Pattern of Antenna 002, 5.06 GHz With Squinted Beam

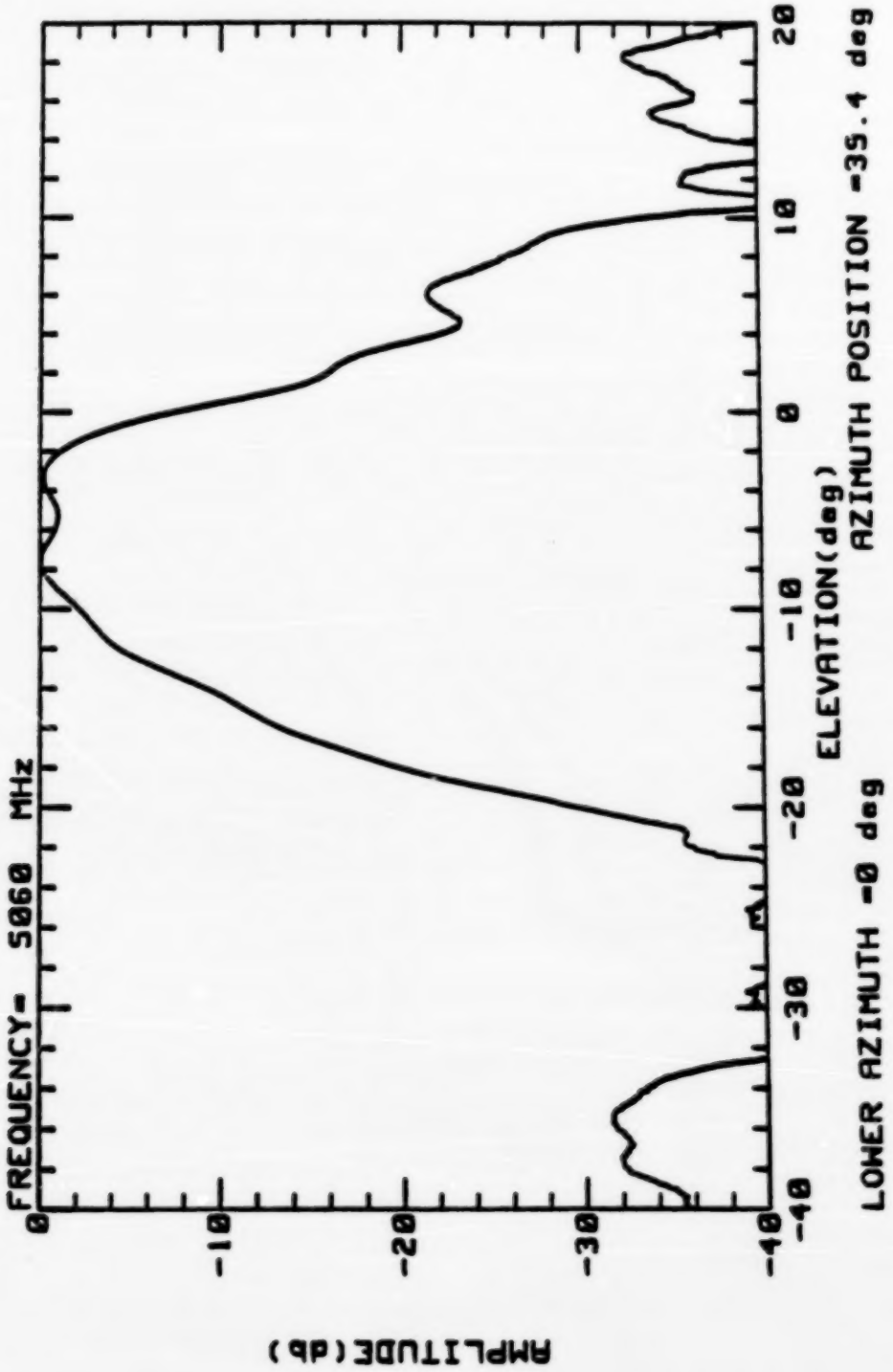

Figure A1-31 Elevation Radiation Pattern of Antenna 002, 5.06 GHz With Squinted Beam

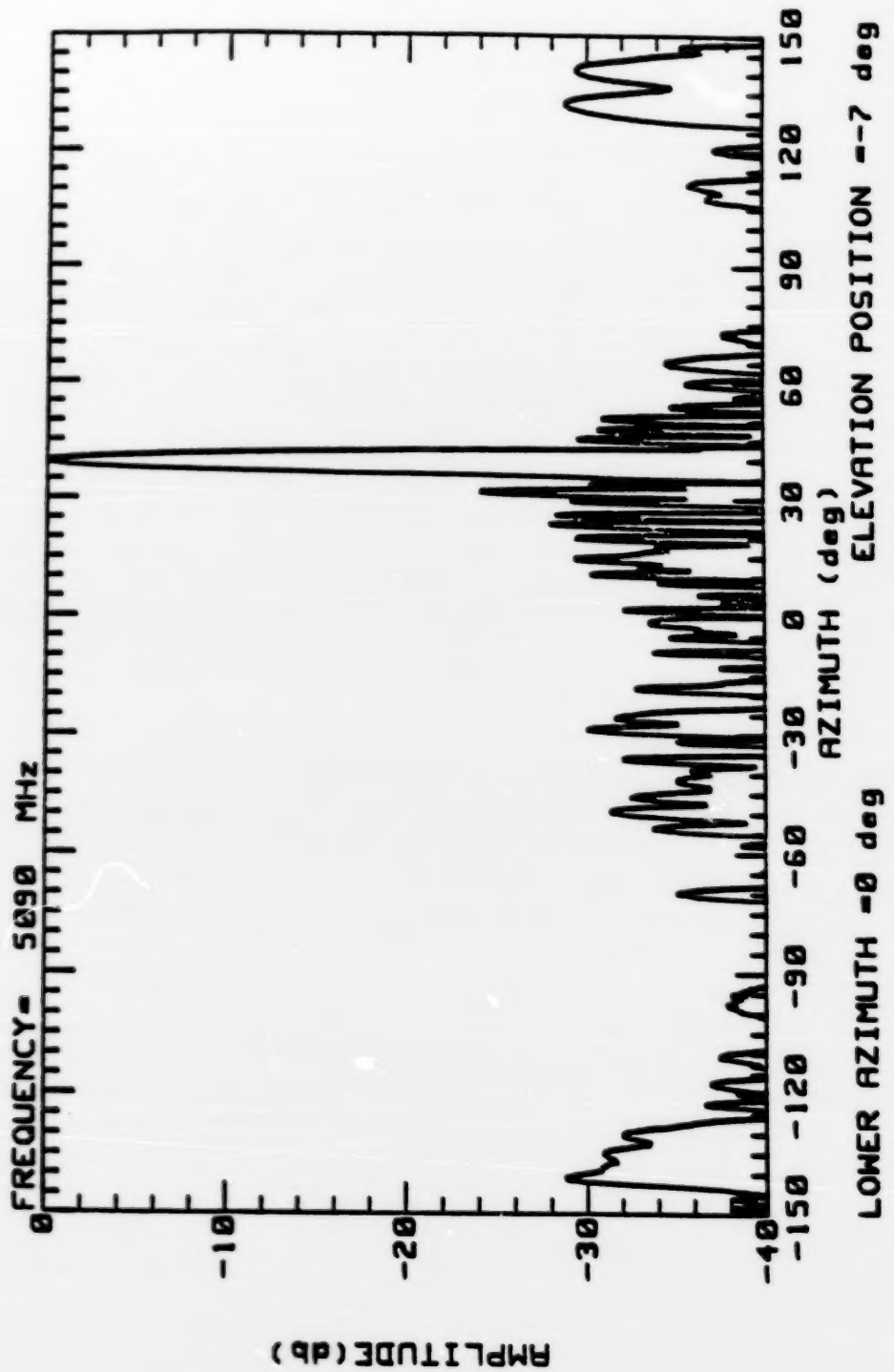

Figure A1-32 Azimuth Radiation Pattern of Antenna 002, 5.09 GHz With Squinted Beam

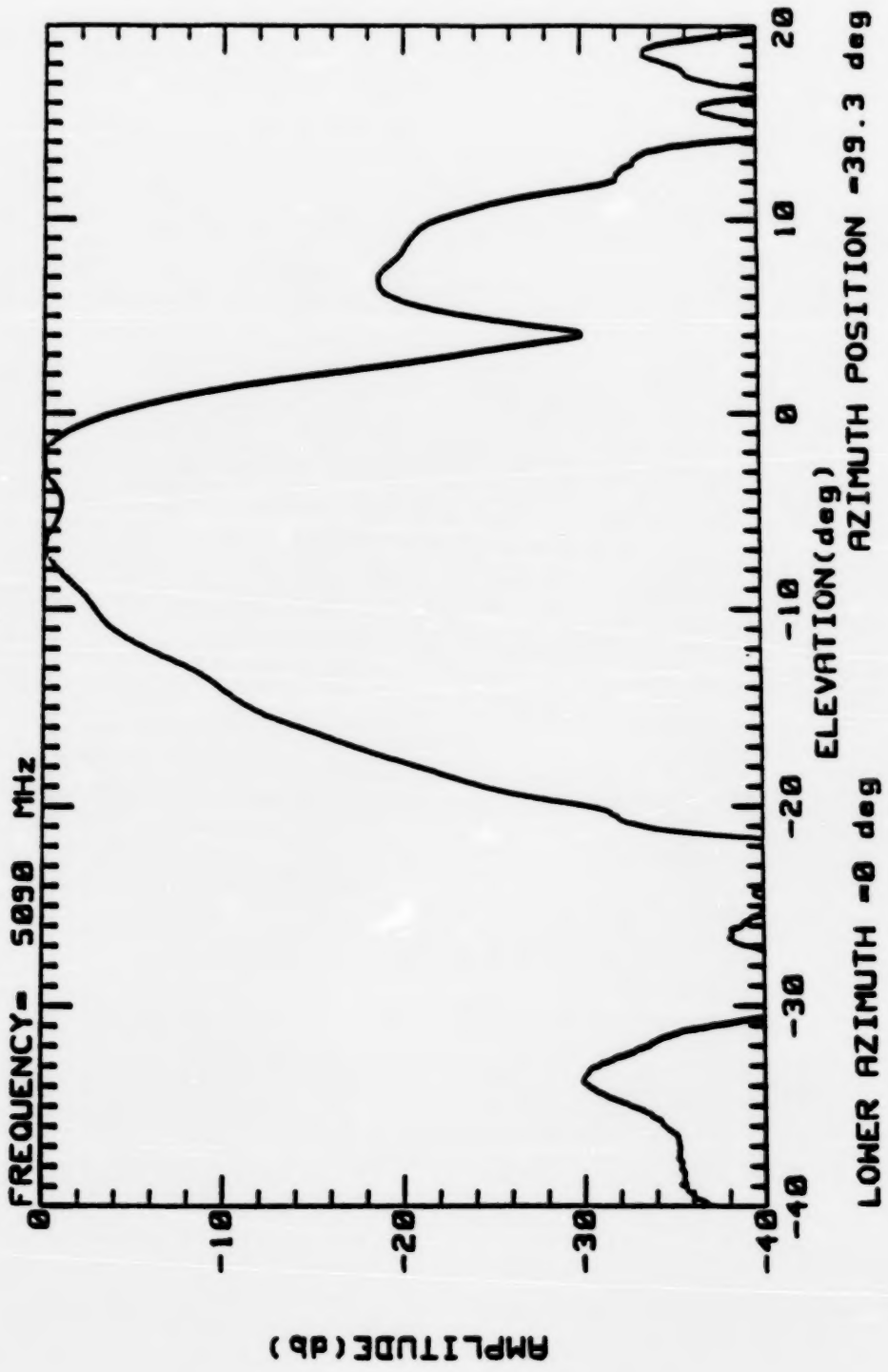

Figure A1-33 Elevation Radiation Pattern of Antenna 002, 5.09 GHz With Squinted Beam